AD_____

Award Number: DAMD17-01-1-0135

TITLE: Identification of Genes Regulated by Proteolysis

PRINCIPAL INVESTIGATOR: Jeffrey W. Harper, Ph.D.

CONTRACTING ORGANIZATION: Harvard Medical School
Boston, MA 02115

REPORT DATE: July 2005

TYPE OF REPORT: Final

PREPARED FOR: U.S. Army Medical Research and Materiel Command
Fort Detrick, Maryland 21702-5012

DISTRIBUTION STATEMENT: Approved for Public Release;
Distribution Unlimited

REPORT DOCUMENTATION PAGE

Form Approved
OMB No. 0704-0188

1. REPORT DATE *(DD-MM-YYYY)*	2. REPORT TYPE	3. DATES COVERED *(From - To)*
01-07-2005	Final	1 Jul 2001 - 30 Jun 2005

4. TITLE AND SUBTITLE
Identification of Genes Regulated by Proteolysis

5a. CONTRACT NUMBER

5b. GRANT NUMBER
DAMD17-01-1-0135

5c. PROGRAM ELEMENT NUMBER

6. AUTHOR(S)
Jeffrey W. Harper, Ph.D.

E-mail: wade_harper@hms.harvard.edu

5d. PROJECT NUMBER

5e. TASK NUMBER

5f. WORK UNIT NUMBER

7. PERFORMING ORGANIZATION NAME(S) AND ADDRESS(ES)
Harvard Medical School
Boston, MA 02115

8. PERFORMING ORGANIZATION REPORT NUMBER

9. SPONSORING / MONITORING AGENCY NAME(S) AND ADDRESS(ES)
U.S. Army Medical Research and Materiel Command
Fort Detrick, Maryland 21702-5012

10. SPONSOR/MONITOR'S ACRONYM(S)

11. SPONSOR/MONITOR'S REPORT NUMBER(S)

12. DISTRIBUTION / AVAILABILITY STATEMENT
Approved for Public Release; Distribution Unlimited

13. SUPPLEMENTARY NOTES

14. ABSTRACT

Substrate selection in ubiquitination reactions is achieved by ubiquitin ligases, which simultaneously bind both the target protein and a ubiquitin conjugating enzyme. We have developed a phosphopeptide based approach to facilitate the identification of ubiquitin ligases (e.g. F-box proteins) that recognize regulatory proteins in a phosphorylation-dependent manner. Thus far, we have used this approach to identify substrates of two F-box proteins, Fbw7 and beta-TRCP. Cyclin E associates with Fbw7 through a phosphodegron near its C-terminus. Experiments in vitro and in vivo have identified critical phosphorylation sites in this degron that are required for interaction with Fbw7. Interestingly, this motif is found in a number of other unstable oncogenic proteins, including c-myc, c-jun, and SREBP. In a second series of studies, we have identified the cell cycle regulatory protein Cdc25A as a target of the beta-TRCP protein. We have found that Chk1 phosphorylates Cdc25A in response to DNA damage to generate a priming event that facilitates phosphorylation of Cdc25A on a motif that then binds to beta-TRCP. Using biochemical and genetic techniques, we demonstrate that this interaction is required for regulated proteolysis of Cdc25A.

15. SUBJECT TERMS
Breast Cancer, protein ubiquitination, technology development

16. SECURITY CLASSIFICATION OF:			17. LIMITATION OF ABSTRACT	18. NUMBER OF PAGES	19a. NAME OF RESPONSIBLE PERSON
a. REPORT	b. ABSTRACT	c. THIS PAGE			USAMRMC
U	U	U	UU	54	19b. TELEPHONE NUMBER *(include area code)*

FOREWORD

Opinions, interpretations, conclusions and recommendations are those of the author and are not necessarily endorsed by the U.S. Army.

_X_ Where copyrighted material is quoted, permission has been obtained to use such material.

_X_ Where material from documents designated for limited distribution is quoted, permission has been obtained to use the material.

_X_ Citations of commercial organizations and trade names in this report do not constitute an official Department of Army endorsement or approval of the products or services of these organizations.

N/A In conducting research using animals, the investigator(s) adhered to the "Guide for the Care and Use of Laboratory Animals," prepared by the Committee on Care and use of Laboratory Animals of the Institute of Laboratory Resources, national Research Council (NIH Publication No. 86-23, Revised 1985).

N/A For the protection of human subjects, the investigator(s) adhered to policies of applicable Federal Law 45 CFR 46.

N/A In conducting research utilizing recombinant DNA technology, the investigator(s) adhered to current guidelines promulgated by the National Institutes of Health.

N/A In the conduct of research utilizing recombinant DNA, the investigator(s) adhered to the NIH Guidelines for Research Involving Recombinant DNA Molecules.

N/A In the conduct of research involving hazardous organisms, the investigator(s) adhered to the CDC-NIH Guide for Biosafety in Microbiological and Biomedical Laboratories.

Table of Contents

Introduction

Protein ubiquitination requires three components: E1, E2, and E3 (Hershko and Ciechanover, 1998). In the first step, a ubiquitin-activating enzyme (E1) is charged with ubiquitin through a thiol-ester linkage. This ubiquitin is then transferred to one of a dozen or so ubiquitin conjugating enzymes (E2) also as a thiol-ester. The ubiquitin is finally transferred from the E2 to one or more lysine residues in the substrate with the aid of an E3 ubiquitin ligase. In essence, E3s function as substrate-specific adaptors by simultaneously binding substrate and the E2, although in some cases, E3s may also serve as an intermediate in the ubiquitin transfer process.

Much of our knowledge of E3s has come from genetic dissection of signaling pathways that involve one or more ubiquitin-dependent events (reviewed in Koepp et al., 1999; Patton et al., 1998). These studies have revealed 3 broad classes of E3s that are likely to be responsible for targeting the ubiquitination of hundreds of proteins: 1) the HECT domain class which includes E6-AP, 2) the ring finger class which include Cbl and MDM2, and 3) the cullin-based ubiquitin ligases which include SCF, VBC, and APC complexes. Given the size of these different protein families, it is clear that many aspects of the biology of these E3s are unexplored. There are at least 40 HECT domain proteins in the human genome and more than 250 ring-finger containing proteins that may be involved in ubiqutination.

The complexity of these systems is perhaps best exemplified by the cullin-based ligases of which the SCF complex is the best understood. These are multicomponent E3s that dock substrates with a core ubiquitin conjugating system via modular substrate specific adaptors (reviewed in Koepp et al., 1999). The core components include a member of the cullin family of proteins, which contains 6 members in mammals, a RING finger protein typified by Rbx1 and APC11, and an E2 (Cdc34 or Ubc4). These core complexes interact with distinct families of substrate specific adaptors to generate a large number of ubiquitin ligases with distinct functions. Our work has focused on the SCF sub-family of cullin-based ubiquitin ligases, which refers to the three major components (Skp1, Cul1, and a member of the F-box family of proteins) (See scheme on left). Through genetic and biochemical studies in budding yeast, we identified Skp1 as a component of the SCF that links Cul1 to F-box proteins (Bai et al., 1996; Skowyra et al., 1997). We also discovered the F-box motif as a Skp1 binding element that is found in a large number of proteins that can bind to particular ubiquitination substrates in a phosphorylation dependent manner (Bai et al., 1996; Skowyra et al., 1997). The timing of ubiquitination and destruction of many proteins are controlled by protein phosphorylation, including cyclin-dependent kinase inhibitors such as p27 and Sic1, and G1 cyclins (cyclin E and Cln proteins). Through biochemical reconstruction of the SCF mediated ubiquitination of Sic1 and Cln1, we were able to demonstrate that distinct F-box proteins recognize distinct targets in a phosphorylation dependent manner and allow ubiquitination via an Rbx1/Cul1 dependent pathway (Skowyra et al., 1997, 1999; Kamura et al., 1999). In addition to the F-box motif that mediates interaction with Skp1, F-box proteins frequently contain C-terminal protein-protein interaction domains (Bai et al., 1996). The most common are WD40 and leucine-rich repeat domains. In an effort to understand the

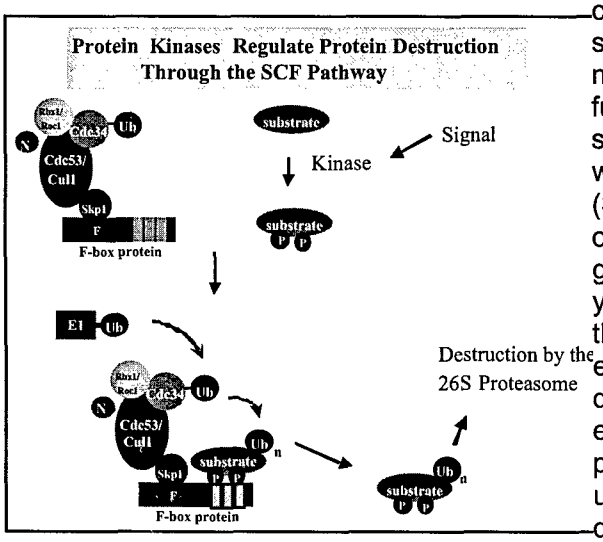

complexity of mammalian F-box proteins, we have isolated a large number of cDNAs encoding F-box proteins (Winston et al., 1999a). In total, >68 distinct mammalian F-box proteins are now known to exist. We have shown that one of these, β-TRCP, is responsible for the ubiquitination of IkB, an inhibitor of the NFkB transcription factor complex required for the cytokine response as well as β-catenin, a transcription factor that functions as an oncogene when not properly destroyed by ubiquitin-mediated proteolysis (Winston et al., 1999b). The Cul2-based ubiquitin ligase has more than 20 known substrate adaptor proteins called SOCS-box proteins (Hilton et al., 1998), one of which is the von Hippel-Lindau tumor suppressor protein (Lisztwan et al., 1999). Although the functions of the vast majority of F-box and SOCS-box proteins are unknown, the finding that the limited number of F-box proteins that have been characterized all function to ubiquitinate multiple target proteins suggests that this family of E3s will be responsible for ubiquitination of possibly hundreds of proteins.

The challenge in the post-genome era will be: 1) to identify proteins whose abundance is regulated, 2) to determine what ubiquitin ligase pathways contribute to destruction of specific targets, and 3) to determine how the activities of particular ligases are controlled. Historically, the identification of ubiquitinated proteins has occurred on a case by case basis, and as such, we have a very limited view of the number and types of proteins in the cell that are controlled by this pathway. Moreover, we have little information that addresses how particular oncogenic events affect either the activities of different classes of ubiquitin ligases or the access of such ligases to their substrates. This is due, in part, to the fact that generally applicable methods are not available for identifying proteins that are destroyed in response to particular stimuli or in particular cellular contexts. In rare cases, it has been possible to use genetic screens in yeast to identify targets of ubiquitin ligases for which mutants were available. However, this approach is generally limited to yeast and even in cases where particular mutants in E3 components are available, substrates have been difficult to identify. In addition, approaches such as two-hybrid systems have not been particularly useful in identifying targets of ubiquitin ligase components such as F-box proteins. Given the large number of substrate adaptors that we and others have identified and that are likely to be identified in the future as a result of genome sequencing efforts, the identification of their important substrates will continue to be a major challenge.

Three complementary approaches are being undertaken to identify ubiquitination targets. In one approach, we are taking advantage of the facile genetics in budding yeast to identify targets of known ubiquitin ligase. Yeast has provided many of the important insights into ubiquitination pathways that have been shown to be general to all eukaryotes. Progress in this area was described in the previous progress report, including a publication in **Science** wherein we reported the identification of an F-box protein – Fbw7 - for human cyclin E. Human cyclin E is a prognostic marker for breast cancer and there is evidence that Fbw7 is mutated in human cancer, consistent with the possibility that it is a tumor suppressor. We have now performed a detailed examination of the biochemical mechanisms used in recognition of Cyclin E by Fbw7 and present these finding below, as well as a recent paper describing these results. Tasks 1 and 2 have been completed and were described in detail in the previous report. As part of task 3, we have designed and utilized a sectoring assay in budding yeast in the hope of identifying E3-substrate pairs. However, this approach has not yet been successful. In a second approach, we are using a collection of F-box proteins as biochemical and genetic reagents to identify substrates. Our progress on the identification of an E3 for Cdc25A – SCF-beta-TRCP - will be presented below. This work has recently been published. Finally, in a third approach, we have attempting to develop general methods to identify substrates in mammalian cells. For the reasons described below, we needed modified our initial objective (Aim 2) in this regard to take advantage of new technology that has emerged since this grant was submitted. Although the final system is still not complete, we think that the approach of RNAi libraries has a good chance of providing a general means by which to identify substrates of ubiquitin ligases.

Body

Development of a library of F-box proteins

We previously reported the identification of 33 human F-box proteins. Through subsequent work, we have now expanded this to more than 68 family members in humans and 70 family members in the mouse. These F-box proteins fall into three classes: Fbws, which contain WD40 repeats, Fbls which contain leucine rich repeats, and Fbxs which contain either no recognized domain or have other classes of protein interaction domains. These C-terminal protein interaction domains are thought to mediate interaction with substrates. We have cloned and sequenced a number of these (more than 50 to date) and have made reagents that allow us to express these genes in human cells. This panel of reagents provides a unique opportunity to employ both yeast genetic systems and biochemical approaches to the identification of ubiquitination targets, the focus of this proposal.

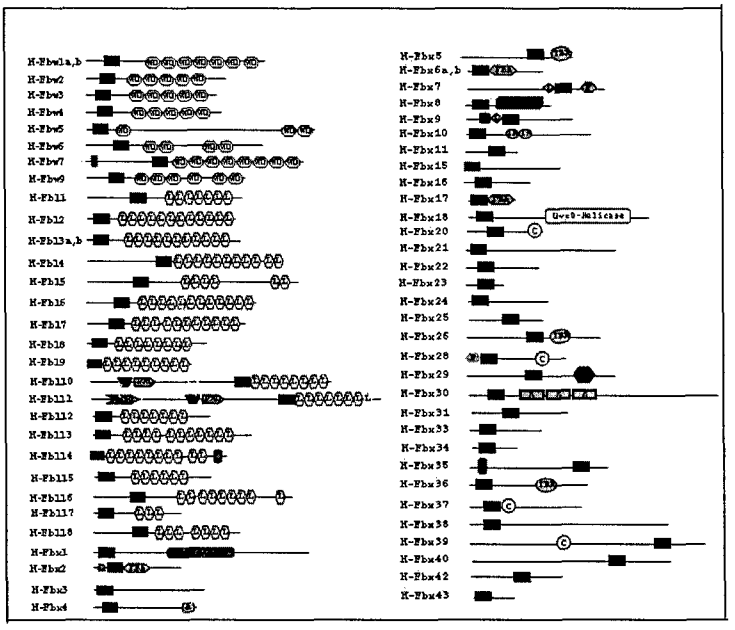

Identification of an F-box protein important for degradation of the breast cancer oncoprotein Cdc25A. Previous work has demonstrated that Cdc25A is an oncogene and is overexpressed in breast cancer (Cangi et al., 2000; Evans, 2000). Cdc25A catalyzes the dephosphorylation of Cdk2, leading to its activation and thereby promoting S-phase entry. Cdc25A is regulated by multiple proteolytic mechanisms, including the anaphase promoting complex. Moreover, recent data indicate that Cdc25A is destroyed in response to DNA damage in a manner that depends upon the Chk1 kinase. Previous data suggested the involvement of an SCF complex in Cdc25A regulation but the identity of the F-box protein involved was not known.

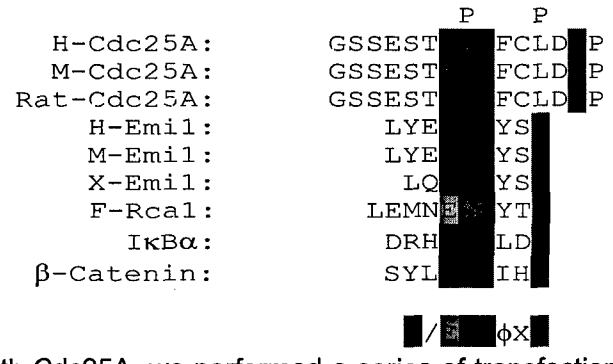

To address this, we first confirmed the previous finding that dominant negative inhibitors of Cul1 lead to stabilization of Cdc25A. Interestingly, this occurs independently of DNA damage. Moreover, we demonstrated that Cul1 associates with Cdc25A in vivo. To search for F-box proteins that interact with Cdc25A, we performed a series of transfection experiments using various F-box proteins and then performed immunoprecipitations using Cdc25A antibodies. We found one F-box protein – β-

TRCP - that consistently interacted with Cdc25A. We previously discovered β-TRCP as an F-box protein that interacts with destruction motifs in IκB and β-catenin. β-TRCP interacts with sequences containing the consensus: DSGIXS where both serine residues are phosphorylated. In the absence of phosphorylation, neither IκB nor β-catenin interact with β-TRCP. We scanned the sequence of Cdc25A for sequences that look like those found in IκB and found a sequence centered on Ser-81 that has similarities to the sequence in IκB. We demonstrated that Cdc25A binds to β-TRCP in a manner that depends upon phosphorylation of Ser-81 and this interaction requires the action of Chk1, a kinase that is activated by ATM/ATR in response to DNA damage. We demonstrated that RNAi against β-TRCP leads to dramatic stabilization of Cdc25A in response to DNA damage and this stabilization is accompanied by a defect in the inter S-phase DNA damage checkpoint. We reconstituted Chk1-dependent ubiquitination of Cdc25A by SCFβ-TRCP in vitro, demonstrating a requirement for phosphorylation of Ser76 by Chk1. Based on these and other data, we hypothesize that Chk1-mediated phosphorylation of Ser-76 in Cdc25A serves as a priming event for phosphorylation of Ser-81 by an as yet unidentified kinase. Future studies are aimed at identifying this kinase. All of this work is reported in the attached **Genes and Development** manuscript by Jin et al., 2003.

Development of retroviral systems for identification of ubiquitination substrates in mammalian cells (Aim 2)

The goal of aim 2 is to develop a retroviral based system for identifying unstable proteins in mammalian cells. Our original plan was to employ GFP-fused cDNA libraries to develop a flow-cytometry based screen that would allow us to identify candidate substrates of particular E3s. Our progress on this was described in the previous report. However, the recent development of RNAi strategies in mammalian cells has radically changed the types of experiments that we can perform. We are now incorporating loss of function type experiments into a new approach to identify substrates that has features of the previously proposed system but is more likely to provide important results. In this approach, we will generate libraries of mammalian cells expressing CFP-tagged cDNAs via integrating retroviral vectors wherein the CFP epitope splices into endogenous genes, creating protein fusions. The CFP-tagged cDNA will be linked via an IRES to GFP such that sub-libraries of cells with defined GFP/CFP ratios can be isolated by live cell sorting. Ablation of particular ubiquitin ligases by RNAi would be expected to lead to increased levels of target proteins, resulting in a shift in the ratio of GFP to CFP in individual cells where the target gene is CFP tagged. Cells displaying altered ratios will be isolated by cell sorting and the identities of recipient genes determined.

The strategy is built upon previous work employing retroviral based tagging of genes (29) using enhanced retroviral mutagen (ERM) vectors. This system has been used to identify dominant proliferative genes. The primary features of these vectors relative to this proposal is that the tagging epitope (CFP for example) under control of its own promoter (CMV for example) is physically linked with splice donor sequences and upon integration into a cellular gene, CFP coding sequences may be spliced into the recipient gene, creating a protein fusion between CFP and the coding sequence of the recipient. Hundreds of thousands of independent integration events occurring in individual cells can be selected by virtue of selectable markers on the retrovirus, allowing the creation of libraries of cells containing a particular gene fused with CFP. An added feature of this system is that even genes that are not normally expressed in the target cell line can come under control of the retroviral derived CMV promoter, thereby allowing expression of otherwise silent genes. We have constructed the tagging tagging vector that expresses two spectrally separated GFP coding sequences from the same CMV driven transcript using an intervening IRES (internal ribosomal entry sequence) (Figure 1). The first GFP is expressed as an

intact protein while the second variant GFP (CFP) lacks a stop codon but contains a splice-donor sequence. Upon integration into a recipient gene, GFP and the CFP fusion proteins should be produced at a constant ratio since they are derived from the same mRNA, although their individual stabilities may be different. Additional versions of this vector have been generated, including CD20 instead of GFP and vectors that splice in two other reading frames. CD20 is a cell surface protein that can be detected immunologically in live cells.

Because the ratio of GFP to CFP-fusion protein should be stable in each recipient cell, groups of cells with particular ratios can be isolated by fluorescence activated cell sorting and then expanded for experimental manuipulation. We are currently in the process of generating MCF7 cells and related breast cancer cell lines that are stably transduced with this vector. Our initial goal is to generate pools of cells that each display a particular ratio of GFP (or CD20) to CFP-fusion protein. We will isolate 10 pools of cells that reflect GFP/CFP ratios ranging from 10 to 0.1. Each pool is expected to contain hundreds of thousands of different integration events. A substantial fraction of these integration events will lead to the production of a fusion protein between CFP and recipient coding sequences. The resulting CFP fusion proteins may represent full-length sequences or may represent fragments of the recipient gene, possibly containing sequences important for regulated turnover. In principle, by making cells with vectors in all three reading frames prior to sorting all cells together, it should be possible to have a larger number of recipient genes represented in the collection of pools. This effort represents Aim 2, tasks7 and 8.

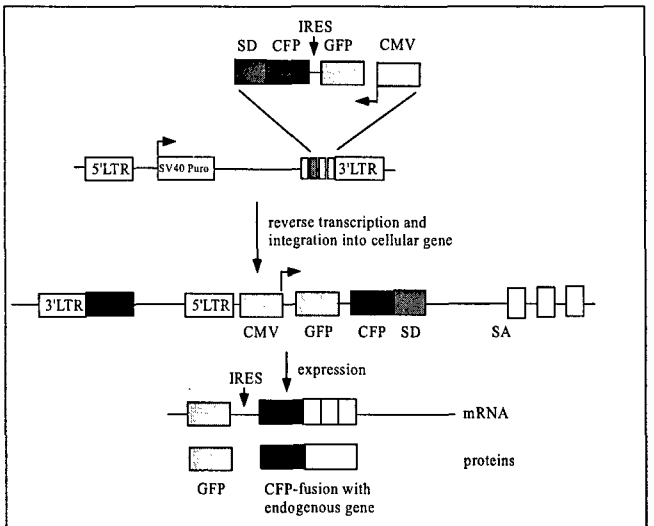

Figure 1. Schematic representation of vectors for generating libraries of cells expressing CFP-fusion proteins after random integration in mammalian cells. CMV drives the expression of a transcript for GFP and CFP/splice donor (SD) linked by an IRES. Integration into an endogenous gene leads to expression of GFP and a CFP-fusion protein with sequences inherited from the endogenous locus. The ratio of GFP and CFP proteins will remain constant in the cell due to the fact that they are both expressed from the same transcript.

A second part of this approach involves the development of RNAi for E3s. As part of a collaboration with Dr. Greg Hannon at Cold Spring Harbor, we have developed retroviral vectors expressing shRNA (short hairpin RNAs) for a large number of ubiquitin ligase components. These shRNAs are made against specific sequences in the E3 component and we have three different sequences per gene, thereby increasing the likelihood that knock-down can be achieved. Each of the shRNAs are under control of the U6 promoter. We are currently preparing DNA for shRNA vectors directed against ~50 F-box proteins which we have identified.

Depletion of a particular ubiquitin ligase by RNAi would be expected to lead to an increase in the abundance of requisite CFP-tagged substrates and this should be reflected in the alteration in the ratio of GFP to CFP. Thus, once pools of cells are established, RNAi will then be used to knock-down particular F-box proteins and cells that display increased levels of CFP-recipient fusion proteins relative to GFP isolated using FACS. Given the window of fluorescence ratios chosen for each pool, we anticipate to be able to identify cells in which the GFP/CFP ratio is decreased by as little as 3 fold. These cells contain tagged candidates for ubiquitination targets of particular F-box proteins. Based on our previous experience with RNAi against other ubiquitin ligases (Fbw7 for example) we easily see a 3-fold increase in cyclin E levels after RNAi (27), in the range we expect to be able to seen by FACS. If necessary, we will reconstruct the system using cyclin E as target to standardize parameters.

Functional analysis of point mutations in Fbw7 found in human cancer

In our previous report, we described our identification of Fbw7 as the F-box protein responsible for ubiquitination of cyclin E. There is now clear evidence of mutations in Fbw7 in human cancer, including ovarian, breast, and endometrial cancers (Moberg et al., 2000; Koepp et al., 2000; Spruck et al., 2002). Our work initially found defects in expression of Fbw7 in breast cancer cell lines relative to normal cell lines. Several point mutations were found in the WD40 repeats of Fbw7, including R385, R425, and R463. We thought that it may be worthwhile to follow up our studies by examining the consequence of these mutations on function. To determine the effect of these mutations on interaction with cyclin E, we introduced these mutations into Fbw7 and examined their interaction with cyclin E. Prior to performing these experiments, we determined the phosphorylation status of cyclin E in mammalian cells and identified several phosphorylation sites that we thought might be important to interaction with Fbw7. We identified phosphorylation at S372, T380, and S384. Peptides containing various phospho-forms of this region of cyclin E were synthesized and tested for binding to Fbw7. Also, the sequence around T62 is similar to the Fbw7 recognition sequence centered at T380, so various phosphopeptides in this region were made as well. Using binding reactions with in vitro translated Fbw7 and phosphopeptides immobilized on agarose, we found that phosphorylation of T380 is sufficient to interact with Fbw7. Phosphorylation of S384 or S372 in the context of T380 phosphorylation had no impact on binding. In addition, phosphorylation of T62 was sufficient to allow for binding but phosphorylation of S58 had no effect on this binding. We next tested the point mutants seen in Fbw7 in cancer for binding to both the T62 peptide and the T380 peptide. We found that cancer derived mutations either did not bind at all to these peptides (R385A) or bound poorly relative to WT Fbw7 (R425A, R463A). The ability of Fbw7 to interact with two different cyclin E derived phosphopeptides could reflect either the presence of two different binding sites or the presence of a single binding site, wherein binding is mutually exclusive. To examine this issue, we performed a competition experiment wherein association of Fbw7 with phospho-T380 peptide was competed with either T62 peptide or with phosphorylated T62 peptide. We found that phosphorylated T62 peptide (but not unphosphorylated peptide) competed for binding to phospho-T380. Therefore, it would appear that a single site is responsible for binding to both of the peptides. Therefore, phosphorylation of either of these sites would be expected to affect turnover of cyclin E by Fbw7. Experiments to examine this are underway, as are experiments that test the interaction between Fbw7 mutants and full-length cyclin E.

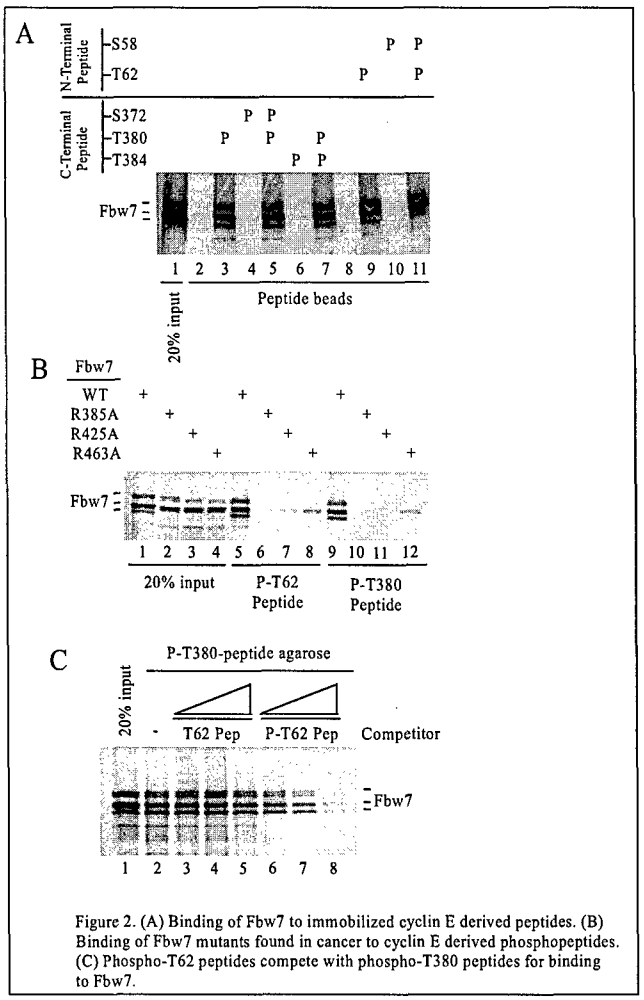

Figure 2. (A) Binding of Fbw7 to immobilized cyclin E derived peptides. (B) Binding of Fbw7 mutants found in cancer to cyclin E derived phosphopeptides. (C) Phospho-T62 peptides compete with phospho-T380 peptides for binding to Fbw7.

Contribution of phosphorylation to Fbw7-mediated cyclin E turnover *in vivo*.

Currently, three distinct isoforms of Fbw7 - α, β, and γ – have been described. These isoforms employ distinct 5' exons encoding unique N-termini fused with 10 common exons. We first asked where these proteins are localized in the cell. However, because anti-Fbw7 antibodies suitable for immunofluorescence are not available, we used transient transfection of Fbw7 expression vectors in which the N-terminus was tagged with a Flag epitope. In 293T cells, we found that both Fbw7α and Fbw7γ are localized primarily in the nucleus (Figure 3A, C). In contrast, Fbw7β is almost exclusively found in the cytoplasm (Figure 3B). We previously reported that Fbw7β has an apparent transmembrane domain near the N-terminus (Koepp et al., 2001) and this may be involved in localizing Fbw7β to ER membranes.

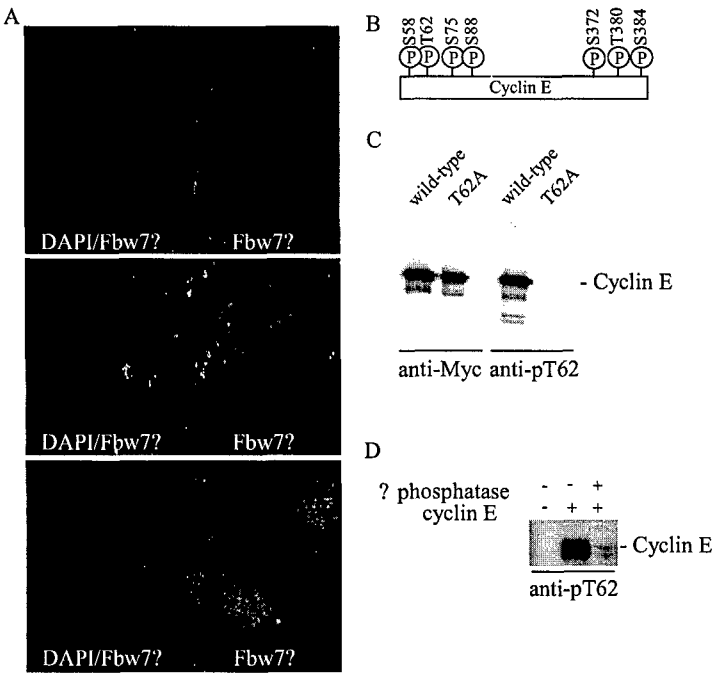

Figure 3. (A) Differential localization of Fbw7 isoforms. Expression plasmids encoding the indicated N-terminally Flag-tagged Fbw7 isoforms were transiently transfected into 293T cells using Fugene 6. After 36 h, cells were subjected to indirect immunofluorescence. Anti-Flag immunofluorescence is in red. Nuclei, stained with DAPI, are in blue. (B) Schematic representation of phosphorylation sites found in cyclin E (see Table 1). (C, D) Antibodies directed at phospho-T62 of cyclin E selectively interact with wild-type cyclin E purified from 293T cells after transient transfection but do not react with cyclin E^{T62A} or with cyclin E treated previously with ? phosphatase. In panel C, 293T cells were transfected with pCMV-Myc-cyclin E DNA and after 48h, cell lysates were immunoprecipitated with anti-Myc antibodies prior to immunoblotting with either anti-Myc antibodies or anti-phosphoT62 antibodies. In panel D, Myc-cyclin E immune complexes were incubated in the presence or absence of ? βhosphatase prior to immunoblotting with anti-phosphoT62 antibodies.

To examine the contribution of multi-site phosphorylation to cyclin E turnover, we employed an *in vivo* degradation assay wherein Myc-cyclin E and Cdk2 are transiently expressed in 293T cells in the presence or absence of Fbw7 isoforms. Expression of Myc-cyclin E and Cdk2 alone led to readily detectable Myc-cyclin E, as determined by immunoblotting of crude cell extracts (Figure 2 in attached manuscript). Co-expression of increasing levels of Flag-Fbw7α led to a dramatic decrease in the steady-state abundance of Myc-cyclin E. All three Fbw7 isoforms, when expressed at comparable levels, were capable of reducing the abundance of cyclin E but had no effect on Cdk2 abundance. These results extend previous results from multiple labs indicating that Fbw7β overexpression can drive cyclin E degradation when overexpressed. As expected, cyclin E^{T380A} and cyclin $E^{T62A;T380A}$ levels were largely unaffected by expression of all three isoforms of Fbw7. This is consistent with a major role for T380 phosphorylation in controlling cyclin E turnover, as determined by pulse chase (Figure 2D in attached manuscript). We then examined the susceptibility of T62A, S88A, S372A and S384A mutations to elimination by Fbw7 isoforms. We found that T62A was substantially defective in elimination by Fbw7β and γ but this defect was much less obvious with the Fbw7α isoform under these conditions (Figure 2 A-C in attached manuscript). However, using lower Fbw7α expression plasmids revealed clear defects in cyclin E^{T62A} turnover (Figure 2F in attached manuscript). We also found that Fbw7β was profoundly defective in eliminating cyclin E^{S384A} (Figure 2B in attached manuscript), while turnover of cyclin E^{S384A} by Fbw7α and γ was less affected (Figure 2A, C in attached manuscript). At higher levels of cyclin E^{S384A} expression plasmid used for transfection, cyclin E^{S384A} was substantially more resistant to turnover by Fbw7α than was wild-type cyclin E (Figure 2G in attached manuscript). Cyclin E^{S372A} and cyclin E^{S88A} were efficiently degraded by all three Fbw7 isoforms (Figure 2A-C in attached manuscript and data not shown for

cyclin E^{S372A}). Control experiments demonstrated comparable levels of all three Fbw7 isoforms in transient transfections (Figure 2E in attached manuscript).

Association of cyclin E phosphorylation site mutants with Fbw7 *in vivo*.
The data described above suggested the possibility that T62, in addition to T380, could be employed for Fbw7 association with cyclin E *in vivo*. To examine whether dual modes of interaction occur with intact cyclin E, binding experiments were performed with a series of cyclin E mutants and Fbw7α after transfection in 293T cells. The ability to accurately assess binding interactions requires that comparable levels of cyclin E mutants be expressed. However, mutation of T380, and to a lesser extent T62, leads to increased steady-state levels of cyclin E in the presence of Flag-Fbw7 expression (data not shown). Therefore, to achieve approximately equal levels of cyclin E expression, we also co-transfected vectors expressing a dominant negative form of Cul1 ($Cul1^{DN}$) which contains the Skp1 binding site but lacks the Rbx1 binding site. This form of Cul1 sequesters Skp1/F-box complexes and leads to stabilization of SCF targets. As expected, expression of $Cul1^{DN}$ leads to equal accumulation of all cyclin E mutants examined, despite the presence of Flag-Fbw7α (Figure 4A, lanes 1-5 in attached manuscript). Extracts from cells expressing mutant cyclin E proteins and Flag-Fbw7α were then subjected to immunoprecipitation using anti-Flag antibodies and the levels of associated cyclin E examined by immunoblotting. Cyclin E efficiently associated with Fbw7α (Figure 4A, lane 1 in attached manuscript). Interestingly, cyclin E^{T380A} was found to associate weakly with Fbw7α (lane 3) but mutation of T62 to alanine in the context of the T380A mutant further reduced the interaction with Fbw7α (Figure 4A, lane 4 in attached manuscript). Mutation of T62 in cyclin E to alanine also led to a reduction in the extent of Fbw7α binding (Figure 4B, lane 2 in attached manuscript).

The reduced association between Fbw7α and cyclin E^{T62A} could reflect either a significant utilization of phosphorylated T62 in binding to Fbw7α or could potentially reflect alterations in the phosphorylation of T380. To examine this issue, we tested the extent of phosphorylation of T380 in the context of the T62A mutation under the same conditions employed in Figure 4A in attached manuscript. Lysates from transfected cells were immunoprecipitated with anti-Myc antibodies and the levels of total cyclin E and T380 phosphorylated cyclin E determined by immunoblotting (Figure 4B in attached manuscript). We found that replacement of T62 with alanine significantly reduced the extent of T380 phosphorylation. The extent of reduction was comparable to the reduction seen in the association of Fbw7□ with cyclin E^{T62A}. Transfection of cyclin E mutants in the absence of Fbw7 and $Cul1^{DN}$ demonstrated that the effect on T380 phosphorylation was independent of these two components (data not shown). Taken together, this data indicates that mutation of T62 affects T380 phosphorylation and the majority of its contribution to Fbw7-mediated turnover appears to be indirect.

Involvement of S384 in recognition of cyclin E by Fbw7. Results described above indicate that cyclin E^{S384A} is partially defective in degradation by Fbw7 with turnover by Fbw7β being affected to the greatest extent. To examine whether this reflects recognition by Fbw7, we compared the ability of Fbw7α and β isoforms to immunoprecipitate cyclin E^{S384A} in transfected 293T cells (Figure 5 in attached manuscript). Interestingly, cyclin E^{S384A} bound more weakly to both Fbw7 isoforms (lanes 3and 6) than did wild-type cyclin E, suggesting a significant decrease in affinity in the context of full-length proteins *in vivo*. Association of cyclin E with Fbw7β was substantially lower than with the α isoform, possibly reflecting the fact that Fbw7β is largely cytoplasmic while cyclin E is largely nuclear. Importantly, cyclin E^{S384A} maintained wild-type levels of T380 phosphorylation, as determined by immunoblots of cyclin E immune complexes using anti-phospho-T380 antibodies (Figure 4B in attached manuscript). All of the work cited here is described in detail in the accompanying manuscript in Journal of Biological Chemistry by Ye et al.

Finally, using a fully recombinant system, we have established a method for cyclin E ubiquitination by an SCF-Fbw7 complex. This system employs all components made in insect cells

or in bacteria. We are currently employing this system to examine the possibility that SCF-Fbw7 function requires that it be a dimeric complex. This system is reported in the **Methods in Enzymology** chapter on the identification of SCF substrates which is in press.

Key Research Accomplishments:

Year 1

*Development of a yeast system for identification of proteins whose stability is regulated by a specific ubiquitin ligase

*The use of a related system to identify F-box proteins involved in cyclin E turnover

*Demonstration that Fbw7 in mammalian cells controls cyclin E levels

Year 2

* Completed an analysis of F-box proteins in the human and mouse genomes, leading to the identification of 68 human and 70 mouse F-box proteins

* Cloned and sequenced 50 human F-box proteins. Each F-box protein was placed into mammalian expression plasmids, facilitating the discovery of substrates

*Identified β-TRCP as a candidate ubiquitin ligase for the breast cancer oncoprotein Cdc25A using a panel of F-box proteins that we identified and cloned, and published the results.

*Developed new retroviral vectors that can be used in a dual fluorescence system to identify ubiquitination targets in combination with RNAi-dependent gene ablation

*Determined the requirements for interaction of cyclin E with Fbw7 and demonstrated that cancer-prone mutations in Fbw7 loose binding with cyclin E phospho-degrons.

Year 3

Performed a systematic analysis of F-box proteins encoded by the human and mouse genomes and reported a systematic nomenclature for this family of proteins. This result led to the identification of similar destruction motifs in c-myc, c-jun, and SREBP, work that we published in collaboration with other labs (see papers listed below).

Completed an analysis of the requirements for recognition of cyclin E by the Fbw7 F-box protein and published the results.

Reportable outcomes.

Publications directly supported by this grant:

Koepp, D., Schaffer, L., Ye, X., Keyomarsi, K., Chu, C., Harper, J.W., and Elledge, S.J. (2001) Phosphorylation-dependent ubiquitination of cyclin E by a conserved SCF^{Fbw7} ubiquitin ligase. **Science** 294, 173-177.

Jin J, Shirogane T, Xu L, Nalepa G, Qin J, Elledge SJ, Harper JW. SCFbeta-TRCP links Chk1 signaling to degradation of the Cdc25A protein phosphatase. **Genes Dev**. 2003; 17: 3062-3074.

Ye, X., Nalepa, G., Welcker, M., Kessler, B., Spooner, E., Qin, J., Elledge, S.J., Clurman, B.E., and Harper, J.W. Recognition of phosphodegron motifs in human cyclin E by the SCFFbw7 ubiquitin ligase. **J. Biol. Chem**. 2004, 279: 50110-50119.

Jin, J., Cardozo, T., Elledge, S.J., Pagano, M., and Harper, J.W. (2004) Systematic analysis and nomenclature for mammalian F-box proteins. **Genes Dev**, 18: 2573-2580

Reviews and papers related to protein ubiquitination published by this lab during the last year:

Zheng, N., Schulman, B.A., Miller, J.J., Wang, P., Jeffrey, P.D., Chu, C., Koepp, D.M., Elledge, S.J., Pagano, M., Conaway, R.C., Conaway, J.W., Harper, J.W., and Pavletich, N.P. (2002) Structure of the Cul1–Rbx1–Skp1–F box^{Skp2} SCF Ubiquitin Ligase Complex. **Nature,** 416, 703-709.

Jin, J. and Harper, J.W. (2002) Ring-finger specificity in SCF driven protein degradation. **Developmental Cell** 2, 685-687.

Nalepa, G., and Harper, J.W. (2002) Efp: A ring of independence? **Nature Medicine**, 8,661-662.

Harper, J.W., Burton, J.L., and Solomon, M.J. (2002) The anaphase promoting complex: It's not just for mitosis anymore. **Genes and Development**, 16, 2179-2206.

Passmore, L., McCormack, E.A., Au, S.W.N., Paul, A., Willison, K.R., Harper, J.W., and Barford, D. (2003) Doc1/Apc10 mediates the E3 ubiquitin ligase activity of the anaphase promoting complex by contributing to APC-substrate recognition. **EMBO J.** 22, 786-796.

Wu, G., Schulman, B., Harper, J.W., and Pavletich, N. (2003) Structure of a β-TrCP1–Skp1–β-catenin complex: destruction-motif binding and lysine specificity of the SCF ubiquitin ligase. **Molecular Cell**, 11:1445-1456.

Jin, J., and Harper, J.W. (2003) A license to Kill: Transcriptional activation and enhanced turnover of Myc by the SCF^{Skp2} ubiquitin ligase. **Cancer Cell**, 3:517-518.

Harper, JW. Neddylating the guardian: Mdm2 catalyzed conjugation of Nedd8 to p53. **Cell** 2004; 188: 2-4.

Ang, XL and Harper, JW. Interwoven ubiquitination oscillators and control of cell cycle transitions. **Sci. STKE** 2004; 13, pe31.

Ang, XL and Harper, JW. SCF-mediated protein degradation and cell cycle control. **Oncogene**, 24, 2860-2870.

Passmore, L., Barford, D., and Harper, J.W. (2004) Purification and assay of the budding yeast anaphase promoting complex. **Methods in Enzymology**, in press.

Jin, J., Ang, XL, Shirogane, T., and Harper, J.W. (2004) Identification of substrates for F-box proteins. **Methods in Enzymology**, in press.

Sundqvist, A., Bengoechea-Alonso, M.T., Ye, X., Lukiyanchuk, V., Jin, J., Harper, J.W., Harper, J.W., and Ericsson, J. (2005) Control of lipid metabolism by phosphorylation-dependent degradation of the SREBP family of transcription factors by SCFFbw7. **Cell Metabolism** 1, 379-391.

Wei, W., Jin, J., Schlisio, S., Harper, J.W., and Kaelin, W.G., Jr. (2005) The v-Jun point mutation allows c-Jun to escapte GSK3-dependent recognition and destruction by the Fbw7 ubiquitin ligase. **Cancer Cell** 8, 25-33.

Welcker M, Orian A, Jin J, Grim JA, Harper JW, Eisenman RN, Clurman BE. The Fbw7 tumor suppressor regulates glycogen synthase kinase 3 phosphorylation-dependent c-Myc protein degradation. **Proc. Natl. Acad. Sci. U.S.A**. 2004; 101:9085-9090.

Invited seminars to discuss the outcome of work funded by this grant:

Control of cell cycle transitions by the SCF ubiquitin ligase. The Cell Cycle, Cold Spring Harbor Laboratory, May 16, 2002

Protein ubiquitination and control of cell division. Division of Medical Oncology, University of Colorado Health Science Center, Denver, CO, July 15, 2002.

Control of cell division by protein phosphorylation and ubiquitin mediated proteolysis. Department of Pathology, Harvard Medical School, September 18, 2002.

Control of cell division by protein phosphorylation and ubiquitin mediated proteolysis. Fred Hutchison Cancer Research Center, November 12, 2002.

Novel targets upstream of the proteasome. Continuing Medical Education Program on Novel Anticancer Agents in the Proteasome Pathway, American Society of Hematology, Philadelphia, PA, December 6, 2002.

Substrate recognition by Cullin-based ubiquitin ligases. NCI Workshop of Ubiquitin Pathways, Rockville MD, December 8, 2002.

The SCF ubiquitin ligase pathway, University of Chicago, February 19, 2003

Substrate specificity of cullin-based ubiquitin ligases, Cold Spring Harbor Laboratory, The ubiquitin Family meeting, April 24, 2003

The ubiquitin-Proteasome Pathway, Karolinska Institute/Baylor College of Medicine Symposium, May 12, 2003

FASEB Symposium, *Ubiquitination and Cellular Regulation* June, 2004

Vallee Foundation Symposium, May 2004

AACR Symposium, *Cell Cycle Regulation* December, 2004

AACR National Meeting, Chair of the *Ubiquitin System in Cancer Symposium*, April 2005

Cold Spring Harbor, *The Ubiquitin Family* May, 2005

Funding applied for using preliminary data from this grant:

National Institutes of Health, R01 – "Functional anatomy of cullin-3 ubiquitin ligases"; Funded in 2004.

National Institutes of Health, R01 – "Transcriptional and post-translational control of the Cdc25A protein"; Funded in 2005.

Employment/Research Opportunities impacted by the grant:

I was recruited to Harvard Medical School to join the Department of Pathology as the Bert and Natalie Vallee Professor of Molecular Pathology, a position I will assume on August 1, 2003. Our research funded by the grant contributed significantly to this recruitment.

Conclusion

The SCF pathway is widely used to control the levels of regulatory proteins. We are using multiple systems – both biochemical and genetic – to identify ubiquitin ligases for important cell cycle regulators as well as to identify substrates of particular ubiquitin ligases. The new system we are developing to identify substrates has the potential to help uncover numerous proteins whose levels are controlled by the ubiquitin pathway and may be involved in the genesis of breast cancer.

References

Bai, C., P. Sen, N. Mathias, K. Hofmann, M. Goebl, J.W. Harper, and S.J. Elledge. 1996. SKP1 connects cell cycle regulation to the ubiquitin proteolysis machinery through a novel motif, the F-box. *Cell*, **86**: 263-274.

Cangi MG, Cukor B, Soung P, Signoretti S, Moreira G Jr, Ranashinge M, Cady B, Pagano M, Loda M. 2000. Role of the Cdc25A phosphatase in human breast cancer. J Clin Invest. 106:753-761.

Evans KL. 2000. Overexpression of CDC25A associated with poor prognosis in breast cancer. Mol Med Today. 2000 6:459.

Hershko, A., and A. Ciechanover. 1998. The ubiquitin system. *Annu Rev Biochem* **67**: 425-479.

Kamura, T., D.M. Koepp, M.N. Conrad, D. Skowyra, R.J. Moreland, O. Iliopoulos, W.S. Lane, W.G. Kaelin Jr., S.J. Elledge, R.C. Conaway, J.W. Harper, and J.W. Conaway. 1999. Rbx1, a component of the VHL tumor suppressor complex and SCF ubiquitin ligase. *Science* **284**: 657-661.

Koepp, D.M., J.W. Harper, and S.J. Elledge. 1999. How the cyclin became a cyclin: regulated proteolysis in the cell cycle. *Cell* **97**: 431-434.

Koepp DM, Schaefer LK, Ye X, Keyomarsi K, Chu C, Harper JW, Elledge SJ. 2001. Phosphorylation-dependent ubiquitination of cyclin E by the SCFFbw7 ubiquitin ligase. Science 294:173-177.

Lorick, K.L., Jensen, J.P., Fang, S., Ong, A.M., Hatakeyama, S. and Weissman, A. 1999. RING fingers mediate ubiquitin-conjugating enzyme (E2)-dependent ubiquitination *PNAS* 96: 11364-11369.

Liu Q, Li MZ, Leibham D, Cortez D, Elledge SJ. 1998. The univector plasmid-fusion system, a method for rapid construction of recombinant DNA without restriction enzymes. *Curr Biol* 8:1300-1309.

Maniatis, T. 1999. A ubiquitin ligase complex essential for the NF-kappaB, Wnt/Wingless, and Hedgehog signaling pathways. *Genes Dev* **13**: 505-510.

Moberg KH, Bell DW, Wahrer DC, Haber DA, Hariharan IK. Archipelago regulates Cyclin E levels in Drosophila and is mutated in human cancer cell lines. Nature. 2001 413:311-6.

Patton, E.E., A.R. Willems, and M. Tyers. 1998. Combinatorial control in ubiquitin-dependent proteolysis: don't Skp the F-box hypothesis. *Trends Genet.* **14**: 236-243.

Skowyra, D., K. Craig, M. Tyers, S.J. Elledge, and J.W. Harper. 1997. F-box proteins are components of E3 complexes and act as receptors to recruit phosphorylated substrates for ubiquitination. *Cell* **91**: 209-219.

Skowyra, D., D.M. Koepp, T. Kamura, M.N. Conrad, R.C. Conaway, J.W. Conaway, S.J. Elledge, and J.W. Harper. 1999. Reconstitution of G1 cyclin ubiquitination with complexes containing SCFGrr1 and Rbx1. *Science* **284**: 662-665.

Spruck CH, Strohmaier H, Sangfelt O, Muller HM, Hubalek M, Muller-Holzner E, Marth C, Widschwendter M, Reed SI. hCDC4 gene mutations in endometrial cancer. Cancer Res. 2002 62:4535-9.

Winston, J.T., P. Strack, P. Beer-Romero, C.Y. Chu, S.J. Elledge, and J.W. Harper. 1999b. The SCFbeta-TRCP-ubiquitin ligase complex associates specifically with phosphorylated destruction motifs in IkappaBalpha and beta-catenin and stimulates IkappaBalpha ubiquitination in vitro. *Genes Dev* **13**:270-283.

Winston, J.T., D.M. Keopp, C. Zhu, S.J. Elledge, and J.W. Harper. 1999a. A family of mammalian F-box proteins. *Current Biology*, 9, 1180-1182.

$SCF^{\beta\text{-}TRCP}$ links Chk1 signaling to degradation of the Cdc25A protein phosphatase

Jianping Jin,[1] Takahiro Shirogane,[1] Lai Xu,[1] Grzegorz Nalepa,[1,3] Jun Qin,[3] Stephen J. Elledge,[2] and J. Wade Harper[1,4]

[1]Department of Pathology and [2]Center for Genetics and Genomics, Department of Genetics, Howard Hughes Medical Institute, Harvard Medical School, Boston, Massachusetts 02115, USA; [3]Verna and Marrs McLean Department of Biochemistry and Molecular Biology, Program in Cell and Molecular Biology, Baylor College of Medicine, Houston, Texas 77030, USA

Eukaryotic cells respond to DNA damage and stalled replication forks by activating protein kinase-mediated signaling pathways that promote cell cycle arrest and DNA repair. A central target of the cell cycle arrest program is the Cdc25A protein phosphatase. Cdc25A is required for S-phase entry and dephosphorylates tyrosine-15 phosphorylated Cdk1 (Cdc2) and Cdk2, positive regulators of cell division. Cdc25A is unstable during S-phase and is degraded through the ubiquitin–proteasome pathway, but its turnover is enhanced in response to DNA damage. Although basal and DNA-damage-induced turnover depends on the ATM-Chk2 and ATR-Chk1 pathways, how these kinases engage the ubiquitin ligase machinery is unknown. Here, we demonstrate a requirement for $SCF^{\beta\text{-}TRCP}$ in Cdc25A turnover during an unperturbed cell cycle and in response to DNA damage. Depletion of β-TRCP stabilizes Cdc25A, leading to hyperactive Cdk2 activity. $SCF^{\beta\text{-}TRCP}$ promotes Chk1-dependent Cdc25A ubiquitination in vitro, and this involves serine 76, a known Chk1 phosphorylation site. However, recognition of Cdc25A by β-TRCP occurs via a noncanonical phosphodegron in Cdc25A containing phosphoserine 79 and phosphoserine 82, sites that are not targeted by Chk1. These data indicate that Cdc25A turnover is more complex than previously appreciated and suggest roles for an additional kinase(s) in Chk1-dependent Cdc25A turnover.

[*Keywords*:]

Received October 2, 2003; revised version accepted November 10, 2003.

In response to DNA damage and DNA replication interference, cells activate an elaborate network of signaling pathways collectively called the DNA damage stress response pathway (Zhou and Elledge 2000). The central conduits of this network are two parallel but partially overlapping protein kinase cascades, the ATM-Chk2 and ATR-Chk1 kinase modules, that transduce the damage signal to downstream effectors involved in cell cycle control, DNA repair, and apoptosis (Zhou and Elledge 2000; Shiloh 2003). ATM primarily responds to DNA double-strand breaks, whereas ATR responds to agents that interfere with DNA replication in addition to double-strand breaks (Zou and Elledge 2003).

The branches of these pathways used in arresting the cell cycle are called checkpoints. In many eukaryotes, the targets of checkpoint pathways are the cyclin-dependent kinases, Cdks, which control multiple cell cycle transitions including the G_1/S transition, late origin firing during S phase, and the G_2/M transition, each of which is inhibited in response to DNA damage. Cells have evolved multiple mechanisms to inhibit Cdk activity. In mammals, the Cdk inhibitor $p21^{Cip1}$ is induced in response to DNA damage through activation of the p53 transcription factor, which is activated and stabilized in response to DNA damage (Giaccia and Kastan 1998; Zhou and Elledge 2000). In addition, levels of cyclin D1 rapidly decrease in response to DNA damage during G_1, leading to redistribution of $p21^{Cip1}$ from Cdk4 to Cdk2 (Agami and Bernards 2000). Cdks are also regulated by inhibitory phosphorylation on tyrosine, which is altered in response to DNA damage (Jin et al. 1997; Rhind et al. 1997; for review, see Takizawa and Morgan 2000; Donzelli and Draetta 2003).

The regulatory mechanisms controlling Cdk phosphorylation have been extensively studied. Tyrosine phosphorylation is regulated by the opposing activities of the tyrosine kinases Wee1 and Myt1, and a group of tyrosine phosphatases known as Cdc25A, Cdc25B, Cdc25C (for review, see Morgan 1997). A direct connec-

[4]Corresponding author.
E-MAIL wade_harper@hms.harvard.edu; FAX (617) 432-2882.
Article published online ahead of print. Article and publication date are at http://www.genesdev.org/cgi/doi/10.1101/gad.1157503.

tion between checkpoint signaling and Cdc25 was established when it was found that the checkpoint kinase Chk1, and later Chk2, could phosphorylate Cdc25C on a site relevant to its checkpoint function in vivo (Peng et al. 1996; Sanchez et al. 1996; Furnari et al. 1997; Matsuoka et al. 1998). Furthermore, these kinases were shown to phosphorylate all three Cdc25 family members, suggesting they were general targets of DNA damage stress response pathways (Sanchez et al. 1996; Matsuoka et al. 1998). Analysis of Chk regulation of Cdc25 from several systems showed that phosphorylation of Cdc25C both inhibited kinase activity (Blasina et al. 1999; Furnari et al. 1999) and maintained Cdc25C in the cytoplasm, where it cannot access Cdk/cyclin complexes efficiently (Zeng et al. 1998; Kumagai and Dunphy 1999; Lopez-Girona et al. 1999; Zeng and Piwnica-Worms 1999). However, mice lacking Cdc25C grow normally and have intact checkpoint responses (Chen et al. 2001), suggesting that other family members may play more prominent roles in Cdk regulation.

A second family member implicated in the damage response is Cdc25A. Cdc25A is capable of removing inhibitory tyrosine phosphorylation from both Cdk1 and Cdk2 kinases to promote entry into and progression through S phase and mitosis (Hoffmann et al. 1994; Vigo et al. 1999; for review, see Donzelli and Draetta 2003). Cdc25A has also been shown to be a phosphorylation target of Chk kinases (Sanchez et al. 1996) and to be regulated by Chk kinases in response to DNA damage (for review, see Donzelli and Draetta 2003). In contrast to regulation of Cdc25C, Cdc25A is destroyed in response to ionizing radiation (IR) and ultraviolet (UV) light through a process involving ubiquitin-mediated proteolysis. During G_1, UV treatment leads to Chk1-dependent elimination of Cdc25A (Mailand et al. 2000) and persistent Cdk2 Y15 phosphorylation. During an unperturbed S phase, Cdc25A is unstable and this instability requires Cdc25A phosphorylation by Chk1 (Falck et al. 2001; Sorensen et al. 2003). IR during S phase leads to accelerated Cdc25A phosphorylation by Chk1 with a concomitant increase in turnover. Defects in this intra-S-phase checkpoint lead to radio-resistant DNA synthesis (RDS; Falck et al. 2001; Xiao et al. 2003). Whereas depletion of Chk1 leads to an RDS phenotype, expression of a Cdk2 mutant that is resistant to inhibitory tyrosine phosphorylation overcomes IR-dependent S-phase arrest (Falck et al. 2001), implicating elimination of Cdc25A in the intra-S-phase checkpoint.

Recent studies indicate that Cdc25A turnover through the ubiquitin pathway involves at least two temporally distinct components (Donzelli et al. 2002; Donzelli and Draetta 2003). During mitotic exit and early G_1, Cdc25A stability is controlled by the anaphase-promoting complex in conjunction with Cdh1. During interphase, however, Cdc25A turnover is dependent on Cul1 (Donzelli et al. 2002), a central component of the SCF (Skp1/Cul1/F-box protein) ubiquitin ligase (Feldman et al. 1997; Skowyra et al. 1997). Precisely how Cul1 promotes turnover of Cdc25A is unknown. In SCF complexes, Cul1 together with the RING-H2 finger protein Rbx1 forms the core ubiquitin ligase that binds ubiquitin-conjugating enzymes (Deshaies 1999; for review, see Koepp et al. 1999). Specificity in these reactions is achieved by a substrate-binding module composed of Skp1 and a member of the F-box family of proteins. F-box proteins interact with Skp1 through the F-box motif (Bai et al. 1996) and with substrates through C-terminal protein interaction domains, including WD40 propellers (Skowyra et al. 1997; Gu et al. 2003; Orlicky et al. 2003). Frequently, association of SCF targets with the requisite F-box protein requires that the substrate be modified, typically by phosphorylation to produce a short peptide motif displaying properties of a phosphodegron (Winston et al. 1999a; Koepp et al. 2001; Nash et al. 2001; Gu et al. 2003; Orlicky et al. 2003).

Here we report that constitutive and DNA-damage-induced turnover of Cdc25A occurs via the $SCF^{\beta\text{-TRCP}}$ ubiquitin ligase. Depletion of β-TRCP by shRNA stabilizes Cdc25A, leading to inappropriately high levels of Cdk2 kinase activity characteristic of a checkpoint defect. Cdc25A ubiquitination by $SCF^{\beta\text{-TRCP}}$ in vitro involves Chk1-dependent phosphorylation principally at S76, consistent with the requirement for Chk1 in vivo. However, Chk1-mediated phosphorylation of Cdc25A does not appear to be sufficient to generate the requisite phosphodegron for β-TRCP recruitment. We find that residues 79–84 of Cdc25A constitute a phosphodegron for recognition by β-TRCP and implicate S79 and S82 as phosphoacceptor sites in this motif. Indeed, S82 is in a sequence context (Asp–Ser–Gly–Phe) reminiscent of previously identified phosphodegrons in the β-TRCP substrates IκBα and β-catenin. We suggest that Chk1-mediated phosphorylation of S75 may promote Cdc25A turnover by facilitating the phosphorylation of the adjacent phosphodegron targeted by β-TRCP.

Results

Involvement of the SCF pathway in DNA-damage-induced Cdc25A turnover

The precise pathways involved in interphase and DNA-damage-mediated turnover of Cdc25A and the role of phosphorylation in this process are unknown. To address these issues, we examined whether DNA-damage-dependent elimination of Cdc25A, like its interphase counterpart, is also involved in the SCF pathway. Cells were transiently transfected with a vector expressing a dominant-negative version of Cul1, $Cul1^{DN}$, which binds to Skp1 but does not associate with the essential ring-finger protein Rbx1 (Donzelli et al. 2002). As expected, $Cul1^{DN}$ expression resulted in accumulation of Cdc25A, as well as other SCF substrates including p27 and cyclin E, in the absence of DNA damage (Fig. 1A). In control transfected cells, ionizing radiation (IR) induced a time-dependent decrease in the abundance of Cdc25A (Fig. 1B, lanes 1–4). However, expression of $Cul1^{DN}$ led to increased Cdc25A abundance throughout the time course (Fig. 1B, lanes 5–8), implicating an SCF-like complex in Cdc25A turnover in response to DNA damage, as well as during

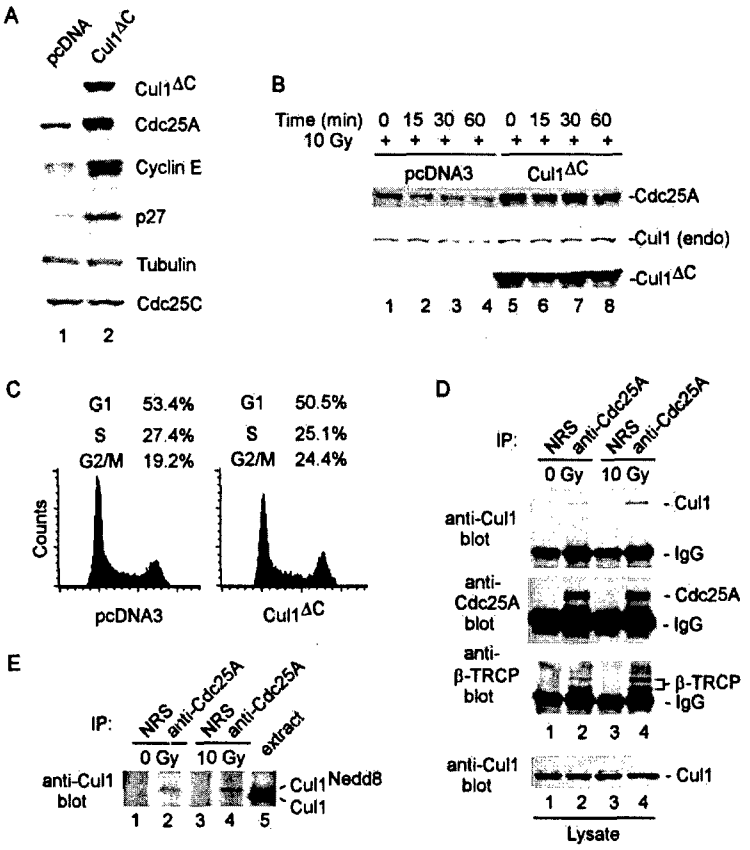

Figure 1. In vivo association of Cdc25A with the $SCF^{\beta\text{-}TRCP}$ ubiquitin ligase. (*A*) Disruption of the Cul1 ubiquitin ligase pathway leads to accumulation of Cdc25A. 293T cells were transfected with vectors expressing an N-terminal fragment of Cul1 (residues 1–452; $Cul1^{DN}$) or empty vector (3 μg) and after 48 h, lysates were subjected to immunoblotting with the indicated antibodies. (*B*) Disruption of the Cul1 pathway blocks DNA-damage-dependent elimination of Cdc25A. 293T cells were transfected with 3 μg of pCMV-$Cul1^{DN}$ or empty vector subjected to ionizing radiation (10 Gy) prior to analysis of total Cdc25A by immunoblotting. (*C*) Effect of $Cul1^{DN}$ on cell cycle control. 293T cells were collected 48 h after transfection with either pcDNA3 or pcDNA3-Cul1DN as described in *B* and then subjected to flow cytometry after staining with propidium iodide. (*D*) Cdc25A associates with endogenous Cul1 and β-TRCP in the presence and absence of DNA damage. 293T cells were treated with IR (10 Gy). Then, 30 min later, cells were lysed and Cdc25A immune complexes were prepared from 1 mg of extract prior to immunoblotting for Cul1. The blot was stripped and reprobed for β-TRCP. The relative levels of Cdc25A, Cul1, and β-TRCP were determined by densitometry. After normalizing for a small (17%) increase in the amount of Cdc25A in the presence of damage, we determined a 1.85- and 2.5-fold increase in Cdc25A-associated β-TRCP and Cul1 levels in response to DNA damage. (*E*) Cdc25A associates specifically with the neddylated and activated form of Cul1. Immune complexes were prepared as in *C* and subjected to electrophoresis together with crude extract (25 μg) to visualize the position of neddylated and unneddylated Cul1. As expected, neddylated Cul1 represents ~5% of the total Cul1 present in crude extracts.

interphase. Flow cytometry (Fig. 1C) indicated that, under these conditions, expression of $Cul1^{DN}$ has only a minor influence on the cell cycle distribution in these cells. Thus, the dramatic stabilization of Cdc25A by $Cul1^{DN}$ does not appear to be caused by an indirect effect of cell cycle position.

We next examined association of Cdc25A with Cul1 in the presence and absence of DNA damage. Consistent with previous studies (Donzelli et al. 2002), endogenous Cdc25A was found to associate with endogenous Cul1 in the absence of DNA damage (Fig. 1D, lane 2). Moreover, Cdc25A was also associated with Cul1 in the presence of IR (10 Gy), and quantification of the blot indicated an ~twofold increase in the quantity of Cdc25A-associated Cul1 (relative to Cdc25A levels) in the presence of DNA damage (Fig. 1D, lane 4). Importantly, Cdc25A was associated exclusively with the neddylated, and therefore potentially activated, form of Cul1 (Fig. 1E).

The β-TRCP F-box protein specifically associates with Cdc25A

Substrate specificity in SCF-driven ubiquitination reactions is controlled by the identity of the F-box protein (Bai et al. 1996). To search for F-box proteins involved in Cdc25A ubiquitination, we cloned and expressed 18 of the 70 known human F-box proteins (Winston et al. 1999b; J. Jin and J.W. Harper, unpubl.) as Myc-tagged protein fusions (Fig. 2). These F-box protein expression plasmids were then individually cotransfected with vectors expressing either GST-Cdc25A or GST as a negative control. F-box proteins associating with GST-Cdc25A were identified by immunoblotting. Two WD40-containing F-box proteins—β-TRCP1 and β-TRCP2—were found to bind efficiently to GST-Cdc25A but not GST alone, and this binding occurred independently of addition of exogenous DNA damaging agents (Fig. 2, lanes 3,5). β-TRCP proteins are derived from distinct genes, yet are closely related in sequence and appear to interact with identical phosphodegrons in several ubiquitinated targets, including β-catenin, IκBα, and Emi1 (Hart et al. 1999; Latres et al. 1999; Winston et al. 1999a; Guardavaccaro et al. 2003). Using previously characterized antibodies that react with both β-TRCP1 and β-TRCP2 (Spiegelman et al. 2000), we found that β-TRCP is present in Cdc25A immune complexes and that the association is enhanced ~twofold in the presence of ionizing irradiation (Fig. 1D, lanes 2,4). These data suggest a pos-

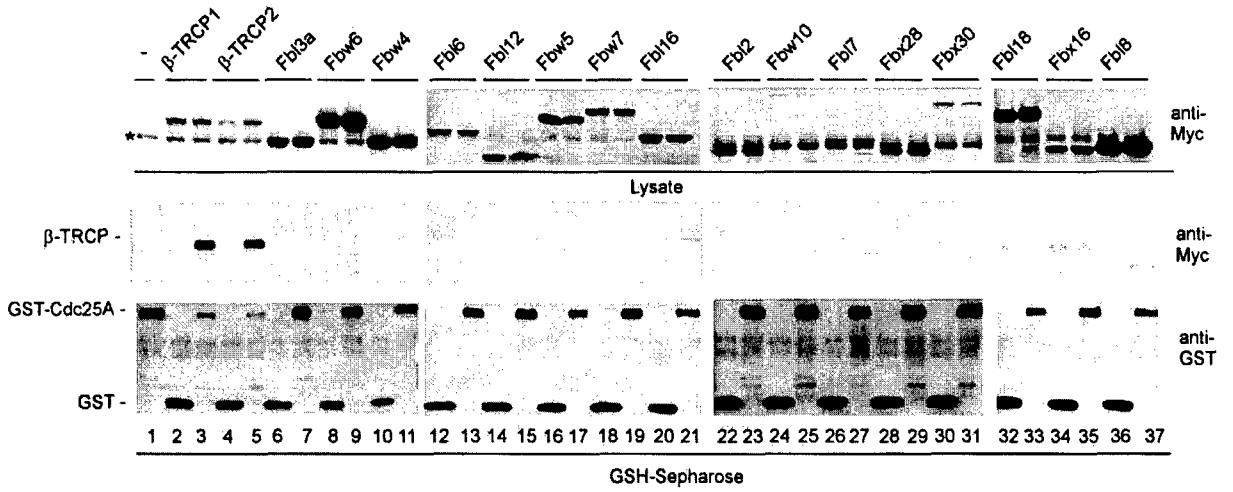

Figure 2. Screening a panel of F-box proteins for association with Cdc25A reveals specific association with β-TRCP1 and β-TRCP2. Cdc25A associates with β-TRCP1 and β-TRCP2. Vectors expressing the indicated Myc-tagged F-box proteins (1 μg) were cotransfected into 293T cells (2-cm dish) with either pCMV-GST or pCMV-GST-Cdc25A (1 μg) and association with GST-Cdc25A determined 48 h later after purification of GSH-Sepharose. A band cross reacting with anti-Myc antibodies in crude extracts is indicated by the asterisk.

sible regulatory connection between β-TRCP and Cdc25A turnover.

Linkage of β-TRCP with elimination of Cdc25A in the presence and absence of DNA damage

We next examined whether expression of β-TRCP can promote Cdc25A ubiquitination in tissue culture cells. 293T cells were transiently transfected with vectors expressing HA-Cdc25A, β-TRCP1, and/or His_6-tagged ubiquitin. After 36 h, guanidine-denatured extracts were subjected to Ni-NTA purification, and bound proteins were immunoblotted with anti-HA antibodies. β-TRCP1 dramatically promoted the formation of high-molecular-weight Cdc25A/His_6-Ub conjugates, when compared with those produced in the absence of exogenous β-TRCP (Fig. 3A, lanes 1,2). Immunoblotting for total Cdc25A in crude cell lysates indicated reduced levels of Cdc25A in cells expressing β-TRCP, when compared with control cell lysates (Fig. 3A, lower panels). Thus, the increased abundance of Cdc25A-ubiquitin conjugates is not a reflection of higher levels of total Cdc25A in this experiment. A similar dramatic reduction in the levels of Cdc25A was also seen when higher quantities of pCMV-β-TRCP were used (Fig. 2, lanes 3,5). None of the other 16 F-box proteins tested displayed an ability to reduce steady-state Cdc25A levels when coexpressed, indicating a high degree of specificity for β-TRCP in this regard.

To examine whether β-TRCP is required for Cdc25A turnover, we initially examined the effects of a dominant negative β-TRCP protein lacking the F-box motif. 293T cells were transfected with vectors expressing β-$TRCP^{\Delta F\text{-}box}$ or $Skp2^{\Delta F\text{-}box}$ as a negative control and then subjected to irradiation (Fig. 3B,C). In this experiment, a modified SDS-PAGE system was used to enhance the separation of phosphorylated and unphosphorylated forms of Cdc25A seen previously (Zhao et al. 2002; Materials and Methods). Cdc25A was eliminated in cells expressing $Skp2^{\Delta F\text{-}box}$ at a rate similar to that found with vector-only control cells (Fig. 3B, lanes 1–3, 7–9), while the levels of Cul1 used as a loading control were constant. In contrast, the levels of the more slowly migrating phosphorylated forms of Cdc25A were elevated in cells expressing β-$TRCP^{\Delta F\text{-}box}$ both in the absence of irradiation and throughout the time course after DNA damage (Fig. 3B, lanes 4–6), suggesting that β-TRCP is important for turnover of Cdc25A in response to its phosphorylation. Rapid turnover of the more rapidly migrating Cdc25A isoforms in this experiment likely reflects a population of cells that did not receive the β-$TRCP^{\Delta F\text{-}box}$ plasmid, as the efficiency of transfection under these conditions is <80% (data not shown). The levels of dominant-negative β-TRCP and Skp2 were maintained throughout the time course (Fig. 3C).

To extend these results, we used vectors expressing shRNA against β-TRCP proteins. The targeting sequence used represents a sequence fully conserved in both β-TRCP1 and β-TRCP2 and has been demonstrated to effectively knock down expression of both isoforms (Fong and Sun 2002), a result confirmed here in 293T and HCT116 cells (Fig. 3D). Expression of β-TRCP shRNA in both 293T and HCT116 cells resulted in accumulation of Cdc25A both in unirradiated cells (Fig. 3E, lane 2) and in cells exposed to IR (lane 4), when compared with control cells expressing shRNA against GFP (lanes 1,3). These data are consistent with a role for β-TRCP in Cdc25A turnover.

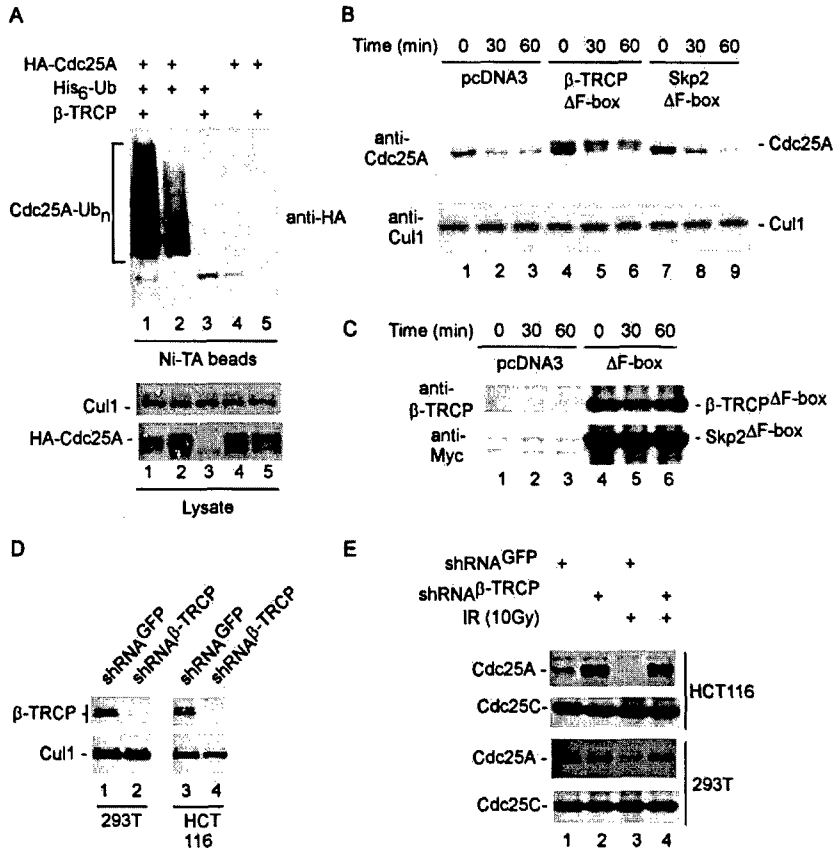

Figure 3. Linkage of β-TRCP to elimination of Cdc25A in the presence and absence of DNA damage. (*A*) Expression of β-TRCP promotes Cdc25A ubiquitination in vivo. 293T cells in 6-cm dishes were transfected with vectors expressing HA-Cdc25A (2 μg), β-TRCP1 (1 μg), and/or His_6-Ub (4 μg). After 36 h, cells were lysed in buffers containing 6 M guanidinium-HCl and His_6-Ub tagged proteins purified on Ni-NTA beads. Proteins were separated by SDS-PAGE and immunoblotted with anti-HA antibodies. Cells from a parallel transfection were lysed using conventional NP-40-containing buffers (see Materials and Methods) and extracts subjected to immunoblotting (*lower* panels) using anti-HA to determine the total abundance of HA-Cdc25A and anti-Cul1 as a loading control. (*B,C*) Accumulation of Cdc25A after DNA damage in the presence of dominant-negative β-TRCP1. 293T cells in 10-cm dishes were transfected with 5 μg of pCMV, pCMV-β-$TRCP^{\Delta F\text{-box}}$, and pCMV-$Skp2^{\Delta F\text{-box}}$. After 48 h, cells were subjected to IR (10 Gy) and lysates were examined by immunoblotting (panel *A*) at the indicated times with anti-Cdc25A and anti-Cul1 antibodies as a loading control. For analysis of Cdc25A, extracts were subjected to a modified SDS-PAGE procedure that provides larger separation of phosphoryated forms of Cdc25A seen previously (Zhao et al. 2002). The expression of β-$TRCP^{\Delta F\text{-box}}$ and $Skp2^{\Delta F\text{-box}}$ was confirmed by immunoblotting (panel *C*). (*D,E*) Knock-down of β-TRCP by shRNA blocks constitutive and DNA-damage-dependent elimination of Cdc25A. The indicated cells were infected with a single retroviruses expressing shRNA targeting both β-TRCP1 and β-TRCP2 as well a retrovirus expressing shRNA against GFP as a negative control. Then, 48 h later, cells were lysed prior to analysis of β-TRCP and Cul1 levels by immunoblotting (panel *D*; see Materials and Methods). (*E*) shRNA-expressing cells were either subjected to ionizing radiation (10 Gy) or left untreated. Cells were lysed 30 min later and 25 μg of extract was subjected to immunoblotting with anti-Cdc25A antibodies. Blots were reprobed with anti-Cdc25C as a loading control.

Depletion of β-TRCP stabilizes Cdc25A and increases cyclin E/Cdk2 activity in the presence and absence of DNA damage

To examine Cdc25A turnover directly, we determined Cdc25A levels in the presence of cyclohexamide with or without depletion of β-TRCP by shRNA and in the presence or absence of DNA damage (Fig. 4A). In 293T cells expressing a control shRNA in the presence or absence of DNA damage, Cdc25A was eliminated with an apparent half-life of 30 min or less (Fig. 4A, lanes 1–8; Fig. 4B). As expected, DNA damage accelerated Cdc25A turnover. In contrast, Cdc25A was dramatically stabilized upon depletion of β-TRCP in both the presence and absence of DNA damage, with an apparent half-life of ~90 min (Fig. 4A, lanes 1–8; Fig. 4B). In addition, the total abundance of Cdc25A was greatly elevated by depletion of β-TRCP, when compared with Cul1 used as a loading control (Fig. 4A, lanes 1–8 vs. lanes 9–16). One explanation for altered Cdc25A turnover is that β-TRCP depletion leads to cell cycle arrest at a point in the cell cycle where Cdc25A is more stable. To examine this possibility, cells from the experiment shown in Figure 4A were processed for flow cytometry in parallel. As shown in Figure 4C, β-TRCP depletion had a negligible effect on the cell cycle distribution of 293T cells when compared with control cells expressing $shRNA^{GFP}$. Thus, β-TRCP is required for Cdc25A turnover in the presence and absence of DNA damage.

Previous studies have demonstrated that depletion of Chk1 leads to increased abundance of Cdc25A with a concomitant increase in the activity of cyclin E/Cdk2, reflecting inappropriate dephosphorylation of Y15 by Cdc25A (Falck et al. 2001; Sorensen et al. 2003). Consistent with this, we find that depletion of β-TRCP leads to increased levels of cyclin E associated kinase activity in both the presence and absence of DNA damage, while the total level of cyclin E-associated Cdk2 is unaffected (Fig. 4D). These data are consistent with a role for both Chk1 and β-TRCP in controlling Cdc25A and cyclin E/Cdk2 activity.

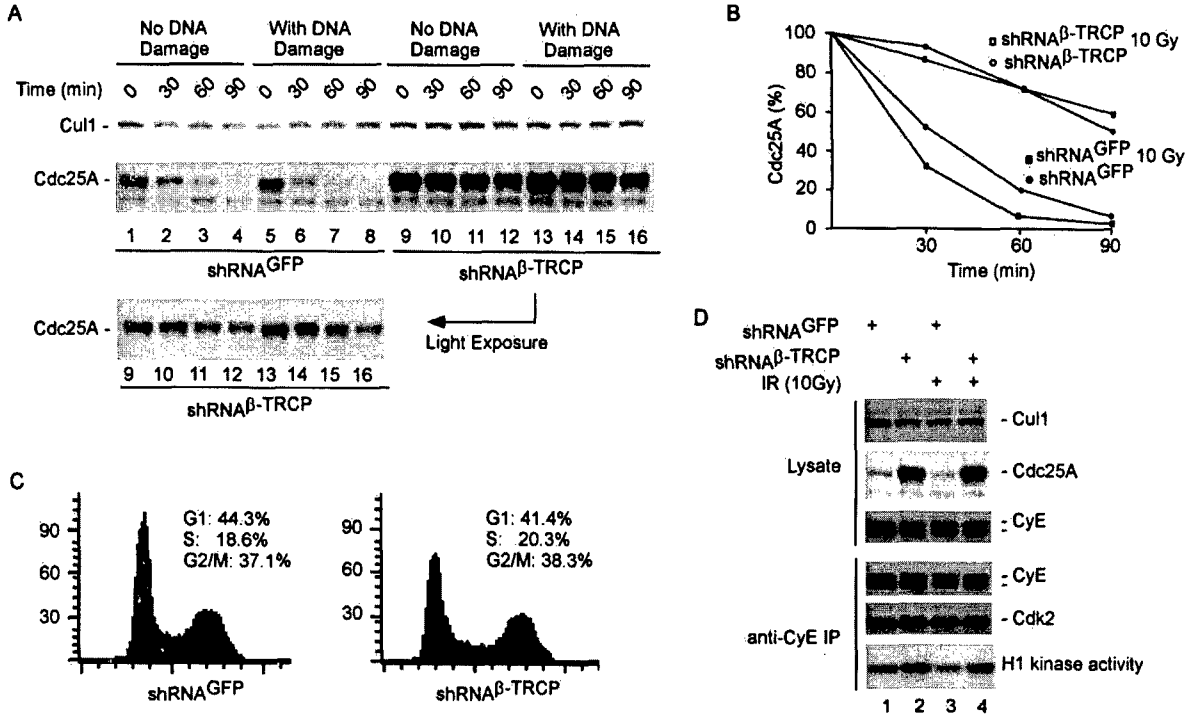

Figure 4. Stabilization of Cdc25A by depletion of β-TRCP in the presence or absence of DNA damage leads to deregulated cyclin E/Cdk2 activity. (*A*,*B*) Turnover of Cdc25A requires β-TRCP. 293T cells were transfected with pSUPER-shRNA^{GFP} or pSUPER-shRNA$^{β\text{-}TRCP}$ using lipofectamine 48 h after dual transfection and then either left untreated or subjected to DNA damage (10 Gy). Translation was immediately blocked by addition of cyclohexamide, and cells lysed at the indicated time points prior to SDS-PAGE. (*F*) Blots were probed with anti-Cdc25A, stripped, and reprobed with anti-Cul1 antibodies. (*G*) Blots of comparable intensity for shRNA^{GFP} and shRNA$^{β\text{-}TRCP}$ were quantified by densitometry. (*C*) Depletion of β-TRCP does not alter cell cycle progression. Cells from *A* were subjected to flow cytometry after staining with propidium iodide. (*D*) Increased cyclin E/Cdk2 kinase activity in cells depleted of β-TRCP. 293T cells were transfected with vectors expressing shRNA against GFP as control or β-TRCP using the dual-transfection protocol. After 48 h, cells were lysed and cyclin E immune complexes assayed for activity using histone H1 as a substrate. Cyclin E immune complexes were generated using a rabbit polyclonal antibody (C-19 from Santa Cruz Biotechnology). Parallel immunoblots were probed for Cdk2 and cyclin E to demonstrate equal loading. The cyclin E immunoblot was probed with a monoclonal antibody (HE12, Santa Cruz Biotechnology). Controls demonstrated a dramatic accumulation of Cdc25A in response to depletion of β-TRCP whereas Cul1 levels remained unchanged.

Chk1-dependent Cdc25A ubiquitination by SCF$^{β\text{-}TRCP}$ in vitro

We next asked whether SCF$^{β\text{-}TRCP1}$ can function as a ubiquitin ligase for Cdc25A in vitro and whether this required phosphorylation of Cdc25A by Chk1. SCF$^{β\text{-}TRCP1}$ complexes were assembled by translation of β-TRCP1 in reticulocyte extracts. Such complexes have been shown to be proficient in ubiquitination of IκBα (Wu et al. 2003). SCF$^{β\text{-}TRCP1}$ complexes were then supplemented with E1, Ubc5, ubiquitin, ATP, and ^{35}S-methionine-labeled Cdc25A added in the presence of wild-type or kinase-dead (KD) Chk1 (Fig. 5A). Cdc25A formed high-molecular-weight products in the presence of wild-type Chk1 (Fig. 5A, lane 2) but not in the presence of Chk1^{KD} or samples lacking kinase (lanes 1,3), and this correlated with a shift in the mobility of Cdc25A in the presence of Chk1 indicative of phosphorylation (lane 2). Although β-TRCP2 was also capable of promoting Chk1-dependent Cdc25 ubiquitination, three other WD40-containing F-box proteins present at equivalent levels (Fbw5, Fbw6, and Fbw7) failed to promote Cdc25A ubiquitination, demonstrating specificity for β-TRCP proteins (Fig. 5B). Addition of the polyubiquitin chain terminator methyl ubiquitin led to the generation of shorter conjugates, demonstrating that the formation of high-molecular-weight Cdc25A species reflected ubiquitination (Fig. 5C). Taken together, these data indicate Cdc25A can be ubiquitinated by SCF$^{β\text{-}TRCP}$ and this process is dependent on Cdc25A phosphorylation by Chk1.

Role of Chk1-dependent phosphorylation in Cdc25A ubiquitination by SCF$^{β\text{-}TRCP}$

Given that Chk1 promotes Cdc25A turnover in response to DNA damage in vivo (Falck et al. 2001; Sorensen et al. 2003) and that Chk1 is required for Cdc25A ubiquitination by SCF$^{β\text{-}TRCP}$ in vitro, we explored the role of Cdc25A phosphorylation in the ubiquitination process. Chk1 is known to phosphorylate Cdc25A on at least five

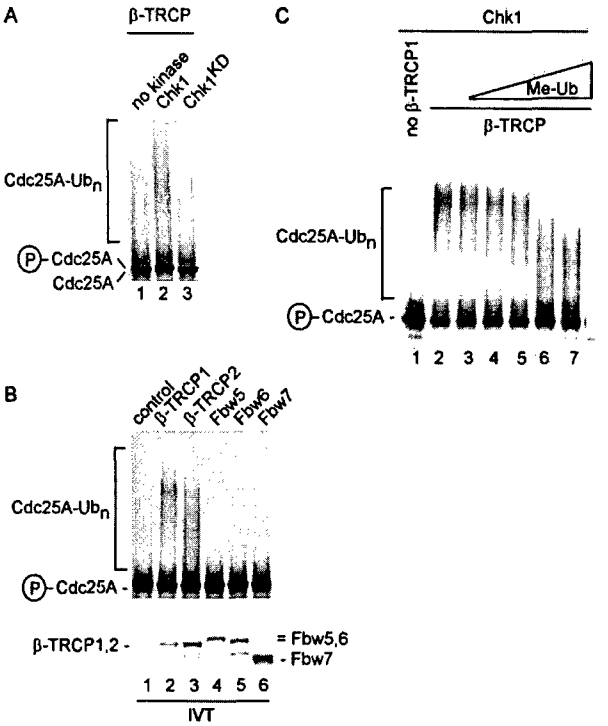

Figure 5. Chk1-dependent ubiquitination of Cdc25A by $SCF^{\beta\text{-}TRCP}$ in vitro. (*A*) Activation of Cdc25A ubiquitination by $SCF^{\beta\text{-}TRCP}$ requires active Chk1. In vitro translated and ^{35}S-methionine-labeled Cdc25A was subjected to ubiquitination of $SCF^{\beta\text{-}TRCP}$ complexes assembled in reticulocyte extracts in the absence of kinase or in the presence of active or inactive Chk1 (100 ng) made in insect cells as described in Materials and Methods. Phosphorylation of Cdc25A by Chk1 leads to a small decrease in electrophoretic mobility, as indicated. (*B*) Both β-TRCP1 and β-TRCP2, but not other WD40-containing F-box proteins, can ubiquitinate Cdc25A in vitro. Assays were performed as in *A* in the presence of Chk1 with the indicated in vitro translated F-box proteins. (*C*) Polyubiquitination of Cdc25A by $SCF^{\beta\text{-}TRCP}$ is attenuated in the presence of methyl ubiquitin. Chk1-dependent Cdc25A ubiquitination reactions were performed in the presence of constant amounts of $SCF^{\beta\text{-}TRCP}$ and increasing concentrations of methyl ubiquitin. The methyl ubiquitin concentrations used were 0.25. 1, 2.5, 25, and 100 μg/mL.

sites: S76, S124, S179, S279, and S293 (Fig. 6A). By mass spectrometry, we demonstrated phosphorylation of S76 and S124 in Cdc25A phosphorylated by our recombinant Chk1 in vitro (Table 1). Early studies indicated a prominent role for phosphorylation of S124 in DNA-damage-dependent Cdc25A turnover (Falck et al. 2001; Sorensen et al. 2003), but more recent work suggests the key involvement of S76 in controlling Cdc25A turnover, particularly in response to ultraviolet radiation (Goloudina et al. 2003; Hassepass et al. 2003). Indeed, DNA damage leads to increased S76 phosphorylation as determined using a phosphospecific antibody to this site (Goloudina et al. 2003). Using our in vitro Cdc25A ubiquitination assay and Cdc25A mutants in which particular phosphorylated serine residues are replaced by alanine, we found that S124 phosphorylation is not required for Cdc25A ubiquitination in vitro (Fig. 6B, lane 6). Moreover, a quadruple mutant lacking S124, S179, S279, and S293 was ubiquitinated by $SCF^{\beta\text{-}TRCP}$, although we did consistently find that the quadruple mutant produced smaller ubiquitin conjugates than were generated with the wild-type protein (Fig. 6B, lanes 1,7). In contrast, replacement of S76 with alanine greatly reduced $SCF^{\beta\text{-}TRCP}$-driven Cdc25A ubiquitination in this assay (Fig. 6B, lane 2). Thus, our biochemical data reveal a critical role for Chk1-mediated phosphorylation of S76 in promoting Cdc25A ubiquitination and is consistent with the involvement of this phosphorylation event in promoting Cdc25A turnover in vivo (Goloudina et al. 2003; Hassepass et al. 2003).

Identification of a novel phosphodegron in Cdc25A

Degrons are considered to be minimal sequences that support recognition of cognate E3s and may possess relevant lysine side chains for ubiquitination. The finding that F-box proteins such as β-TRCP and Cdc4 frequently interact with short phosphopeptide motifs has led to the use of the term "phosphodegron" to refer to short sequences capable of interacting specifically with particular F-box proteins (Nash et al. 2001), although these sequences may not themselves contain relevant lysines for ubiquitination. The β-propeller of β-TRCP is known to interact with a phosphodegron containing the sequence DpSGΦXpS, where pS is phospho-serine and Φ is a hydrophobic amino acid (Spencer et al. 1999; Winston et al. 1999a; Gu et al. 2003). Both the aspartate and glycine residues in this motif are required for high-affinity interactions. However, none of the known Chk1 phosphorylation sites in Cdc25A, including S76, would be expected to create a classical β-TRCP recognition motif. This suggested that either β-TRCP is recognizing phosphorylated Cdc25A through a nonclassical phosphodegron or that additional phosphorylation events are involved. Scanning the Cdc25A sequence, we identified a single region (DSGFCLDSP, residues 81–89) that displayed characteristics of the classical β-TRCP recognition motif and is located adjacent to S76 (Fig. 6A). In particular, the first four residues of this motif conform to a portion of the known β-TRCP recognition motif or phosphodegron (Fig. 6A).

To examine the possible involvement of this region, we first determined the effect of mutation of S82 to alanine. This residue corresponds to phospho-S33 in β-catenin, which interacts with a network of hydrogen bonds involving R285 and S325 in β-TRCP (Fig. 6D). Interestingly, $Cdc25A^{S82A}$ was not ubiquitinated by $SCF^{\beta\text{-}TRCP}$ in vitro, suggesting the involvement of this motif in Cdc25A ubiquitination (Fig. 6B, lane 4). We next considered the possibility that S88 may potentially be involved in recognition, in which case, β-TRCP would need to accommodate alternative spacing between phospho-serine residues in the phosphodegron. However, we found that $Cdc25A^{S88A}$ was ubiquitinated with an efficiency similar to that found with the wild-type protein

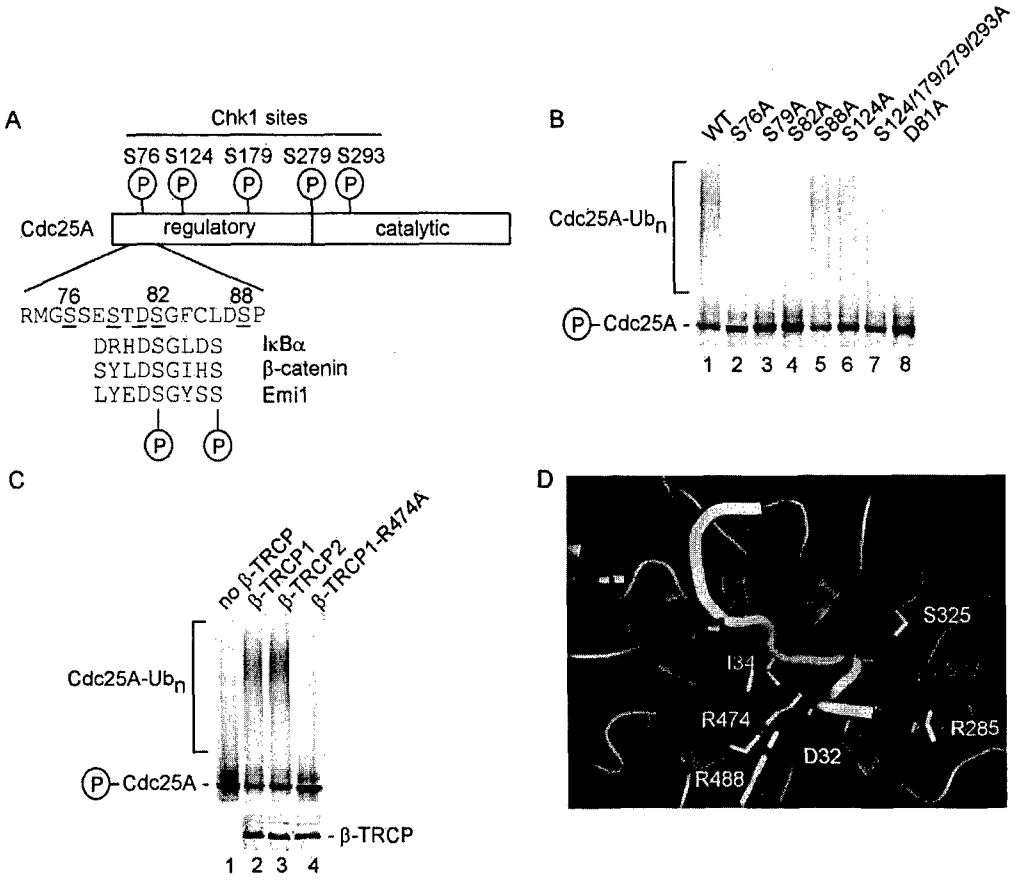

Figure 6. Chk1 phosphorylation sites in Cdc25A are required for $SCF^{\beta\text{-}TRCP}$-mediated ubiquitination but do not appear to constitute the major Cdc25A phosphodegron. (*A*) Schematic representation of Chk1 phosphorylation sites in Cdc25A and comparison of a putative phosphodegron in Cdc25A with the IκBα, β-catenin, and Emi1 phosphodegron recognized by β-TRCP. The Cdc25A residues are designated based on GenBank accession number AAH18642. (*B*) Identification of residues in Cdc25A important for Chk1-dependent ubiquitination. The indicated Cdc25A mutants were used in $SCF^{\beta\text{-}TRCP}$-driven ubiquitination reactions in the presence of Chk1. (*C*) Arg 474 in β-TRCP1 is required for Chk1-dependent Cdc25A ubiquitination. Ubiquitination of Chk1-phosphorylated Cdc25A was performed in the presence of β-TRCP1 or an R474A mutant. An aliquot of each β-TRCP synthesis reaction was supplemented with ^{35}S-methionine to demonstrate equal expression of β-TRCP proteins (*lower* panel). (*D*) Three-dimensional structure of β-TRCP bound to the phosphodegron of β-catenin depicting the interaction of D32 and phosphoserine-33 (pS33) in the phosphodegron with R474 and R285 in β-TRCP. Graphics were generated using Pymol.

(Fig. 6B, lane 5). We also noted that Cdc25A contains an additional serine residue at residue 79, which could potentially be part of the phosphodegron. We found that mutation of S79 to alanine abolished Cdc25A ubiquitination by $SCF^{\beta\text{-}TRCP}$ (Fig. 6B, lane 3).

Additional mutagenesis experiments indicate the direct involvement of a phosphodegron containing phospho-S82 in Cdc25A recognition by β-TRCP. Mutation of D81 in Cdc25A abolished ubiquitination by β-TRCP in vitro (Fig. 6B, lane 8). D81 corresponds to D32 in β-catenin, which is frequently mutated in stabilized alleles of β-catenin (see Wu et al. 2003). In the β-catenin/β-TRCP crystal structure, D32 (which is invariant in β-TRCP substrates) is buried in the β-propeller and forms hydrogen bonds with R474 and Y488 (Fig. 6D). Previous studies indicate that replacement of R474 with alanine blocks IκBα ubiquitination by $SCF^{\beta\text{-}TRCP}$, revealing that this interaction is crucial for recognition of canonical β-TRCP targets (Wu et al. 2003). Likewise, we found that R474 in β-TRCP is required for Chk1-dependent Cdc25A ubiquitination (Fig. 6C, lane 4), consistent with the proposed interaction with D80 in Cdc25A.

Synthetic phosphopeptides have been useful in defining phosphodegrons in cyclin E, β-catenin, IκBα, and Sic1 (Winston et al. 1999a; Koepp et al. 2000; Nash et al. 2001). Therefore, we directly examined whether sequences containing the DSG motif in Cdc25 could function as a phosphodegron. Immobilized peptides spanning this candidate phosphodegron were found to interact efficiently with β-TRCP when S82 or both S79 and S82 were phosphorylated, whereas the phospho-S79 peptide bound slightly better than the unphosphorylated control peptide (Fig. 7A). In contrast, a peptide containing phospho-S76, the site of Chk1 phosphorylation, displayed no detectable interaction with β-TRCP in this assay (Fig. 7A), consistent with the idea that Chk1-mediated phos-

Table 1. *Mass spectral analysis of Cdc25A phosphorylation by Chk1*

Tryptic fragment	Residues	Number of phosphates	Calculated average mass[b] (D)	Measured average mass[b] (D)
6[a]	73–94	1, S76[c]	2217.4	2218
12–13[a]	121–148	1, S124[d]	3320.4	3321
12–15	121–152	1	3801.1	3801
35–40	323–377	1	6119.0	6120

[a]These phosphopeptides were sequenced with LC/MS/MS.
[b]Average mass of dephosphorylated form.
[c]Phosphorylation of S77 in addition to S76 was also detected at lower levels.
[d]Phosphorylation of S126 in addition to S124 was also detected at lower levels.

phorylation of this site is not sufficient for β-TRCP recognition. A larger Cdc25A peptide (residues 66–92) also failed to interact with β-TRCP when phosphorylated on S76 but did associate when phosphorylated on S82 (Fig. 7B).

To more accurately determine the relative affinities of various Cdc25A-derived phosphopeptides for β-TRCP, we developed a competition assay using β-TRCP-driven Cdc25A ubiquitination (Fig. 7C). In principle, this approach avoids the concentration and steric effects sometimes seen with immobilized peptides. Neither the unphosphorylated peptide nor the singly phosphorylated peptides containing phospho-S76 was capable of blocking Cdc25A ubiquitination in this assay (Fig. 7C, lanes 3–6, 23–26). In contrast, a doubly phosphorylated S79/S82 peptide, and to a lesser extent a singly phosphorylated S79 peptide, were capable of inhibiting Cdc25A ubiquitination by $SCF^{\beta\text{-}TRCP}$ as judged by both the lower levels of ubiquitin conjugates and the increased abundance of unmodified Cdc25A (lanes 9–12). The peptide containing phospho-S82 reduced the extent of polyubiquitination (lanes 13–16). Interestingly, the extent of inhibition by the phospho-S79/S82 peptide was comparable to that observed with the phosphodegron from IκBα (Winston et al. 1999a) when examined in the same concentration range (Fig. 7D). Taken together, these data indicate that S79 and S82 are central components of the Cdc25A phosphodegron recognized by β-TRCP and indi-

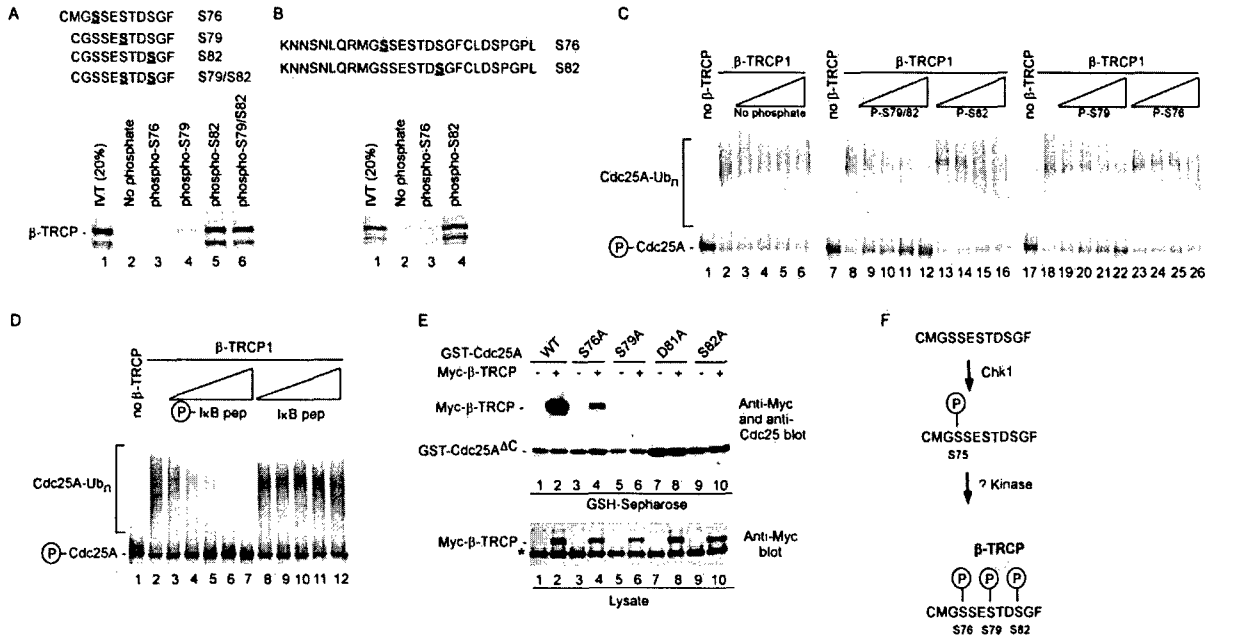

Figure 7. Involvement of a novel phosphodegron in Cdc25A centered at S82 in association with β-TRCP in vivo. (*A*,*B*) A Cdc25A-derived phosphodegron containing at phospho-S79 and phospho-S82 binds β-TRCP in vitro. The indicated synthetic peptides spanning S76–S82 in Cdc25A in phosphorylated or unphosphorylated forms were immobilized on agarose beads and used in binding reactions with in vitro translated and ^{35}S-methionine-labeled β-TRCP1. Bound proteins were separated by SDS-PAGE and visualized by autoradiography. Peptides in *A* were coupled to Sulfo-link agarose through an N-terminal cysteine while peptides in *B* were coupled to Affigel-10 through the side chain of the N-terminal lysine. (*C*) Cdc25A-derived phosphodegrons inhibit ubiquitination of Cdc25A by $SCF^{\beta\text{-}TRCP}$ in vitro. Assays were performed as described in Figure 5 in the presence of the indicated peptides at 2, 10, 20, and 40 μg/mL. (*D*) Cdc25A ubiquitination is blocked by an IκBα phosphodegron. Phosphorylated or unphosphorylated synthetic peptides encompassing the IκBα phosphodegron were used in competition reactions with Chk1-dependent Cdc25A ubiquitination. The concentrations of peptides used were 2, 10, 20, 40, and 100 μg/mL. (*E*) Vectors expressing the indicated $Cdc25A^{\Delta C}$ proteins were cotransfected into 293T cells with a vector expressing Myc-tagged β-TRCP (1 μg each). After 36 h, cells were lysed and subjected to GSH-Sepharose pull-down assays. Blots were probed with anti-Myc antibodies and reprobed with andi-Cdc25A antibodies to demonstrate similar protein levels. The protein labeled with the asterisk is the endogenous c-Myc protein. (*F*) Model for recognition of Cdc25A by β-TRCP in response to phosphorylation by Chk1. See text for details.

cate that Chk1 phosphorylation alone is not sufficient to create the requisite epitopes for β-TRCP recognition. The data also indicate that Cdc25A and IκBα use at least partially overlapping binding sites in β-TRCP.

Recognition of β-TRCP by Cdc25A in vivo requires a phosphodegron anchored by S82

To verify the involvement of residues 76 to 82 in β-TRCP recognition in vivo, GST-Cdc25A$^{\Delta C}$ containing the N-terminal regulatory domain (Fig. 7E) and mutant versions in which S76, S79, D81, and S82 were individually replaced with alanine were tested for binding after expression in 293T cells (Fig. 6D). Mutation of S76 reduced binding by ~10-fold (lane 4 vs. lane 2), whereas mutation of S79, D81, and S82 bound even less efficiently (lanes 6,8,10 vs. lane 2). Taken together, these in vitro and in vivo data strongly implicate a novel phosphodegron in Cdc25A centered at S82 as being important for its association with the β-TRCP ubiquitin ligase.

Discussion

β-TRCP is involved in a large number of seemingly unrelated processes. β-TRCP controls phosphorylation-mediated destruction or processing of several transcriptional regulators, including IκB, β-catenin, ATF-4, and p105$^{NF\kappa B}$ (Latres et al. 1999; Spencer et al. 1999; Winston et al. 1999a; Fong and Sun 2002). Moreover, β-TRCP controls multiple cell cycle-related processes, including centrosome duplication in *Drosophila* and destruction of the mitotic regulator Emi1 during mitosis (Wojcik et al. 2000; Guardavaccaro et al. 2003). Our data now implicate β-TRCP1 and β-TRCP2 in control of Cdc25A turnover during both a normal cell cycle and in response to DNA damage. We have shown that endogenous Cdc25A forms complexes with SCF$^{\beta\text{-TRCP}}$ in the presence or absence of DNA damage. Moreover, depletion of β-TRCP by shRNA stabilizes Cdc25A in the presence or absence of DNA damage, and SCF$^{\beta\text{-TRCP}}$ can ubiquitinate Cdc25A in a Chk1-dependent manner in vitro. Several lines of biochemical evidence suggest the involvement of a novel phosphodegron in Cdc25A containing phospho-S79 and phospho-S82 in β-TRCP recognition. Chk1 appears to be required, but not sufficient, to generate this novel phosphodegron. Previous studies indicate that Cdc25A is phosphorylated by Chk1 during a normal cell cycle, probably during S phase, leading to its instability during S and G_2 phases (Sorensen et al. 2003). This process is accelerated in response to DNA damage (Sorensen et al. 2003). Chk1 is essential for cell proliferation in mammals (Liu et al. 2000), and maintaining low levels of Cdc25A during S and G_2 phases could represent a component of its essential functions. Inappropriately high levels of Cdc25A during DNA replication could influence the kinetics of S-phase progression and thereby affect the fidelity of DNA synthesis.

Our biochemical experiments indicate that Cdc25A turnover is more complex than previously appreciated. Early models suggested that phosphorylation of Cdc25A by Chk1 at multiple sites might be required for Cdc25A turnover. Our reconstitution studies indicate that of all the Chk1 sites in Cdc25A, only S76 phosphorylation plays a prominent role in facilitating SCF$^{\beta\text{-TRCP}}$-dependent Cdc25A ubiquitination in vitro, consistent with recent work on the role of this residue in Cdc25A turnover in vivo (Goloudina et al. 2003; Hassepass et al. 2003). Other known Chk1 sites in Cdc25A (S124, S179, S279, and S293) are not required for ubiquitination in vitro but could, nevertheless, be important for turnover in vivo. One possibility is that phosphorylation affects the site(s) of ubiquitination, which has recently been shown to affect the kinetics of proteasome-mediated destruction of an SCF substrate Sic1 (Petroski and Deshaies 2003). Moreover, we also note that we consistently see the formation of shorter ubiquitin conjugates with the Cdc25A mutant lacking these four Chk1 sites, which could affect the efficiency of recruitment to the proteasome.

Although Chk1-mediated phosphorylation is required for Cdc25A turnover in vivo and ubiquitination by SCF$^{\beta\text{-TRCP}}$ in vitro, it appears that Chk1 activity is not sufficient for this process. First, Chk1 kinases are known to preferentially phosphorylate R-X-X-S/T motifs (O'Neill et al. 2002). Although all of the known Chk1 sites in Cdc25A conform to this consensus sequence, none is expected to generate phosphodegrons of the type known to interact with β-TRCP. Consistent with this, peptides containing phospho-S76 failed to interact with β-TRCP in a direct binding assay. Moreover, these peptides did not efficiently inhibit Cdc25A ubiquitination in vitro. Second, mass spectral analysis of bacterial Cdc25A phosphorylated in vitro by recombinant Chk1 revealed strong phosphorylation of S76 and S124 (>90%), but no phosphorylation at S79 or S82 was detected, indicating that Chk1 cannot directly phosphorylate these two sites. Finally, bacterial Cdc25A that was previously phosphorylated by Chk1 was not a substrate for ubiquitination by purified SCF$^{\beta\text{-TRCP}}$ complexes in vitro that are competent for IκB ubiquitination (data not shown).

We propose that β-TRCP recognizes a novel phosphodegron in Cdc25A. This sequence contains a DSG motif characteristic of all previously identified β-TRCP targets (Emi1, β-catenin, IκBα, p105$^{NF\kappa B}$). Several lines of evidence implicate this degron in β-TRCP recognition. First, point mutations in Cdc25A that remove S79 or S82 abolish ubiquitination by SCF$^{\beta\text{-TRCP}}$ in vitro and association with β-TRCP in transfected cells. Second, point mutations in the aspartate of the DSG motif, or in its complementary ligand in the WD40 propeller of β-TRCP, R474, abolish ubiquitination by SCF$^{\beta\text{-TRCP}}$. Finally, synthetic Cdc25A peptides containing phospho-S79 and phospho-S82 alone can associate with β-TRCP in vitro and can block Cdc25A ubiquitination by SCF$^{\beta\text{-TRCP}}$ in a competition assay, as can a canonical phosphodegron from IκBα.

The simplest explanation for these results is that generation of the phosphodegron in Cdc25A involves two critical steps (Fig. 7F). In the first step, Chk1 phosphorylates S76. In the second step, S76-phosphorylated

Cdc25A is then phosphorylated by one or more kinases on S82 and S79 to generate the phosphodegron recognized by β-TRCP. In the case of our in vitro Cdc25A ubiquitination assay, where S76 and Chk1 are required, this second kinase activity appears to be provided by one or more kinases in the reticulocyte extract. According to this model, Chk1 may perform a priming function that facilitates modification of S79 and/or S82. Other β-TRCP substrates also use analogous priming reactions. For example, β-catenin is phosphorylated by casein kinase I on T41 and T45, and this facilitates phosphorylation of S33 and S37 by GSK3β in a sequential mechanism (Liu et al. 2002). At present, we cannot exclude the possibility that Cdc25A is constitutively phosphorylated on S82/S79 and that Chk1 in a second step induces a conformational change in the adjacent S79/S82 phosphodegron that allows it to be recognized by β-TRCP or protects these residues from rapid dephosphorylation. The finding that $Cdc25A^{S76A}$ displays detectable, albeit greatly reduced, association with β-TRCP in vivo, whereas $Cdc25A^{S82A}$ mutants display no detectable binding, suggests that S76 phosphorylation is not an absolute requirement for S79/S82 phosphorylation. A determination of the mechanism by which Chk1 promotes formation of the degron awaits identification of relevant kinases. In this regard, one candidate kinase is casein kinase Iα. However, addition of two specific casein kinase Iα inhibitors (CKI-7, US Biologicals; IC261, Calbiochem) continuously throughout Cdc25A translation, Chk1 phosphorylation, and in vitro ubiquitination assay failed to block Cdc25A ubiquitination (data not shown). It is also possible that additional cofactors may be involved in Cdc25A turnover independent of the kinases involved. For example, Cks1 is required for p27 ubiquitination by SCF^{Skp2} (for review, see Harper 2001).

The discovery of a role for β-TRCP in Cdc25A turnover now sets the stage for the elucidation of the interplay between regulatory mechanisms responsible for directing the destruction of Cdc25A and control of cell cycle transitions. Although Chk1 is a critical player in this regard, our studies reveal a previously unanticipated level of complexity in the targeting of Cdc25A for ubiquitination involving other participants. These new players may themselves be targets of regulation intended to control cell cycle progression. In addition to targeting Cdc25A for degradation, positive feedback mechanisms involving Cdk1 phosphorylation have been implicated in stabilization of Cdc25A to promote mitotic entry (Mailand et al. 2002). How these competing regulatory pathways interface with the Chk1 pathway to control Cdc25A stability remains to be determined.

Materials and methods

Plasmids

F-box proteins were generated by PCR and cloned into pUNI50 (Liu et al. 1998) prior to sequence analysis. Details of these constructs will be published elsewhere. For expression, pUNI50 constructs were recombined with pCMV-Myc-lox-RS (pJP150) using Cre recombinase, placing N-terminally Myc_3-tagged F-box proteins under control of the CMV promoter. The pUNI backbone was then removed by RS-mediated recombination. Vectors for expression of CDC25A and mutants were generated using pENTR vectors and recombined into the indicated bacterial or mammalian expression construct using clonase (Invitrogen). To generate retroviral vectors expressing $shRNA^{GFP}$ and $shRNA^{\beta\text{-}TRCP}$, double-stranded oligonucleotides were cloned into a modified version of pSuper-retro (Oligoengine, Inc.) wherein the puromycin marker was replaced with an expression cassette for enhanced cyan fluorescence protein (ECFP). The sequences used were: humanized *Renilla* GFP, GGACTTC CCCGAGTACCACttcaagagaGTGGTACTCGGGGAAGTCCtt; β-TRCP, GTGGAATTTGTGGAACATCttcaagagaGATGTTC CACAAATTCCACtt (gene-specific sequences are in caps, and hairpin sequences are underlined). Point mutations in Cdc25A were generated using a QuickChange mutagenesis kit (Stratagene). $Cdc25A^{\Delta C}$ encodes amino acids 1–100 and was generated by PCR prior to cloning into pcDNA3. Vectors for expression of $\beta\text{-}TRCP^{R474A}$ are from a previous study (Wu et al. 2003). pCMV-$\beta\text{-}TRCP^{\Delta F\text{-}box}$ and pCMV-$Skp2^{\Delta F\text{-}box}$ were provided by R. Benarous and L. Larsson, respectively.

Protein interactions

293T cells were cultured in DMEM supplemented with 10% fetal bovine serum (5% CO_2). Transfections were performed using Lipofectamine 2000 (Invitrogen), except in the case of retrovirus production, where calcium-phosphate-mediated DNA transfer was used. At the indicated time, cells were lysed in extraction buffer (25 mM Tris-HCl at pH7.5, 150 mM NaCl, 0.5% nonidet P-40, 1 mM EDTA, 10 mM β-glycerol phosphate, 10 mM *p*-nitrophenyl phosphate, 0.1 μM okadaic acid, and 5 mM NaF). Extracts were subjected to direct Western blot analysis or complex purification using the indicated affinity reagent. For determining Cdc25A ubiquitination in vivo using His_6-Ub, cells were lysed in buffer containing 6M guanidinium hydrochloride in 0.1 M sodium phosphate buffer (pH 8.0) prior to binding to Ni-NTA resin. Where indicated, cells were subject to γ-irradiation (10 Gy) using a Cobalt source. Antibodies against Cdc25A were from Neomarker, Inc. Anti-Cul1 was from Zymed. Anti-cyclin E and Cdc25C antibodies were from Santa Cruz Biotechnology. Anti-β-TRCP was from a previous study and has been shown to interact with both β-TRCP1 and β-TRCP2 (Spiegelman et al. 2000).

β-TRCP suppression

Knock-down of β-TRCP was performed using retroviral-mediated transfer of vectors expressing shRNA for β-TRCP1 and β-TRCP2 or GFP as a negative control. 293T or HCT116 cells were infected with retroviruses. The experiments were performed at 48 h postinfection. In some experiments, lipofectamine-2000-mediated transfection of shRNA in pSUPER vectors was performed. 293T cells were transfected twice in 24 h. Then, 48 h later, cells were subjected to γ-irradiation (10 Gy) or left untreated. At the indicated time, cell extracts were generated and used for direct analysis by immunoblotting with the indicated antibodies. In some experiments, cyclohexamide (25 μg/mL) was added immediately after DNA damage. To verify β-TRCP knock-down, lysates (500 μg, 100 μL) were incubated with 20 μL of agarose-IκB phosphodegron beads prior to immunoblotting, as described (Winston et al. 1999a). This step is required to enrich for β-TRCP as available antibodies do not specifically interact with β-TRCP in crude extracts. Cell cycle

analysis was performed using propidium iodide essentially as described (Ye et al. 2003). Histone H1 kinase assays were performed as described (Ye et al. 2003). With the exception of Figure 3A, all SDS-PAGE separations were performed using 8%–12% gradient minigels (Invitrogen). Figure 3A used a 15-cm 10% polyacrylamide gel, which gave higher resolution of Cdc25A isoforms observed previously (Zhao et al. 2002).

In vitro ubiquitination

Cdc25A ubiquitination was performed using in vitro ^{35}S-methionine-labeled Cdc25A (2.5 µL) in the presence of insect-cell-derived Chk1 or Chk1^{KD} (100 ng), E1 ubiquitin-activating enzyme (50 ng), Ubc5 (200 ng), ubiquitin (1 mg/mL), 1 µM ubiquitin aldehyde, 2.3 µL of in vitro translated F-box protein, and 4 mM ATP in a total volume of 10 µL (30 min, 30°C). In some experiments, methyl ubiquitin (Boston Biochemicals) was used as a chain terminator or synthetic peptides derived from the IκBα phosphodegron (Winston et al. 1999a) or Cdc25A used as a competitive inhibitor. Phosphorylated or unphosphorylated peptides encompassing the Cdc25A phosphodegron and containing a N-terminal cysteine were synthesized by Tufts Medical School Protein Core Facility or by Invitrogen and coupled to Sulfo-link agarose (Pierce) or Affigel-10 (Biorad) at 1 mg/mL. Binding reactions were performed with 10 µL of peptide agarose beads in combination with 5 µL of in vitro translated ^{35}S-methionine-labeled β-TRCP1 in a total of 100 µL of extraction buffer. Beads were washed three times with extraction buffer prior to SDS-PAGE and autoradiography.

Phosphorylation analysis

Mass spectral analysis of bacterial Cdc25A previously phosphorylated with Chk1 was performed using established procedures. Mass spectral analysis of phosphopeptides was performed using Matrix-assisted laser desorption/ionization mass spectrometry (MALDI/TOF) with delayed extraction (Voyager-DE, Perseptive Biosystems) as described (Zhang et al. 1998). An electrospray ion trap mass spectrometer (LCQ, Finnigan) coupled on-line with a capillary high-pressure liquid chromatograph (Magic 2002) was used for identification of phosphorylation sites.

Acknowledgments

We thank S. Blacklow and G. Wu for assistance with Pymol. This work was supported by NIH grants to J.W.H. and S.J.E and by the Department of Defense (to J.W.H.). J.J. was supported by a Department of Defense Postdoctoral Fellowship. T.S. was supported by the Japanese Society for Science. S.J.E. is an Investigator of the Howard Hughes Medical Institute.

The publication costs of this article were defrayed in part by payment of page charges. This article must therefore be hereby marked "advertisement" in accordance with 18 USC section 1734 solely to indicate this fact.

References

Agami, R. and Bernards, R. 2000. Distinct initiation and maintenance mechanisms cooperate to induce G_1 cell cycle arrest in response to DNA damage. *Cell* **102:** 55–66.

Blasina, A., de Weyer, I.V., Laus, M.C., Luyten, W.H., Parker, A.E., and McGowan, C.H. 1999. A human homologue of the checkpoint kinase Cds1 directly inhibits Cdc25 phosphatase. *Curr. Biol.* **9:** 1–10.

Chen, M.S., Hurov, J., White, L.S., Woodford-Thomas, T., and Piwnica-Worms, H. 2001. Absence of apparent phenotype in mice lacking Cdc25C protein phosphatase. *Mol. Cell. Biol.* **21:** 3853–3861.

Deshaies, R.J. 1999. SCF and Cullin/Ring H2-based ubiquitin ligases. *Annu. Rev. Cell Dev. Biol.* **15:** 435–467.

Donzelli, M. and Draetta, G.F. 2003. Regulating mammalian checkpoints through Cdc25 inactivation. *EMBO Rep.* **4:** 671–677.

Donzelli, M., Squatrito, M., Ganoth, D., Hershko, A., Pagano, M., and Draetta, G.F. 2002. Dual mode of degradation of Cdc25 A phosphatase. *EMBO J.* **21:** 4875–4884.

Ducruet, A.P. and Lazo, J.S. 2003. Regulation of Cdc25A half-life in interphase by cyclin-dependent kinase 2 activity. *J. Biol. Chem.* (in press).

Falck, J., Mailand, N., Syljuasen, R.G., Bartek, J., and Lukas, J. 2001. The ATM–Chk2–Cdc25A checkpoint pathway guards against radioresistant DNA synthesis. *Nature* **410:** 842–847.

Falck, J., Petrini, J.H., Williams, B.R., Lukas, J., and Bartek, J. 2002. The DNA damage-dependent intra-S phase checkpoint is regulated by parallel pathways. *Nat. Genet.* **30:** 290–294.

Feldman, R.M., Correll, C.C., Kaplan, K.B., and Deshaies, R.J. 1997. A complex of Cdc4p, Skp1p, and Cdc53p/cullin catalyzes ubiquitination of the phosphorylated CDK inhibitor Sic1p. *Cell* **91:** 221–230.

Fong, A. and Sun, S.C. 2002. Genetic evidence for the essential role of β-transducin repeat-containing protein in the inducible processing of NF κ-B2/p100. *J. Biol. Chem.* **277:** 22111–22114.

Furnari, B., Rhind, N., and Russell, P. 1997. Cdc25 mitotic inducer targeted by chk1 DNA damage checkpoint kinase. *Science* **277:** 1495–1497.

Furnari, B., Blasina, A., Boddy, M.N., McGowan, C.H., and Russell, P. 1999. Cdc25 inhibited in vivo and in vitro by checkpoint kinases Cds1 and Chk1. *Mol. Biol. Cell* **10:** 833–845.

Giaccia, A.J. and Kastan, M.B. 1998. The complexity of p53 modulation: Emerging patterns from divergent signals. *Genes & Dev.* **12:** 2973–2983.

Goloudina, A., Yamaguchi, H., Chervyakova, D.B., Appella, E., Fornace Jr., A.J., and Bulavin, D.V. 2003. Regulation of human Cdc25A stability by serine 75 phosphorylation is not sufficient to activate a S phase checkpoint. *Cell Cycle* **2:** 473–478.

Guardavaccaro, D., Kudo, Y., Boulaire, J., Barchi, M., Busino, L., Donzelli, M., Margottin-Goguet, F., Jackson, P.K., Yamasaki, L., and Pagano, M. 2003. Control of meiotic and mitotic progression by the F box protein β-Trcp1 in vivo. *Dev. Cell* **4:** 799–812.

Harper, J.W. 2001. Protein destruction: Adapting roles for Cks proteins. *Curr. Biol.* **11:** R431–R435.

Hassepass, I., Voit, R., and Hoffmann, I. 2003. Phosphorylation at serine-75 is required for UV-mediated degradation of human Cdc25A phosphatase at the S-phase checkpoint. *J. Biol. Chem.* **278:** 29824–29829.

Hoffmann, I., Draetta, G., and Karsenti, E. 1994. Activation of the phosphatase activity of human cdc25A by a cdk2-cyclin E dependent phosphorylation at the G_1/S transition. *EMBO J.* **13:** 4302–4310.

Jin, P., Gu, Y., and Morgan, D.O. 1996. Role of inhibitory CDC2 phosphorylation in radiation-induced G_2 arrest in human cells. *J. Cell Biol.* **134:** 963–970.

Koepp, D.M., Harper, J.W., and Elledge, S.J. 1999. How the cyclin became a cyclin: Regulated proteolysis in the cell cycle. *Cell* **97:** 431–434.

Koepp, D.M., Schaefer, L.K., Ye, X., Keyomarsi, K., Chu, C., Harper, J.W., and Elledge, S. 2001. Phosphorylation-depen-

dent ubiquitination of cycin E by SCF^{Fbw7} ubiquitin ligase. *Science* **294:** 173–177.

Kumagai, A. and Dunphy, W.G. 1999. Binding of 14–3–3 proteins and nuclear export control the intracellular localization of the mitotic inducer Cdc25. *Genes & Dev.* **13:** 1067–1072.

Latres, E., Chiaur, D.S., and Pagano, M. 1999. The human F box protein β-Trcp associates with the Cul1/Skp1 complex and regulates the stability of β-catenin. *Oncogene* **18:** 849–854.

Liu, Q., Li, M.Z., Leibham, D., Cortez, D., and Elledge, S.J. 1998. The univector plasmid-fusion system, a method for rapid construction of recombinant DNA without restriction enzymes. *Curr. Biol.* **8:** 1300–1309.

Liu, Q., Guntuku, S., Cui, X.S., Matsuoka, S., Cortez, D., Tamai, K., Luo, G., Carattini-Rivera, S., DeMayo, F., Bradley, A., et al. 2000. Chk1 is an essential kinase that is regulated by Atr and required for the G_2/M DNA damage checkpoint. *Genes & Dev.* **14:** 1448–1459.

Liu, C., Li, Y., Semenov, M., Han, C., Baeg, G.H., Tan, Y., Zhang, Z., Lin, X., and He, X. 2002. Control of β-catenin phosphorylation/degradation by a dual-kinase mechanism. *Cell* **108:** 837–847.

Lopez-Girona, A., Furnari, B., Mondesert, O., and Russell, P. 1999. Nuclear localization of Cdc25 is regulated by DNA damage and a 14–3–3 protein. *Nature* **397:** 172–175.

Mailand, N., Falck, J., Lukas, C., Syljuasen, R.G., Welcker, M., Bartek, J., and Lukas, J. 2000. Rapid destruction of human Cdc25A in response to DNA damage. *Science* **288:** 1425–1429.

Mailand, N., Podtelejnikov, A.V., Groth, A., Mann, M., Bartek, J., and Lukas, J. 2002. Regulation of G_2/M events by Cdc25A through phosphorylation-dependent modulation of its stability. *EMBO J.* **21:** 5911–5920.

Matsuoka, S., Huang, M., and Elledge, S.J. 1998. Linkage of ATM to cell cycle regulation by the Chk2 protein kinase. *Science* **282:** 1893–1897.

Morgan, D.O. 1997. Cyclin-dependent kinases: Engines, clocks, and microprocessors. *Annu. Rev. Cell Dev. Biol.* **13:** 261–291.

Nash, P., Tang, X., Orlicky, S., Chen, Q., Gertler, F.B., Mendenhall, M.D., Sicheri, F., Pawson, T., and Tyers, M. 2001. Multisite phosphorylation of a CDK inhibitor sets a threshold for the onset of DNA replication. *Nature* **414:** 514–521.

O'Neill, T., Giarratani, L., Chen, P., Iyer, L., Lee, C.H., Bobiak, M., Kanai, F., Zhou, B.B., Chung, J.H., and Rathbun, G.A. 2002. Determination of substrate motifs for human Chk1 and hCds1/Chk2 by the oriented peptide library approach. *J. Biol. Chem.* **277:** 16102–16115.

Orian, A., Gonen, H., Bercovich, B., Fajerman, I., Eytan, E., Israel, A., Mercurio, F., Iwai, K., Schwartz, A.L., and Ciechanover, A. 2000. $SCF^{\&beta\text{-}TrCP}$ ubiquitin ligase-mediated processing of NF-κB p105 requires phosphorylation of its C-terminus by IκB kinase. *EMBO J.* **19:** 2580–2591.

Peng, C.Y., Graves, P.R., Thoma, R.S., Wu, Z., Shaw, A.S., and Piwnica-Worms, H. 1997. Mitotic and G_2 checkpoint control: Regulation of 14–3–3 protein binding by phosphorylation of Cdc25C on serine 216. *Science* **277:** 1501–1505.

Petroski, M.D. and Deshaies, R.J. 2003. Context of multiubiquitin chain attachment influences the rate of Sic1 degradation. *Mol. Cell* **11:** 1435–1444.

Rhind, N., Furnari, B., and Russell, P. 1997. Cdc2 tyrosine phosphorylation is required for the DNA damage checkpoint in fission yeast. *Genes & Dev.* **11:** 504–511.

Shiloh, Y. 2003. ATM and related protein kinases: Safeguarding genome integrity. *Nat. Rev. Cancer* **3:** 155–168.

Skowyra, D., Craig, K.L., Tyers, M., Elledge, S.J., and Harper, J.W. 1997. F-box proteins are receptors that recruit phosphorylated substrates to the SCF ubiquitin-ligase complex. *Cell* **91:** 209–219.

Sorensen, C.S., Syljuasen, R.G., Falck, J., Schroeder, T., Ronnstrand, L., Khanna, K.K., Zhou, B.B., Bartek, J., and Lukas, J. 2003. Chk1 regulates the S phase checkpoint by coupling the physiological turnover and ionizing radiation-induced accelerated proteolysis of Cdc25A. *Cancer Cell* **3:** 247–258.

Spencer, E., Jiang, J., and Chen, Z.J. 1999. Signal-induced ubiquitination of IκBα by the F-box protein Slimb/β-TrCP. *Genes & Dev.* **13:** 284–294.

Spiegelman, V.S., Tang, W., Katoh, M., Slaga, T.J., and Fuchs, S.Y. 2002. Inhibition of HOS expression and activities by Wnt pathway. *Oncogene* **21:** 856–860.

Takizawa, C.G. and Morgan, D.O. 2000. Control of mitosis by changes in the subcellular location of cyclin-B1-Cdk1 and Cdc25C. *Curr. Opin. Cell Biol.* **12:** 658–665.

Vigo, E., Muller, H., Prosperini, E., Hateboer, G., Cartwright, P., Moroni, M.C., and Helin, K. 1999. CDC25A phosphatase is a target of E2F and is required for efficient E2F-induced S phase. *Mol. Cell. Biol.* **19:** 6379–6395.

Winston, J.T., Strack, P., Beer-Romero, P., Chu, C.Y., Elledge, S.J., and Harper, J.W. 1999a. The $SCF^{\beta\text{-}TRCP}$-ubiquitin ligase complex associates specifically with phosphorylated destruction motifs in IκBα and β-catenin and stimulates IκBα ubiquitination in vitro. *Genes & Dev.* **13:** 270–283.

Winston, J.T., Koepp, D.M., Zhu, C., Elledge, S.J., and Harper, J.W. 1999b. A family of mammalian F-box proteins. *Curr. Biol.* **9:** 1180–1182.

Wojcik, E.J., Glover, D.M., and Hays, T.S. 2000. The SCF ubiquitin ligase protein slimb regulates centrosome duplication in *Drosophila*. *Curr. Biol.* **10:** 1131–1134.

Wu, G., Xu, G., Schulman, B.A., Jeffrey, P.D., Harper, J.W., and Pavletich, N.P. 2003. Structure of a β-TrCP1–Skp1–β-catenin complex: Destruction motif binding and lysine specificity of the $SCF^{\beta\text{-}TrCP1}$ ubiquitin ligase. *Mol. Cell* **11:** 1445–1456.

Xiao, Z., Chen, Z., Gunasekera, A.H., Sowin, T.J., Rosenberg, S.H., Fesik, S., and Zhang, H. 2003. Chk1 mediates S and G_2 arrests through Cdc25A degradation in response to DNA-damaging agents. *J. Biol. Chem.* **278:** 21767–21773.

Ye, X., Wei, Y., Nalepa, G., and Harper, J.W. 2003. The cyclin E/Cdk2 substrate p220NPAT is required for S-phase entry, histone gene expression, and Cajal Body maintenance in human somatic cells. *Mol. Cell. Biol.* (in press).

Zeng, Y. and Piwnica-Worms, H. 1999. DNA damage and replication checkpoints in fission yeast require nuclear exclusion of the Cdc25 phosphatase via 14–3–3 binding. *Mol. Cell. Biol.* **19:** 7410–7419.

Zeng, Y., Forbes, K.C., Wu, Z., Moreno, S., Piwnica-Worms, H., and Enoch, T. 1998. Replication checkpoint requires phosphorylation of the phosphatase Cdc25 by Cds1 or Chk1. *Nature* **395:** 507–510.

Zhang, X., Herring, C.J., Romano, P.R., Szczepanowska, J., Brzeska, H., Hinnebusch, A.G., and Qin, J. 1998. Identification of phosphorylation sites in proteins separated by polyacrylamide gel electrophoresis. *Anal. Chem.* **70:** 2050–2059.

Zhao, H., Watkins, J.L., and Piwnica-Worms, H. 2002. Disruption of the checkpoint kinase 1/cell division cycle 25A pathway abrogates ionizing radiation-induced S and G_2 checkpoints. *Proc. Natl. Acad. Sci.* **99:** 14795–14800.

Zhou, B.B. and Elledge, S.J. 2000. The DNA damage response: Putting checkpoints in perspective. *Nature* **408:** 433–439.

Zou, L. and Elledge, S.J. 2003. Sensing DNA damage through ATRIP recognition of RPA–ssDNA complexes. *Science* **300:** 1542–1548.

THE JOURNAL OF BIOLOGICAL CHEMISTRY
Vol. 279, No. 48, Issue of November 26, pp. 50110–50119, 2004
Printed in U.S.A.

Recognition of Phosphodegron Motifs in Human Cyclin E by the SCF^{Fbw7} Ubiquitin Ligase*

Received for publication, August 11, 2004, and in revised form, September 9, 2004
Published, JBC Papers in Press, September 13, 2004, DOI 10.1074/jbc.M409226200

Xin Ye[a], Grzegorz Nalepa[b,c,d], Markus Welcker[e], Benedikt M. Kessler[a,f], Eric Spooner[a], Jun Qin[b,c], Stephen J. Elledge[g,h,i,j], Bruce E. Clurman[e], and J. Wade Harper[a,k]

From the [a]Department of Pathology, [g]Center for Genetics and Genomics, [h]Department of Genetics, and [i]Howard Hughes Medical Institute, Harvard Medical School, Boston, Massachusetts 02115, the [b]Program in Cell and Molecular Biology and [c]Verna and Marrs McLean Department of Biochemistry, Baylor College of Medicine, Houston, Texas 77030, and the [e]Division of Clinical Research, Fred Hutchinson Cancer Research Center, Seattle, Washington 98109

Turnover of cyclin E is controlled by SCF^{Fbw7}. Three isoforms of Fbw7 are produced by alternative splicing. Whereas Fbw7α and -γ are nuclear and the β-isoform is cytoplasmic in 293T cells, all three isoforms induce cyclin E destruction in an *in vivo* degradation assay. Cyclin E is phosphorylated on Thr^{62}, Ser^{88}, Ser^{372}, Thr^{380}, and Ser^{384} *in vivo*. To examine the roles of phosphorylation in cyclin E turnover, a series of alanine point mutations in each of these sites were analyzed for Fbw7-driven degradation. As expected, mutation of the previously characterized residue Thr^{380} to alanine led to profound defects of cyclin E turnover, and largely abolished association with Fbw7. Mutation of Thr^{62} to alanine led to a dramatic reduction in the extent of Thr^{380} phosphorylation, suggesting an indirect effect of this mutation on cyclin E turnover. Nevertheless, phosphopeptides centered at Thr^{62} associated with Fbw7, and residual binding of cyclin E^{T380A} to Fbw7 was abolished upon mutation of Thr^{62}, suggesting a minor role for this residue in direct association with Fbw7. Mutation of Ser^{384} to alanine also rendered cyclin E resistant to degradation by Fbw7, with the largest effects being observed with Fbw7β. Cyclin E^{S384A} associated more weakly with Fbw7α and -β isoforms but was not defective in Thr^{380} phosphorylation. Analysis of the localization of cyclin E mutant proteins indicated selective accumulation of cyclin E^{S384A} in the nucleus, which may contribute to the inability of cytoplasmic Fbw7β to promote turnover of this cyclin E mutant protein.

Flux through signaling pathways is controlled, in large part, by regulated protein destruction and reversible protein phosphorylation. During the last few years, it has become clear that, in many cases, protein destruction is initiated by site-specific phosphorylation of the target protein, which then facilitates the interaction of the target protein with the destruction machinery. Much of the ubiquitination that occurs in response to protein phosphorylation occurs via the SCF ubiquitin ligase pathway. Phosphorylated proteins are ubiquitinated by an E1-E2[1] thiol-ester cascade, wherein the E2 is brought to the phosphorylated substrate via an SCF E3 (1–3). SCF complexes are composed of a core ubiquitin ligase containing the scaffold Cul1, a ring finger protein called Rbx1/Roc1, and an adaptor protein called Skp1 (4–8). Rbx1 associates with and activates E2s including Cdc34 (7, 9), whereas Skp1 interacts simultaneously with Cul1 and with a member of the F-box family of proteins (10). F-box proteins constitute a large family (more than 70 members in humans) of specificity factors that link diverse substrates with ubiquitination machinery (3, 11–13).[2] Many F-box proteins contain C-terminal protein-protein interaction domains including WD40 and leucine-rich repeats that allow for specific target recognition. Several F-box proteins, including Cdc4 and Grr1 in yeast and β-TRCP (β-transducin-repeat containing protein), Skp2, and Fbw7 in humans, have been demonstrated to interact with target proteins in a phosphorylation-dependent manner (5, 14–19, 20–23). Structural and biochemical analysis of the cyclin-dependent kinase inhibitor Sic1, a target of the SCF^{Cdc4} complex, has revealed a complex relationship between Sic1 phosphorylation events and recognition by WD40 repeats in Cdc4 (18, 24). In essence, a minimum of six phosphorylation events are required for recognition through a single phosphodegron binding site on Cdc4. Each of these phosphorylation events generates phosphodegrons that are, in isolation, suboptimal for tight binding with Cdc4 (18, 24). In contrast, structural analysis of the β-TRCP F-box protein responsible for destruction of IκBα and β-catenin indicates that two phosphorylation events are recognized as a unit by a specific network of basic residues (25). The extent to which other substrates of the Cdc4 class of F-box proteins require multiple phosphorylation events is unknown.

In this work, we have examined how phosphorylation is used to regulate the interaction of the human G_1 cyclin, cyclin E, with the WD40 containing F-box protein, Fbw7. Fbw7 is most closely related to Cdc4 in budding yeast (17, 21, 26) and has

* This work was supported in part by National Institutes of Health (NIH) Grant AG11095 (to J. W. H. and S. J. E.), by NCI, NIH Grant CA102742 (to B. E. C.), by Department of Defense Grants DAMD 17-01-01-0135 (to J. W. H.) and DAMD 17-02-1-0292 (to G. N.), and by the Leukemia and Lymphoma Society (to M. W.). Support for mass spectrometry was provided by NIH Grant ROI 62502, a grant from the Harvard Center for Neurodegeneration and Repair, and a grant from the Alexander and Margaret Stewart Trust Foundation (to B. M. K and Hidde Ploegh). The costs of publication of this article were defrayed in part by the payment of page charges. This article must therefore be hereby marked "*advertisement*" in accordance with 18 U.S.C. Section 1734 solely to indicate this fact.

[d] Present address: Dept. of Pathology, Harvard Medical School, 77 Ave. Louis Pasteur, Boston, MA 02115.

[f] Supported by a Multiple Myeloma Research Foundation Senior Research Award.

[j] A member of the Howard Hughes Medical Institute.

[k] To whom correspondence should be addressed: Dept. of Pathology, Harvard Medical School, 77 Ave. Louis Pasteur, Boston, MA 02115. Tel.: 617-432-6590; Fax: 617-432-6591; E-mail: wade_harper@hms.harvard.edu.

[1] The abbreviations used are: E1, ubiquitin-activating enzyme; E2, ubiquitin carrier protein; E3, ubiquitin-protein isopeptide ligase; Cdk, cyclin-dependent kinase; MS, mass spectrometry.

[2] J. Jin and J. W. Harper, unpublished data.

been implicated in the turnover of not only cyclin E but Notch (27), c-Myc (28–30), and c-Jun (31) as well. RNAi against Fbw7 in humans or its *Drosophila* ortholog *Ago* leads to increased levels of cyclin E in tissue culture cells (17, 21), and mutations in *Ago* affect cyclin E levels in the *Drosophila* (26). In addition, mice deficient in Fbw7 die during embryogenesis (~10.5 days postcoitum) and both the embryo and the placenta display stabilization of cyclin E and Notch (32). Finally, Fbw7 can ubiquitinate cyclin E *in vitro* (17, 21). Mammalian cyclin E functions to activate cyclin-dependent kinase 2 (Cdk2) at the G_1/S transition. Previous work has demonstrated that phosphorylation of Thr^{380} in cyclin E, in part via an autophosphorylation mechanism, is required for its rapid turnover (33, 34). This residue can also be phosphorylated by GSK3β to promote turnover (35). Although mutation of Thr^{380} to alanine greatly stabilizes cyclin E, its turnover *in vivo* or ubiquitination *in vitro* is not completely eliminated (17, 21). Recent studies have also implicated phosphorylation of Thr^{62} and Ser^{384} in cyclin E turnover by Fbw7β (21, 35), but whether this reflects direct or indirect effects in Fbw7 recognition is not clear. Thr^{62} conforms to a Cdk2 consensus site but the identity of kinases involved in Thr^{62} phosphorylation are currently unknown (35). Available data indicates that phosphorylation of Thr^{62} is required for phosphorylation of Ser^{58} by GSK3β (35). Phosphorylation of Ser^{384} is dependent upon interaction of cyclin E with active Cdk2, and it has been proposed that Ser^{384} is directly phosphorylated by Cdk2 (35).

To understand in greater detail how Fbw7 recognizes cyclin E and promotes its turnover, we have used mass spectrometry to confirm and extend recent peptide mapping studies of cyclin E phosphorylation and have performed a series of biochemical and mutagenic experiments that examine the role of multiple phosphorylation events in recognition and turnover of cyclin E by three specific isoforms of Fbw7, α, β, and γ. The data indicate both direct and indirect roles for Thr^{62} in binding to Fbw7. Whereas synthetic peptides encompassing Thr^{62} bind Fbw7 in a phosphorylation-dependent manner, the major effect seen upon mutation of Thr^{62} to alanine is a dramatic reduction in the extent of Thr^{380} phosphorylation, suggesting an indirect effect of the T62A mutation on cyclin E degradation through the Thr^{380} degron. Nevertheless, residual association of cyclin E^{T380A} with Fbw7 is reduced upon mutation of Thr^{62} to alanine. Mutation of Ser^{384} to alanine reduced turnover of cyclin E by all three isoforms of Fbw7, although the effects seen with Fbw7β were much greater than that observed with α and γ. Cyclin E^{S384A} associated more weakly than wild-type cyclin E with both Fbw7α and Fbw7β. Unlike other cyclin E mutants examined, cyclin E^{S384A} appeared to be preferentially retained in the nucleus, partially explaining the reduced ability of cytoplasmic Fbw7β to promote cyclin E turnover.

MATERIALS AND METHODS

Plasmids, Transfections, and Immunofluorescence—The pCS2-Myc-cyclin E expression plasmid employed was from a previous study (33). Mutations were generated using the Gene Editor System (Promega). Vectors for expression of FLAG-Fbw7α, -β, and -γ were created in pCMV-FLAG (Sigma). To create an Fbw7γ expression plasmid, PCR was used to amplify Fbw7γ-specific sequences from a brain cDNA library. The oligonucleotides used were as follows: forward, GATCAAGCTTATGTCAAAACCGGGAAAACCTACTC; reverse, TGTCTGAGCTGCTTGTAGCAGGTC. The 570-bp PCR product was digested with HindIII and BspMI and ligated into the pCMV-FLAG-Fbw7 backbone previously digested with HindIII and BspMI, and the product was confirmed by DNA sequencing. Plasmids used for expression of untagged Fbw7 mutants were described previously (17). To generate an expression plasmid for dominant negative Cul1, sequences encoding amino acids 1–453 were cloned into pcDNA3 (12). 293T cells were maintained in Dulbecco's modified Eagle's medium containing 10% fetal bovine serum. The indicated quantities of DNA were used in either calcium phosphate- or Fugene 6 (Roche Applied Science)-mediated transfections. Thirty-six hours after transfection, cells were either lysed in 25 mM Tris-HCl, 100 mM NaCl, 0.1% Triton X-100, 10 mM β-glycerol phosphate, 10 mM NaF, and protease inhibitors (Roche Applied Science) or were processed for immunofluorescence.

Microscopy and Image Analysis—For immunofluorescence, cells transfected with cyclin E or Fbw7$\alpha/\beta/\gamma$ plasmids were grown on ultrathin cover slides (Fisher) and fixed in methanol or 4% paraformaldehyde in phosphate-buffered saline followed by permeabilization with 0.2% Triton X-100 for 10 min. Cells were then blocked with 5% goat serum (Sigma) for 30 min, incubated with primary antibodies (anti-Myc or anti-FLAG at 1:100) for 1 h, washed five times with phosphate-buffered saline, incubated with fluorochrome-conjugated secondary antibody for 1 h, and generously washed. Nuclei were then counterstained with 4′,6′-diamidino-2-phenylindole, and cells were mounted in SlowFade Light Antifade reagent (Molecular Probes, Inc., Eugene, OR). To visualize subcellular localization of Fbw7 isoforms, images were taken on a Nikon/DeltaVision deconvolution microscope (Applied Precision) as a series of 0.2-μm-thick Z-sections and processed with a Softworx image work station. Each image represents single transcellular Z-section.

For fluorescence signal quantification, cells were fixed and immunostained as described above 48 h post-transfection with the indicated wild type and mutant cyclin E-expressing plasmid. Images were recorded with an empirically chosen, constant exposure time on an Olympus BX60 microscope fitted with a Hammamatsu CCD camera. For processing, an ImagePro Plus work station (Media Cybernetics Inc.) was employed. Fluorescence intensity profiles were measured and averaged along intranuclear or intracytoplasmic linear tracks, and obtained values were normalized against internal background controls for each visual field. Results were calculated as $y = \Delta(x(N_{norm}/C_{norm}); wt(N_{norm}/C_{norm}))$, using averaged *N/C* ratios for 15 cells/construct. Statistical significance was confirmed by analysis of variance.

Immunoprecipitation and Protein Interactions—To examine cyclin E degradation, lysates from transfected cells were subjected to immunoblotting using anti-Myc (9E10) antibodies (Covance). To examine cyclin E turnover, cells were transfected with the indicated plasmids, and 36 h later, cells were cultured for 1 h in methionine-free medium prior to pulse labeling with [^{35}S]methionine (0.1 mCi/ml). Twenty minutes later, [^{35}S]methionine-containing medium was replaced with fresh medium containing 10 mM cold methionine. Extracts made at the indicated times were used for immunoprecipitation with anti-Myc antibodies. Immune complexes were subjected to SDS-PAGE, autoradiography, and quantitation using a PhosphorImager (Amersham Biosciences). To examine association of FLAG-Fbw7α with cyclin E post-transfection, extracts were subjected to immunoprecipitation with anti-FLAG antibodies, and immune complexes were immunoblotted with anti-Myc antibodies. To examine the extent of cyclin E phosphorylation at Thr^{380}, anti-cyclin E immune complexes were separated by SDS-PAGE and immunoblotted with anti-phospho-Thr^{380} antibodies (Santa Cruz Biotechnology, Inc., Santa Cruz, CA), and the blot was subsequently stripped and reprobed with anti-Myc antibodies. The absence of reactivity of anti-phospho-Thr^{380} antibodies with cyclin E^{T380A} points to the specificity of the antibodies employed. For peptide binding experiments, the indicated synthetic peptides were coupled to Affi-Gel-10 beads (Bio-Rad) at a concentration of 1 mg/ml. Immobilized peptides (7 μl) were incubated with the indicated *in vitro* translation products (5 μl) in a total volume of 120 μl of NETN (25 mM Tris-HCl, pH 7.8, 100 mM NaCl, 1 mM EDTA, and 0.1% Nonidet P-40). Complexes were washed three times with 1 ml of NETN prior to SDS-PAGE and autoradiography. In some cases, Thr^{62}-containing peptides were employed as competitor. Antibodies against a synthetic peptide containing Thr^{62} (SLIPpTPDK) were made by Phospho-Solutions, Inc. (Aurora, CO).

Mass Spectrometry—Recombinant cyclin E was produced in insect cells as a glutathione *S*-transferase fusion protein as described (17). To produce mammalian cell-derived cyclin E for mass spectrometry, pCS2-Myc-cyclin E was transfected into four 150-mm dishes using Fugene 6. Subsequently, Myc-cyclin E was isolated using immobilized 9E10 antibodies and purified by SDS-PAGE for mass spectral analysis. Approximately 500 ng of cyclin E was recovered for mass spectral analysis, based on Coommassie Blue staining (data not shown). Mass spectral analysis of phosphopeptides in cyclin E was performed using matrix-assisted laser desorption ionization mass spectrometry with delayed extraction (Voyager-DE; Perseptive Biosystems, Framingham, MA). Unless otherwise noted, an electrospray ion trap mass spectrometer (LCQ; Finnigan, San Jose, CA) coupled on-line with a capillary high pressure liquid chromatograph (Magic 2002, Auburn, CA) was used for identification of phosphorylation sites. Cyclin E$^{81-98}$ was sequenced by

TABLE I
Analysis of cyclin E phosphorylation by mass spectrometry

Tryptic fragment	Calculated mass	Observed mass	
		293T	Insect cells
	Da	*Da*	
F14–15 (aa 81–98)[a]	1934.3	2014.2 (1P)	2014. 5[b] (1P)
F41–43 (aa 362–386)	2608.0	2848.2 (3P), 2768.5 (2P), 2688.1 (1P)	2848.3[b] (3P), 2768.2 (2P), 2688.2 (1P)
F42–43 (aa 363–386)	2479.8		2640.0[b] (2P), 2560.0 (1P)

[a] aa, amino acids.
[b] Phosphopeptides sequenced by liquid chromatography/MS/MS.

liquid chromatography/mass spectrometry/mass spectrometry (liquid chromatography/MS/MS) using a Q-TOF micro (Micromass).

RESULTS

Analysis of Cyclin E Phosphorylation in Vivo—Previous studies of cyclin E have demonstrated that mutation of Thr^{380} or Thr^{62} to nonphosphorylatable alanine leads to partial stabilization of cyclin E in transfected cells, whereas simultaneous mutation of both leads to further stabilization (21). Additionally, these mutations lead to reduced ubiquitination efficiency *in vitro* (17, 21). Precisely how these phosphorylation events facilitate recognition by Fbw7 is unclear. In addition, it is possible that additional phosphorylation events in cyclin E are important for recognition by Fbw7. Recent studies have identified five cyclin E phosphorylation sites, Ser^{58}, Ser^{75}, Ser^{372}, Thr^{380}, and Ser^{384}, by conventional peptide mapping (35). Using mass spectrometry, we confirmed and extended these results in cyclin E purified from mammalian cells after transfection with a pCMV-Myc-cyclin E expression plasmid and in cyclin E expressed in insect cells with Cdk2 (Table I). In brief, various forms of cyclin E$^{363–386}$ were found to contain either two or three phosphates, as determined by treatment with calf intestinal phosphatase. Peptide sequencing by liquid chromatography/MS/MS identified Ser^{372}, Thr^{380}, and Ser^{384} as sites of phosphorylation in the triply phosphorylated peptide (Table I). Peptide sequencing of the cyclin E$^{81–98}$ peptide by liquid chromatography/MS/MS demonstrated phosphorylation on Ser^{88} (Table I and data not shown). Ser^{88} in cyclin E has not been previously shown to be phosphorylated but does conform to a minimal Cdk2 consensus site. In these experiments, we did not observe phosphopeptides containing either Ser^{58}, which is known to be phosphorylated (35), or Thr^{62}, possibly due to the large size and cysteine-rich character of the predicted tryptic peptide. Therefore, antibodies directed at phospho-Thr^{62} were generated using a synthetic peptide as antigen. Immunoblotting of affinity-purified Myc-tagged wild-type or T62A cyclin E with these antibodies revealed specific interaction with wild-type but not T62A cyclin E (Fig. 1*C*). Moreover, treatment of Myc-cyclin E with λ-phosphatase resulted in loss of reactivity toward the phospho-Thr^{62} antibody, consistent with a specific phosphorylation-dependent interaction (Fig. 1*D*). These data indicate that cyclin E is phosphorylated on Thr^{62} in tissue culture cells. Overall, these data lead to the conclusion that cyclin E is phosphorylated on at least three sites in the C terminus and at least four sites near the N terminus (Fig. 1*B*).

Contribution of Phosphorylation to Fbw7-mediated Cyclin E Turnover in Vivo—Currently, three distinct isoforms of Fbw7 (α, β, and γ) have been described (17, 21, 36). These isoforms employ distinct 5′ exons encoding unique N termini fused with 10 common exons. We first asked where these proteins are localized in the cell. However, because anti-Fbw7 antibodies suitable for immunofluorescence are not available, we used transient transfection of Fbw7 expression vectors in which the N terminus was tagged with a FLAG epitope. In 293T cells, we found that both Fbw7α *and Fbw7*γ are localized primarily in the nucleus (Fig. 1, *A* and *C*). In contrast, Fbw7β is almost exclusively found in the cytoplasm (Fig. 1*B*). We previously reported that Fbw7β has an apparent transmembrane domain near the N terminus (17), and this may be involved in localizing Fbw7β to endoplasmic reticulum membranes. An in depth analysis of cis-acting signals important for proper localization will be reported elsewhere.[3]

To examine the contribution of multisite phosphorylation to cyclin E turnover, we employed an *in vivo* degradation assay wherein Myc-cyclin E and Cdk2 are transiently expressed in 293T cells in the presence or absence of Fbw7 isoforms (35). Expression of Myc-cyclin E and Cdk2 alone led to readily detectable Myc-cyclin E, as determined by immunoblotting of crude cell extracts (Fig. 2, *A–C*). Co-expression of increasing levels of FLAG-Fbw7α led to a dramatic decrease in the steady-state abundance of Myc-cyclin E. All three Fbw7 isoforms, when expressed at comparable levels, were capable of reducing the abundance of cyclin E but had no effect on Cdk2 abundance. These results extend previous results from multiple laboratories indicating that Fbw7β overexpression can drive cyclin E degradation when overexpressed (21, 35). As expected, cyclin E^{T380A} and cyclin E$^{T62A/T380A}$ levels were largely unaffected by expression of all three isoforms of Fbw7. This is consistent with a major role for Thr^{380} phosphorylation in controlling cyclin E turnover, as determined by pulse-chase (Fig. 2*D*). We then examined the susceptibility of T62A, S88A, S372A, and S384A mutations to elimination by Fbw7 isoforms. We found that T62A was substantially defective in elimination by Fbw7β and -γ, but this defect was much less obvious with the Fbw7α isoform under these conditions (Fig. 2, *A–C*). However, using lower Fbw7α expression plasmids revealed clear defects in cyclin E^{T62A} turnover (Fig. 2*F*). We also found that Fbw7β was profoundly defective in eliminating cyclin E^{S384A} (Fig. 2*B*), whereas turnover of cyclin E^{S384A} by Fbw7α and -γ was less affected (Fig. 2, *A* and *C*). At higher levels of cyclin E^{S384A} expression plasmid used for transfection, cyclin E^{S384A} was substantially more resistant to turnover by Fbw7α than was wild-type cyclin E (Fig. 2*G*). Cyclin E^{S372A} and cyclin E^{S88A} were efficiently degraded by all three Fbw7 isoforms (Fig. 2, *A–C*, and data not shown for cyclin E^{S372A}). Control experiments demonstrated comparable levels of all three Fbw7 isoforms in transient transfections (Fig. 2*E*).

Phosphorylation of Thr^{380} in the C-terminal Phosphodegron of Cyclin E Is Sufficient for Interaction with Fbw7—Given the multisite phosphorylation of cyclin E in residues flanking Thr^{380}, we next examined the contribution of individual phosphorylation events to recognition by Fbw7 in the context of short peptide phosphodegrons. Previous studies have demonstrated that short phosphopeptides are specifically recognized by WD40-containing F-box proteins (17, 18, 22). Synthetic peptides spanning amino acids 361–388 of cyclin E (cyclin E$^{361–388}$) were synthesized in various phosphorylated and unphosphorylated forms that mimic phosphorylation *in vivo* (Fig. 3*A*), coupled to agarose beads, and then tested for binding to *in vitro*

[3] B. E. Clurman and M. Welcker, unpublished data.

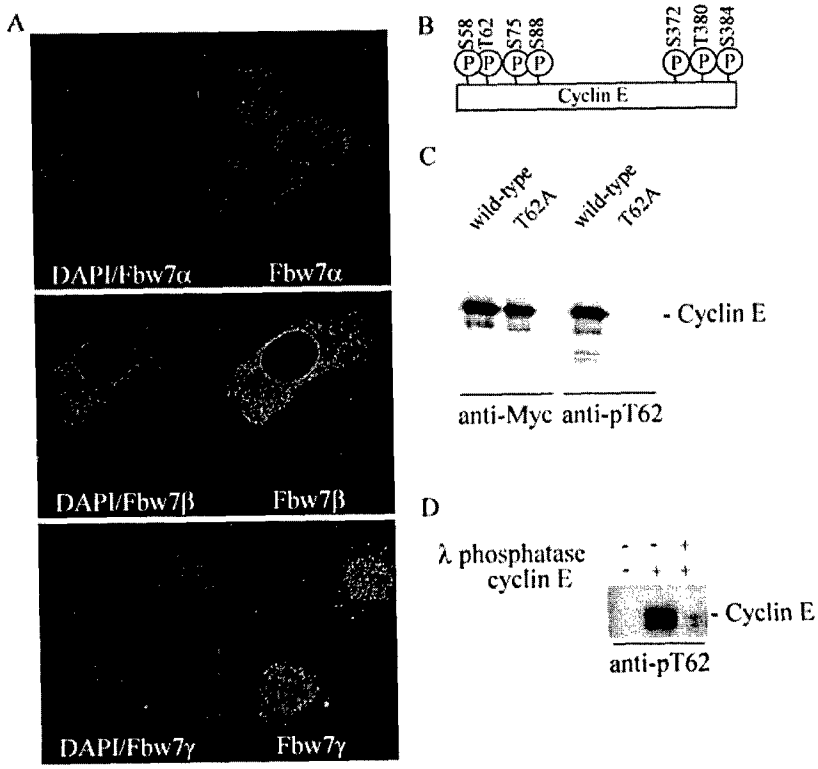

FIG. 1. *A*, differential localization of Fbw7 isoforms. Expression plasmids encoding the indicated N-terminally FLAG-tagged Fbw7 isoforms were transiently transfected into 293T cells using Fugene 6. After 36 h, cells were subjected to indirect immunofluorescence. Anti-FLAG immunofluorescence is shown in *red*. Nuclei, stained with 4′,6′-diamidino-2-phenylindole, are shown in *blue*. *B*, schematic representation of phosphorylation sites found in cyclin E (see Table I). *C* and *D*, antibodies directed at phospho-Thr^{62} of cyclin E selectively interact with wild-type cyclin E purified from 293T cells after transient transfection but do not react with cyclin E^{T62A} or with cyclin E treated previously with λ-phosphatase. *C*, 293T cells were transfected with pCMV-Myc-cyclin E DNA, and after 48 h, cell lysates were immunoprecipitated with anti-Myc antibodies prior to immunoblotting with either anti-Myc antibodies or anti-phospho-Thr^{62} antibodies. In *D*, Myc-cyclin E immune complexes were incubated in the presence or absence of λ-phosphatase prior to immunoblotting with anti-phospho-Thr^{62} antibodies.

translated Fbw7 (Fig. 3*B*). As expected, unphosphorylated cyclin E$^{361-388}$ did not associate with Fbw7 (Fig. 3*B*, *lane 2*). In addition, we found that phosphorylation of either Ser^{372} of Ser^{384} alone did not support Fbw7 binding (Fig. 3*B*, *lanes 4* and *6*). In contrast, cyclin E$^{361-388}$ peptides containing phosphorylation at Thr^{380} alone (*lane 4*) or in combination with Ser^{372} and Ser^{384} (*lanes 5* and *7*) interacted efficiently with Fbw7. In the context of Thr^{380} phosphorylation, phosphorylation at either Ser^{372} or Ser^{384} did not enhance association with Fbw7 (Fig. 3*B*, *lanes 5* and *7*). Thus, within the context of immobilized peptides *in vitro*, phosphorylation of Thr^{380} appears to be the major determinant in Fbw7 binding to the C-terminal phosphodegron.

Interaction of Fbw7 with a Phosphodegron Centered at Thr^{62}—Mutation of Thr^{62} to alanine leads to reduced cyclin E turnover upon expression of Fbw7 (Fig. 2) (21). A major question that emerges is whether cyclin E employs phosphorylated Thr^{62} as a phosphodegron or whether the effects on cyclin E abundance are indirect. The budding yeast Fbw7 isolog Cdc4 is known to preferentially interact with sequences having the consensus (I/L)(P/I/L)pTPP (where pT represents phosphotyrosine) (18). Whereas positions −2 and −1 in the potential Thr^{62} degron are compatible with this consensus, peptide array data would indicate that the potential Thr^{62} phosphodegron would be blocked from binding, due to the presence of lysine at +3 (18). In model peptides, those containing lysine or arginine at +3 were found to not interact with Cdc4. To directly examine whether the Thr^{62} region can act as a phosphodegron, we synthesized peptides encompassing Thr^{62} in phosphorylated and unphosphorylated forms and tested them for binding to Fbw7 as described above (Fig. 3, *A* and *B*). In addition, we also synthesized peptides that contained phosphoserine at position 58 (35). Fbw7 did not interact with unphosphorylated cyclin E$^{50-69}$ or with cyclin E$^{50-69}$ phosphorylated at Ser^{58} (Fig. 3*A*, *lanes 8* and *10*). However, Fbw7 did interact with Thr^{62}-phosphorylated cyclin E$^{50-69}$ (Fig. 3*B*, *lane 9*). The extent of interaction was similar to that seen with Thr^{380} phosphorylated cyclin E$^{361-388}$ (Fig. 3*B*, *lane 3*). The interaction of Thr^{62}-phosphorylated cyclin E$^{50-69}$ was not enhanced by phosphorylation at Ser^{58} in the context of this synthetic phosphodegron (Fig. 3*B*, *lane 11*). Thus, phosphorylation of Thr^{62} could, in principle, serve to directly target cyclin E to Fbw7.

Distinct Phosphodegrons in Cyclin E Interact with an Overlapping Binding Site on Fbw7—The finding that Fbw7 can interact with two distinct phosphodegrons in cyclin E in the context of synthetic peptides raises the question of whether these distinct motifs interact with Fbw7 through the same recognition site. To examine this issue, two experiments were performed. One approach took advantage of a collection of point mutations in the WD40 propeller of Fbw7, which are known to reduce binding to phosphorylated cyclin E. In particular, three arginine residues (Arg^{385}, Arg^{425}, and Arg^{463}, using the Fbw7β protein as reference) (Fig. 3*E*) have been shown to be important for interaction with human cyclin E (17), and the equivalent residues in Cdc4 have been shown to be important for binding to Sic1 and phosphodegrons derived from Sic1 (18) (Fig. 3*F*). We reasoned that if Thr^{62}- and Thr^{380}-derived peptides interact in a similar way with Fbw7, then mutations in these arginine residues would decrease binding to both phosphopeptides. To examine this, these three Fbw7 mutants were produced by *in vitro* translation and tested for interaction with phospho-Thr^{62}- and phospho-Thr^{380}-containing peptides. We found that the R385A mutant was strongly defective in association with both the Thr^{62}- and the Thr^{380}-based peptides, with the interaction being undetectable (Fig. 3*C*, *lanes 6* and *10*). Mutations in Arg^{425} and Arg^{463} displayed reduced interactions compared with wild-type controls, but interaction with both the Thr^{62}- and Thr^{380}-derived peptides were reduced to similar extents. These data are consistent with the idea that overlapping binding sites are used to bind both peptides.

If similar binding sites are used by both peptides, one would expect that the presence of one peptide in solution would compete with Fbw7 for binding to the second peptide immobilized to agarose. To establish this competition assay, Fbw7 was added to mixtures of immobilized phospho-Thr^{380} cyclin E$^{361-388}$ peptide and increasing amounts of either phos-

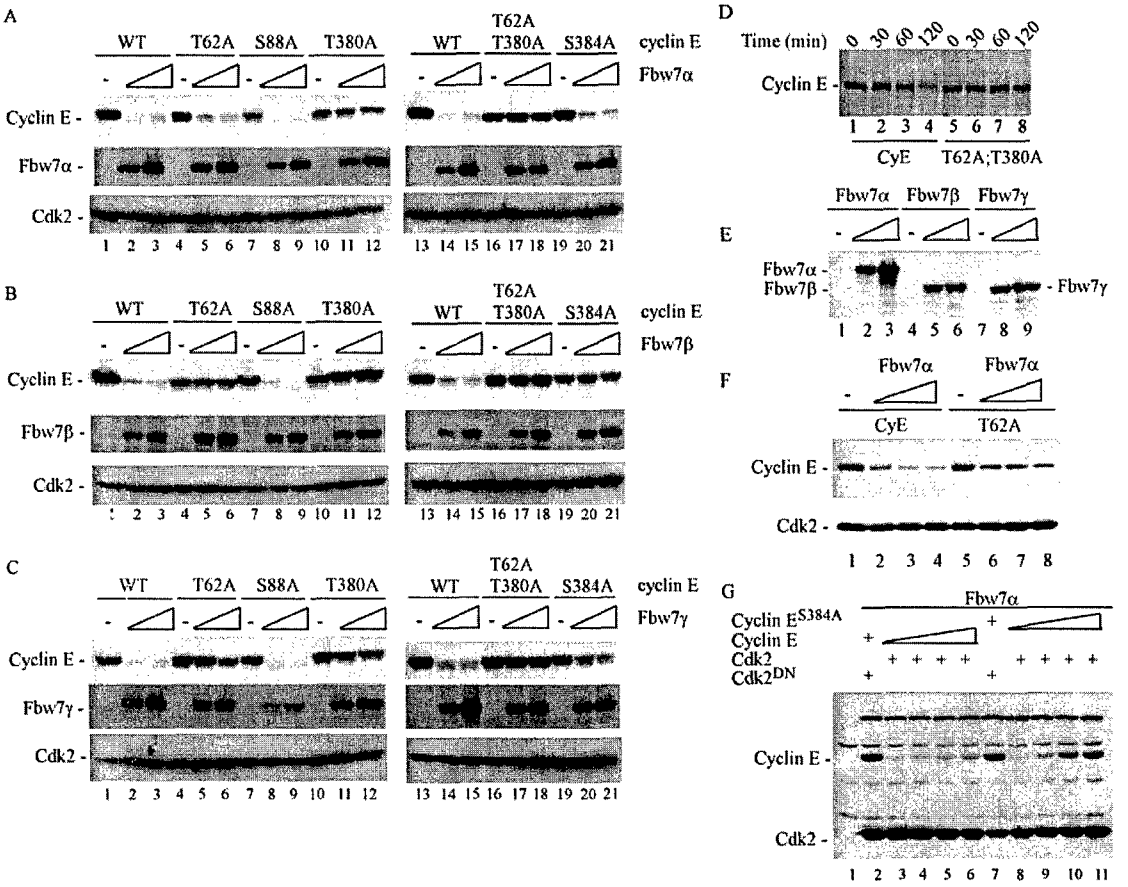

FIG. 2. ***In vivo* degradation of cyclin E phosphorylation site mutants by Fbw7 isoforms.** *A–C*, plasmids expressing the indicated FLAG-tagged Fbw7 isoforms were transfected into 293T cells (6-cm dish) together with vectors expressing Myc-tagged cyclin E mutants and Cdk2. After 36 h, cells were lysed, and immunoblots were probed with either anti-FLAG, anti-Cdk2, or anti-Myc antibodies. The quantities of plasmids employed were 1.5 and 3.0 μg for pCMV-FLAG-Fbw7, 0.3 μg for pCS2-Myc-cyclin E, and 1.5 μg of pCMV-Cdk2. *D*, pulse-chase analysis of Fbw7α-driven cyclin E turnover in 293T cells. Pulse-chase experiments were performed as described under "Materials and Methods." *E*, similar levels of Fbw7 proteins are expressed in cyclin E turnover assays. Extracts from co-transfection studies performed in Fig. 3, *A–C* (*lanes 1–3*), were subjected to immunoblotting using anti-FLAG antibodies to demonstrate comparable levels of Fbw7 proteins. *F*, analysis of cyclin E^{T62A} turnover by Fbw7α at lower Fbw7α/cyclin E ratios. Transfections were performed in 10-cm dishes using 2 μg of pCS2-Myc-cyclin E, 4 μg of pCMV-Cdk2, and 0, 2, 4, and 8 μg of pCMV-Fbw7α expression plasmids. *G*, constant amounts of pCMV-Fbw7α (0.25 μg) and pCMV-Cdk2 (3 μg) expression plasmids were co-transfected with increasing amounts of pCMV-Myc-cyclin E or pCMV-Myc-cyclin E^{S384A} plasmids (0.3, 0.6, 0.9, or 1.2 μg). After 48 h, extracts were subjected to immunoblotting with anti-cyclin E and anti-Cdk2 antibodies.

phorylated or unphosphorylated cyclin E$^{50-69}$ peptide in solution. After mixing, the extent of association of Fbw7 with immobilized cyclin E$^{361-388}$ was determined by SDS-PAGE (Fig. 3*D*). Whereas unphosphorylated Thr^{62} cyclin E$^{50-69}$ had no effect on the association of Fbw7 with cyclin E$^{361-388}$, phospho-Thr^{62} cyclin E$^{50-69}$ dramatically decreased the efficiency of Fbw7 association with cyclin E$^{50-69}$ (Fig. 3*D*). Taken together, these data indicate that Fbw7 is capable of interacting with phospho-Thr^{62} and phospho-Thr^{380} peptides through a single interaction site composed of a cluster of arginine residues.

Association of Cyclin E Phosphorylation Site Mutants with Fbw7 in Vivo—The data described above suggested the possibility that Thr^{62}, in addition to Thr^{380}, could be employed for Fbw7 association with cyclin E *in vivo*. To examine whether dual modes of interaction occur with intact cyclin E, binding experiments were performed with a series of cyclin E mutants and Fbw7α after transfection in 293T cells. The ability to accurately assess binding interactions requires that comparable levels of cyclin E mutants be expressed. However, mutation of Thr^{380}, and to a lesser extent Thr^{62}, leads to increased steady-state levels of cyclin E in the presence of FLAG-Fbw7 expression (data not shown). Therefore, to achieve approximately equal levels of cyclin E expression, we also co-transfected vectors expressing a dominant negative form of Cul1 (Cul1^{DN}), which contains the Skp1 binding site but lacks the Rbx1 binding site. This form of Cul1 sequesters Skp1·F-box complexes and leads to stabilization of SCF targets (16, 37). As expected, expression of Cul1^{DN} leads to equal accumulation of all cyclin E mutants examined, despite the presence of FLAG-Fbw7α (Fig. 4*A*, *lanes 1–5*). Extracts from cells expressing mutant cyclin E proteins and FLAG-Fbw7α were then subjected to immunoprecipitation using anti-FLAG antibodies, and the levels of associated cyclin E were examined by immunoblotting. Cyclin E efficiently associated with Fbw7α (Fig. 4*A*, *lane 1*). Interestingly, cyclin E^{T380A} was found to associate weakly with Fbw7α (*lane 3*), but mutation of Thr^{62} to alanine in the context of the T380A mutant further reduced the interaction with Fbw7α (Fig. 4*A*, *lane 4*). Mutation of Thr^{62} in cyclin E to alanine also led to a reduction in the extent of Fbw7α binding (Fig. 4*B*, *lane 2*).

The reduced association between Fbw7α and cyclin E^{T62A} could reflect either a significant utilization of phosphorylated Thr^{62} in binding to Fbw7α or could potentially reflect alterations in the phosphorylation of Thr^{380}. To examine this issue, we tested the extent of phosphorylation of Thr^{380} in the context of the T62A mutation under the same conditions employed in Fig. 4*A*. Lysates from transfected cells were immunoprecipitated with anti-Myc antibodies, and the levels of total cyclin E-

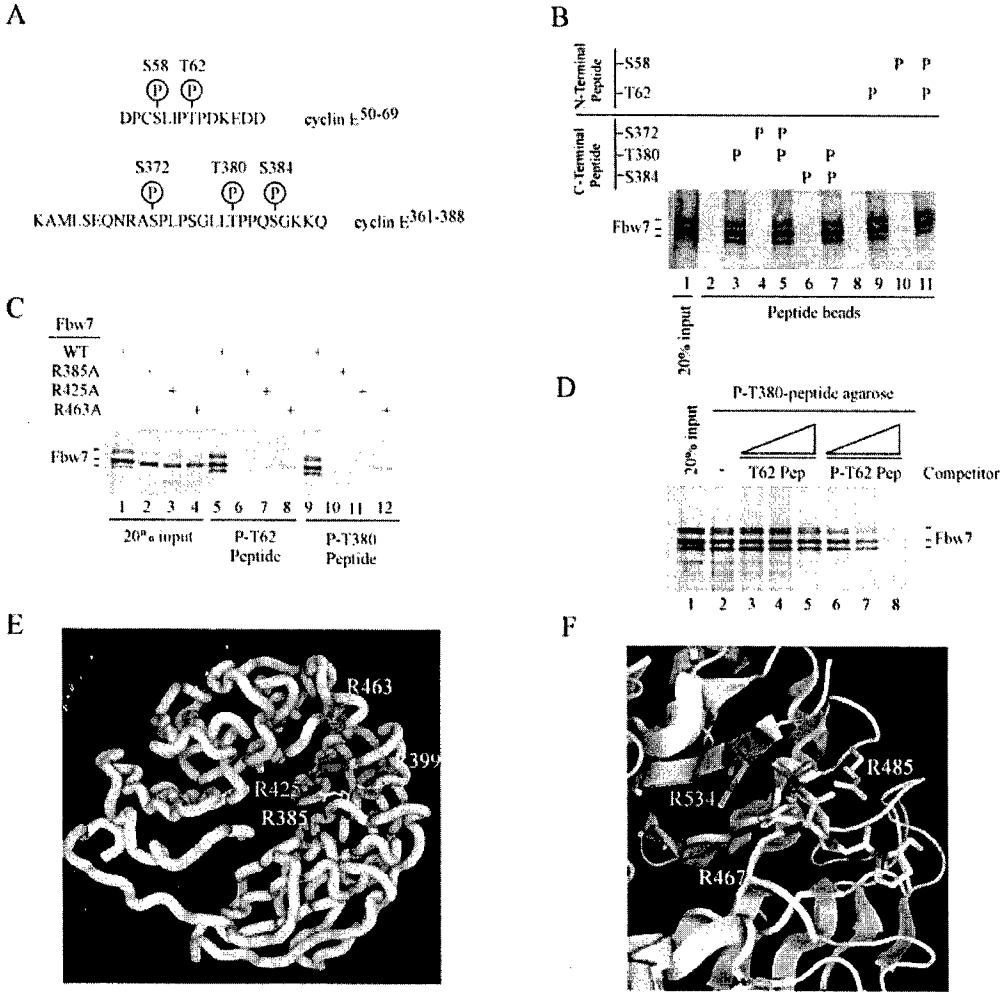

FIG. 3. **Recognition of Fbw7 by cyclin E phosphodegrons centered at Thr^{62} and Thr^{380}.** *A*, amino acid sequences of phosphopeptide degrons used in these studies. *B*, phosphorylation dependence for degron association. Cyclin E$^{361-388}$ and cyclin E$^{50-69}$, phosphorylated at the indicated positions, were immobilized on agarose beads and used in *in vitro* binding reactions with Fbw7β. With cyclin E$^{361-388}$, phosphorylation at Thr^{380} was sufficient for interaction (*lane 3*). With cyclin E$^{50-69}$, phosphorylation of Thr^{62} was sufficient for interaction (*lane 9*). *C*, arginine residues in the WD40-propeller of Fbw7β are required for association of the cyclin E$^{50-69}$ phosphodegron. Binding assays using the indicated immobilized peptides were performed using *in vitro* translated Fbw7 mutants. *D*, phospho-Thr^{62} cyclin E$^{50-69}$ competes with phospho-Thr^{380} cyclin E$^{361-388}$ for association with Fbw7. Fbw7 binding with immobilized phospho-Thr^{380} cyclin E$^{361-388}$ was performed in the presence of phosphorylated or unphosphorylated cyclin E$^{50-59}$. The quantities of soluble peptide used were 0, 25, 50, and 100 μg. *E*, model of the human Fbw7 WD40 propeller generated using Swissmodel with yeast Cdc4 as the template. Arg^{385}, Arg^{425}, and Arg^{463} implicated in association with cyclin E-derived phosphodegrons are shown, as is Arg^{399}, which is implicated on the basis of the Cdc4/phosphodegron structure. *F*, structure of Cdc4 bound to a phosphodegron containing the sequence LpTPP (24). The phosphodegron is shown in *green*, with the phosphate in *purple*. Arg^{467}, Arg^{485}, and Arg^{534} in Cdc4 correspond to Arg^{385}, Arg^{399}, and Arg^{425} in human Fbw7. Graphics were generated using Pymol.

and Thr^{380}-phosphorylated cyclin E determined by immunoblotting (Fig. 4*B*). We found that replacement of T62 with alanine significantly reduced the extent of Thr^{380} phosphorylation. The extent of reduction was comparable with the reduction seen in the association of Fbw7α with cyclin E^{T62A}. Transfection of cyclin E mutants in the absence of Fbw7 and Cul1^{DN} demonstrated that the effect on Thr^{380} phosphorylation was independent of these two components (data not shown). Taken together, these data indicate that mutation of Thr^{62} affects Thr^{380} phosphorylation, and the majority of its contribution to Fbw7-mediated turnover appears to be indirect.

Involvement of Ser^{384} in Recognition of Cyclin E by Fbw7—Results described above indicate that cyclin E^{S384A} is partially defective in degradation by Fbw7 with turnover by Fbw7β being affected to the greatest extent. To examine whether this reflects recognition by Fbw7, we compared the ability of Fbw7α and -β isoforms to immunoprecipitate cyclin E^{S384A} in transfected 293T cells (Fig. 5). Interestingly, cyclin E^{S384A} bound more weakly to both Fbw7 isoforms (*lanes 3* and *6*) than did wild-type cyclin E, suggesting a significant decrease in affinity in the context of full-length proteins *in vivo*. Association of cyclin E with Fbw7β was substantially lower than with the α isoform, possibly reflecting the fact that Fbw7β is largely cytoplasmic, whereas cyclin E is largely nuclear. Importantly, cyclin E^{S384A} maintained wild-type levels of Thr^{380} phosphorylation, as determined by immunoblots of cyclin E immune complexes using anti-phospho-T380 antibodies (Fig. 4*B*).

Mutation of Ser^{384} Affects the Nuclear/Cytoplasmic Ratio of Cyclin E—As stated above, the Fbw7β isoform was profoundly defective in degradation of cyclin E^{S384A} in transfection experiments, whereas the α and γ isoforms were less defective. Because our previous experiment revealed that Fbw7α and Fbw7γ are predominantly nuclear, whereas Fbw7β is localized to the cytoplasm, we examined whether the inability of Fbw7β to degrade cyclin E^{S384A} could result from aberrant intracellular shuttling of this mutant. Previous studies have demonstrated that cyclin E shuttles from the nucleus to the cytoplasm (38). To determine whether cyclin E^{S384A} accumulates in the

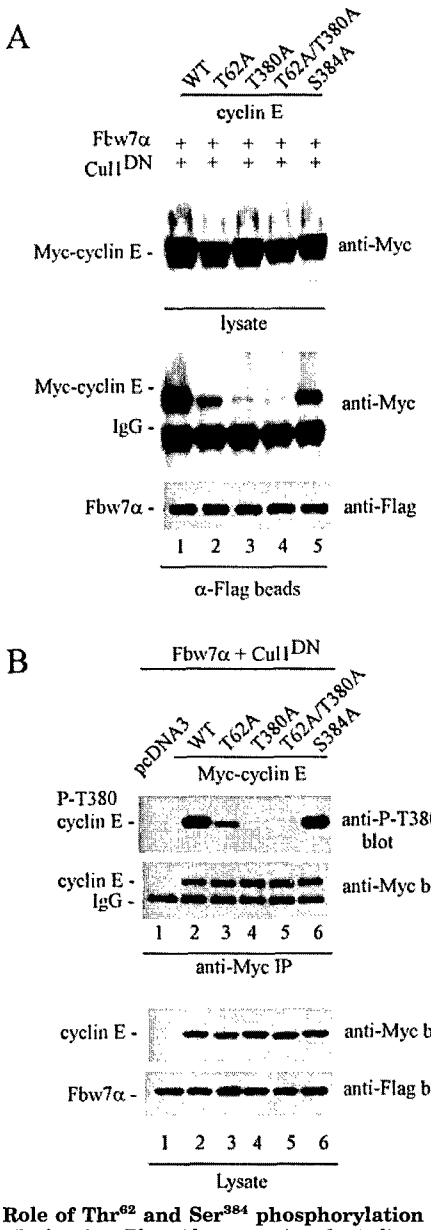

FIG. 4. **Role of Thr^{62} and Ser^{384} phosphorylation in assembly with Fbw7α *in vivo*.** Plasmids expressing the indicated Myc-tagged cyclin E proteins were co-transfected with plasmids expressing FLAG-Fbw7α in the presence of pCMV-Cul1^{DN}. After 36 h, lysates were either directly immunoblotted for cyclin E or subjected to immunoprecipitation using anti-FLAG antibodies prior to immunoblotting. *B*, anti-cyclin E immune complexes were subjected to immunoblotting with anti-phospho-Thr^{380} antibodies, and the blot was stripped and reprobed with anti-cyclin E antibodies. Corresponding cell extracts were probed with anti-Myc antibodies to detect cyclin E and anti-FLAG antibodies to detect Fbw7α.

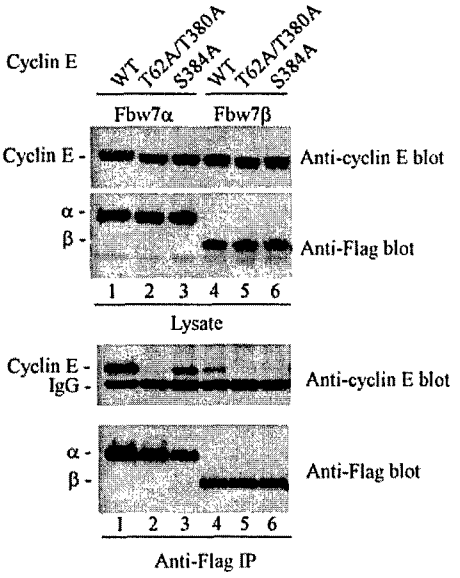

FIG. 5. **Mutation of Ser^{384} in cyclin E reduces association with Fbw7α and β isoforms.** Vectors expressing wild-type cyclin E and the indicated cyclin E mutants were cotransfected with vectors expressing Cul1^{DN} and either FLAG-Fbw7α or FLAG-Fbw7β. After 36 h, lysates were either directly immunoblotted for cyclin E or subjected to immunoprecipitation using anti-FLAG antibodies prior to immunoblotting.

nucleus more efficiently than wild-type cyclin E or other cyclin E mutants that are prone to Fbw7β-mediated degradation, we measured the nuclear/cytoplasmic ratios for cyclin E and the mutants used in this study (Fig. 6). The indicated plasmids were expressed in 293T cells and the levels of cytoplasmic and nuclear cyclin E were determined by immunofluorescence and quantitative image analysis (Fig. 6*B*). Wild-type cyclin E as well as the T62A, S88A, and T380A mutants displayed comparable nuclear/cytoplasmic ratios. In contrast, the nuclear/cytoplasmic ratio of cyclin E^{S384A} was 2-fold larger, indicating defects in nuclear export for this mutant protein (Fig. 6*A*). Thus, defects in turnover of cyclin E^{S384A} by Fbw7β may reflect both decreased affinity and decreased accessibility due to nuclear accumulation of this cyclin E mutant.

DISCUSSION

WD40 repeats in F-box proteins serve as receptors for recognition of phosphodegrons (5, 24, 25). Two distinct WD40/phosphodegron complexes have been examined structurally. The *Saccharomyces cerevisiae* Cdc4 WD40 propeller uses multiple arginine residues to interact with a single phosphothreonine in phosphodegrons derived from Sic1 or cyclin E (24), whereas human β-TRCP employs a large basic surface to interact with dual phosphoserines in a β-catenin-derived phosphodegron (25). Interestingly, the ability of Cdc4 to interact with its sole essential G_1 target, the Cdk inhibitor Sic1, depends upon the number of G_1 Cdk-generated phosphodegrons present in Sic1 (18). In general, each of these phosphodegrons binds weakly to Cdc4 in isolation, but occupancy of six sites allows for facile Sic1 ubiquitination and turnover. The use of a large number of relatively weak interactions allows for ultrasensitivity in the response of Sic1 turnover to G_1 Cdk activity (reviewed in Refs. 39 and 40). The extent to which other SCF^{Cdc4} substrates use multiple phosphorylation events to control turnover is unclear.

In this report, we examined how phosphorylation regulates the interaction of cyclin E with its cognate E3, SCF^{Fbw7}. Fbw7, the closest homolog of Cdc4 in the human genome, exists as three distinct isoforms, α, β, and γ, which display tissue-specific expression patterns (17, 21, 26, 36). Differences in Fbw7 isoforms are concentrated at the N terminus and are not expected *per se* to affect association with substrates via the C-terminal WD40 repeats. The localization properties of endogenous Fbw7 isoforms are unknown due to the absence of antibodies suitable for immunofluorescence. Therefore, we employed transient transfection of epitope-tagged versions of Fbw7α, -β, and -γ to examine the localization properties of these proteins. Fbw7α and -γ are found in the nucleus in 293T cells, whereas Fbw7β appears to be exclusively cytoplasmic. The localization of Fbw7β in the cytoplasm probably reflects the presence of a transmembrane domain not present in the α and γ isoforms (17, 36). Co-expression of Fbw7β with a vector expressing an endoplasmic reticulum marker (GFP-ER) dem-

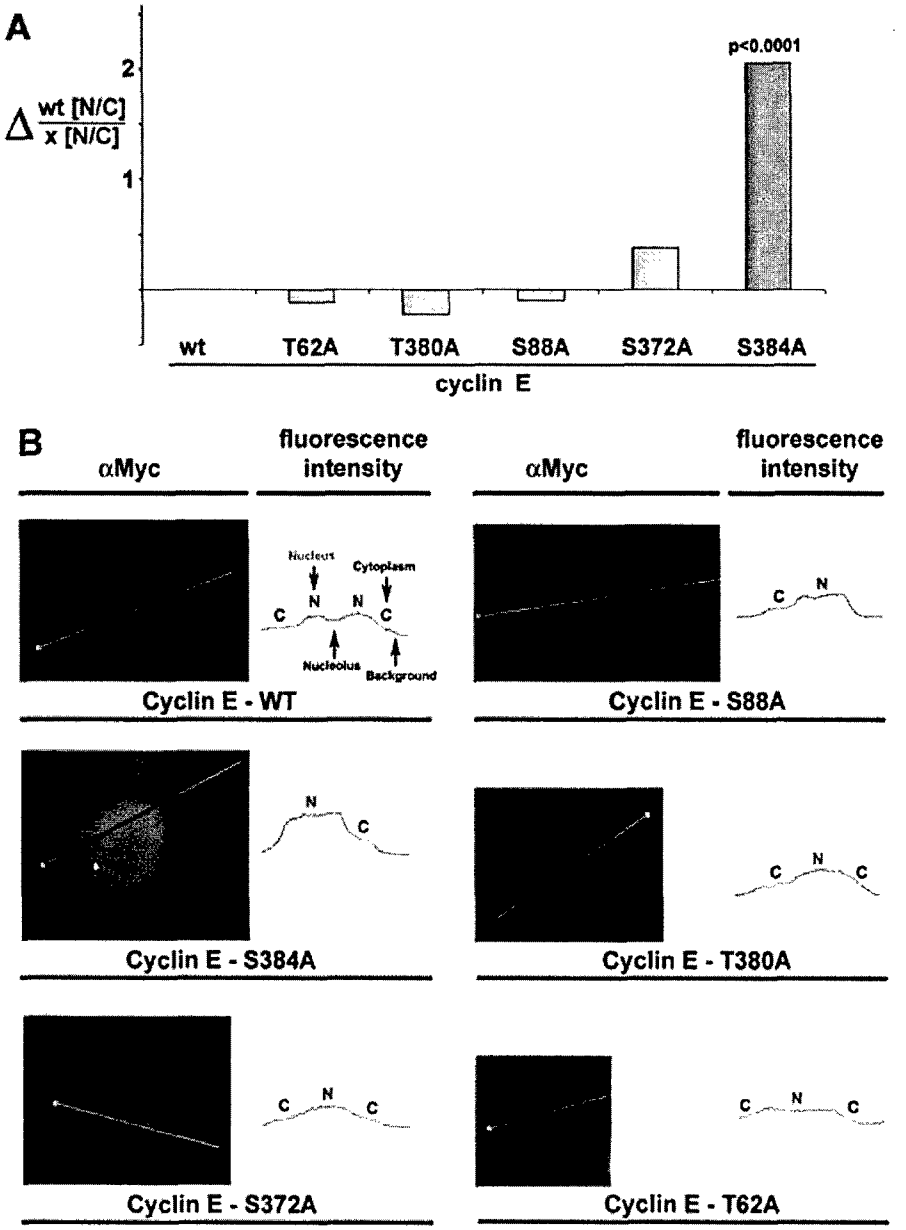

FIG. 6. **Mutation of Ser^{384} to alanine affects subcellular shuttling of cyclin E.** *A*, quantitative analysis of nuclear/cytoplasmic fluorescence intensity ratio in 293T cells subjected to indirect immunofluorescence 48 h post-transfection with five phosphorylation-deficient cyclin E point mutants (T62A, T380A, S88A, and S372A) and wild-type cyclin E reveals significantly enhanced nuclear accumulation of cyclin E^{S384A} protein as compared with wild-type cyclin E and four other cyclin E mutants. The quantities of all plasmids utilized and the exposure times were constant (1.0 μg and 1 s, respectively). Results represent averaged and normalized ($N_x/C_x - N_{wt}/C_{wt}$) values for 15 cells for each construct. *B*, representative cells expressing wild-type cyclin E as well as cyclin E phosphorylation-deficient mutants and respective immunofluorescence profiles are shown. *N*, nucleus; *C*, cytoplasm.

onstrated significant overlap of the fluorescence patterns, suggesting that Fbw7β is at least partially associated with endoplasmic reticulum membranes (data not shown).

Cyclin E has long been known to be phosphorylated on Thr^{380} through an autocatalytic function involving Cdk2 (33, 34), but recent experiments (35) also suggest a role for GSK3β in this process, functioning in an apparently redundant manner with Cdk2. Mutation of Thr^{380} to alanine leads to significant stabilization of cyclin E, implicating this phosphorylation event in cyclin E turnover. A role for this residue is also consistent with the finding that phosphopeptides encompassing Thr^{380} are capable of binding to Fbw7 (17). However, evidence of the involvement of Thr^{62} and Ser^{384} has also been presented (21, 35). Mutation of Thr^{62} partially stabilizes cyclin E to Fbw7β overexpression (35) and enhances the stabilization of the cyclin E^{T380A} mutant (21). However, Thr^{62} has not been demonstrated to be phosphorylated *in vivo*, and it is not clear whether it plays a direct or indirect role in cyclin E turnover. Likewise, mutation of Ser^{384} to alanine also leads to partial stabilization of cyclin E in an Fbw7β-driven turnover assay (35), again through an unknown mechanism. Although the finding that cytoplasmic Fbw7β overexpression can promote degradation of cyclin E (which is primarily nuclear) seems counterintuitive, we note that cyclin E is initially synthesized in the cytoplasm, where it assembles with Cdk2. In this context, newly synthesized cyclin E was generated by ectopic expression in the assays performed here and may be readily destroyed via an Fbw7β-mediated mechanism. Moreover, cyclin E is known to shuttle from the nucleus to the cytoplasm in a Crm1-independent pathway (38). Thus, elevated levels of Fbw7β, through the destruction of cytoplasmic cyclin E, could force the equilibrium in favor of nuclear export, thereby leading to depletion of the nuclear pool of cyclin E. Further studies are required to determine what Fbw7 isoforms are directly involved in cyclin E turnover *in vivo*.

In this paper, we systematically examined the role of various phosphorylation events in the interaction between cyclin E and Fbw7 as well as the ability of individual Fbw7 isoforms to promote turnover of various phosphorylation site mutants in cyclin E. We initially used mass spectrometry to establish

phosphorylation sites in cyclin E. Consistent with recent data using conventional peptide mapping (35), we found that cyclin E is phosphorylated on three sites near the C terminus (Ser^{372}, Thr^{380}, and Ser^{384}). Whereas Thr^{380} is phosphorylated directly by Cdk2, Ser^{384} does not conform to a Cdk2 site, yet its phosphorylation is Cdk2-dependent (35). We also detected phosphorylation of Ser^{88}, a candidate Cdk2 site that was not identified previously. As with other studies (35), we were unable to unequivocally identify Thr^{62}-phosphorylated peptides by mass spectrometry, possibly due to the large size of this tryptic peptide. However, phosphospecific antibodies against Thr^{62} unequivocally demonstrated that Thr^{62} in cyclin E is phosphorylated in 293T cells. However, the stoichiometry of phosphorylation of this residue and how this process is regulated is currently unknown.

Two parallel series of experiments were performed to examine the consequences of phosphorylation at these sites. First, we examined the ability of Fbw7 isoforms to promote cyclin E degradation *in vivo*. Wild-type cyclin E was efficiently degraded by all three Fbw7 isoforms, as were cyclin E^{S88A} and cyclin E^{S372A}. As expected, we found that mutation of Thr^{380}, and to a lesser extent Thr^{62}, led to defects in cyclin E turnover. This defect was independent of Fbw7 isoform. Cyclin E^{S384A} also displayed defects in turnover, but degradation by Fbw7β was affected to the greatest extent. We note that high levels of cyclin E^{S384A} are also substantially resistant to degradation induced by Fbw7α. The stoichiometric relationship between cyclin E and Fbw7 isoforms *in vivo* is not known, and further studies need to be performed to understand what Fbw7 isoforms are most important for cyclin E turnover *in vivo*.

We then went on to examine how various phosphorylation events in cyclin E promote the interaction with Fbw7. Initially, we used phosphopeptides centered at Thr^{380} and Thr^{62} and tested these for binding to Fbw7 *in vitro*. Phosphorylation of Thr^{380} is sufficient to allow for interaction of the C-terminal phosphodegron with Fbw7. Peptides phosphorylated at Ser^{372} or Ser^{384} alone were not capable of interacting with Fbw7, and phosphorylation at these sites did not enhance interaction of phospho-Thr^{380} peptides with Fbw7 in the context of the *in vitro* binding assay. Consistent with this, cyclin E^{T380A} demonstrated a greatly reduced ability to interact with Fbw7α in transfected cells. These data are consistent with previous studies indicating that a single phosphorylation event in a related cyclin E-derived peptide is sufficient for interaction with budding yeast Cdc4 *in vitro* (18). Interestingly, we found that peptides containing phospho-Thr^{62} were also capable of interacting efficiently with Fbw7, whereas phosphorylation of Ser^{58} did not support interaction with cyclin E. The interaction of phospho-Thr^{62}-containing peptides with Fbw7 required the same Fbw7 binding site as used by Thr^{380} peptides. Thus, in principle, this Thr^{62} phosphorylation could be involved directly in cyclin E recognition by Fbw7 independent of Thr^{380} phosphorylation. To examine this issue further, we determined the effects of replacement of Thr^{62} by alanine on the interaction of cyclin E with Fbw7 *in vivo*. The major effect found with cyclin E^{T62A} is a dramatic reduction in the extent of Thr^{380} phosphorylation, as measured using a phosphospecific antibody against Thr^{380}, indicating at least a partially indirect effect of this mutation on interaction with and turnover by Fbw7α. However, residual association of cyclin E^{T380A} with Fbw7α was reduced further upon mutation of Thr^{62}, indicating a direct, albeit small, contribution of Thr^{62} to Fbw7α recognition. The mechanism by which mutation of Thr^{62} to alanine affects phosphorylation of Thr^{380} is unknown. Although the direct contribution of Thr^{62} to cyclin E turnover appears to be small under the conditions examined here, we cannot exclude the possibility that Thr^{62} phosphorylation may be used in particular circumstances and be a major determinant of cyclin E degradation. For example, the stoichiometry of phosphorylation under the conditions examined here may be small relative to that of Thr^{380} phosphorylation, but this need not always be the case *in vivo*. Identification of the Thr^{62} kinase is required to address this issue in greater depth.

Our data as well as that of Welcker *et al.* (35) indicate that mutation of Ser^{384} to alanine blocks effective turnover of cyclin E by Fbw7. As assessed by immunoprecipitation in transfected cells, mutation of Ser^{384} to alanine substantially reduces the association of cyclin E with Fbw7, suggesting that Ser^{384} phosphorylation contributes to binding to Fbw7. Using quantitative imaging, we found that, with the exception of cyclin E^{S384A}, all of the other cyclin E proteins tested displayed indistinguishable nuclear/cytoplasmic ratios when transiently expressed in 293T cells. However, cyclin E^{S384A} displayed a dramatic (more than 2-fold) increase in the nuclear/cytoplasmic ratio. Thus, the defects seen in degradation of cyclin E^{S384A} by Fbw7β may reflect, in part, the inaccessibility of the cyclin E^{S384A} mutant with the Fbw7β isoform. Interestingly, c-Myc has recently been demonstrated to be ubiquitinated by SCF^{Fbw7} in a phosphorylation-dependent manner (28, 29). In this case, Thr^{58} is phosphorylated by GSK3β, and Ser^{62} is phosphorylated by a mitogen-activated protein kinase. In this case, Thr^{58} phosphorylation depends absolutely on prior phosphorylation of Ser^{62}. The phosphodegron in c-Myc (LPpTPPLpSP) is quite similar to that found in cyclin E (LLpTPPQpSG). Because of the dependence of Ser^{62} phosphorylation on Thr^{58} phosphorylation, it has not been possible to examine whether Ser^{62} phosphorylation contributes to association of c-Myc with Fbw7, but in the case of synthetic peptides, the Thr^{58} phosphopeptide binds to Fbw7 independently of Ser^{62} phosphorylation (28). Taken together, our studies reveal a complex interplay between phosphorylation of cyclin E and control of its degradation by Fbw7 and reveal that mutational analysis of cyclin E can in some cases lead to apparent indirect effects in its turnover by altering phosphorylation and/or localization.

REFERENCES

1. Deshaies, R. J. (1999) *Annu. Rev. Cell Dev. Biol.* **15,** 435–467
2. Koepp, D. M., Harper, J. W., and Elledge, S. J. (1999) *Cell* **97,** 431–434
3. Patton, E.E., Willems, A. R., and Tyers, M. (1998) *Trends Genet.* **14,** 236–243
4. Feldman, R. M., Correll, C. C., Kaplan, K. B., and Deshaies, R. J. (1997) *Cell* **91,** 221–230
5. Skowyra, D., Craig, K. L., Tyers, M., Elledge, S. J., and Harper, J. W. (1997) *Cell* **91,** 209–219
6. Patton, E. E., Willems, A. R., Sa, D., Kuras, L., Thomas, D., Craig, K. L., and Tyers, M. (1998) *Genes Dev.* **12,** 692–705
7. Seol, J. H., Feldman, R. M., Zachariae, W., Shevchenko, A., Correll, C. C., Lyapina, S., Chi, Y., Galova, M., Claypool, J., Sandmeyer, S., Nasmyth, K., Shevchenko, A., and Deshaies, R. J. (1999) *Genes Dev.* **13,** 1614–1626
8. Zheng, N., Schulman, B. A., Song, L., Miller, J. J., Jeffrey, P. D., Wang, P., Chu, C., Koepp, D. M., Elledge, S. J., Pagano, M., Conaway, R. C., Conaway, J. W., Harper, J. W., and Pavletich, N. P. (2002) *Nature* **416,** 703–709
9. Skowyra, D., Koepp, D. M., Kamura, T., Conrad, M. N., Conaway, R. C., Conaway, J. W., Elledge, S. J., and Harper, J. W. (1999) *Science* **284,** 662–665
10. Bai, C., Sen, P., Hofmann, K., Ma, L., Goebl, M., Harper, J. W., and Elledge, S. J. (1999) *Cell* **86,** 263–274
11. Cenciarelli, C., Chiaur, D. S., Guardavaccaro, D., Parks, W., Vidal, M., and Pagano, M. (1999) *Curr. Biol.* **9,** 1177–1179
12. Kipreos, E. T., and Pagano, M. (2000) *Genome Biol.* **1,** 3002.1–3002.7
13. Winston, J. T., Koepp, D. M., Zhu, C., Elledge, S. J., and Harper, J. W. (1999) *Curr. Biol.* **9,** 1180–1182
14. Carrano, A. C., Eytan, E., Hershko, A., and Pagano, M. (1999) *Nat. Cell Biol.* **1,** 193–199
15. Latres, E., Chiaur, D. S., and Pagano, M. (1999) *Oncogene* **18,** 849–854
16. Jin, J., Shirogane, T., Xu, L., Nalepa, G., Qin, J., Elledge, S. J., and Harper, J. W. (2003) *Genes Dev.* **17,** 3062–3074
17. Koepp, D. M., Schaefer, L. K., Ye, X., Keyomarsi, K., Chu, C., Harper, J. W., and Elledge, S. J. (2001) *Science* **294,** 173–177
18. Nash, P., Tang, X., Orlicky, S., Chen, Q., Gertler, F. B., Mendenhall, M. D., Sicheri, F., Pawson, T., and Tyers, M. (2001) *Nature* **414,** 514–521
19. Shirane, M., Hatakeyama, S., Hattori, K., Nakayama, K., and Nakayama, K. (1999) *J. Biol. Chem.* **274,** 28169–28174
20. Spencer, E., Jiang, J., and Chen, Z. J. (1999) *Genes Dev.* **13,** 284–294
21. Strohmaier, H., Spruck, C. H., Kaiser, P., Won, K.-A., Sangfelt, O., and Reed,

S. I. (2001) *Nature* **413,** 316–322
22. Winston, J. T., Strack, P., Beer-Romero, P., Chu, C. Y., Elledge, S. J., and Harper, J. W. (1999) *Genes Dev.* **13,** 270–283
23. Yaron, A., Hatzubai, A., Davis, M., Lavon, I., Amit, S., Manning, A. M., Andersen, J. S., Mann, M., Mercurio, F., and Ben-Neriah, Y. (1998) *Nature* **396,** 590–594
24. Orlicky, S., Tang, X., Willems, A. R., Tyers, M., and Sicheri, F. (2003) *Cell* **112,** 243–256
25. Wu, G., Xu, G., Schulman, B. A., Jeffrey, P. D., Harper, J. W., and Pavletich, N. P. (2003) *Mol. Cell* **11,** 1445–1456
26. Moberg, K. H., Bell, D. W., Wahrer, D. C. R., Haber, D. A., and Hariharan, I. K. (2001) *Nature* **413,** 311–316
27. Hubbard, E. J., Wu, G., Kitajewski, J., and Greenwald, I. (1997) *Genes Dev.* **11,** 3182–3193
28. Welcker, M., Orian, A., Jin, J., Grim, J. A., Harper, J. W., Eisenman, R. N., and Clurman, B. E. (2004) *Proc. Natl. Acad. Sci. U. S. A.* **101,** 9085–9090
29. Yada, M., Hatakeyama, S., Kamura, T., Nishiyama, M., Tsunematsu, R., Imaki, H., Ishida, N., Okumura, F., Nakayama, K., and Nakayama, K. I. (2004) *EMBO J.* **23,** 2116–2125
30. Moberg, K. H., Mukherjee, A., Veraksa, A., Artavanis-Tsakonas, S., and Hariharan, I. K. (2004) *Curr. Biol.* **14,** 965–974
31. Nateri, A. S., Riera-Sans, L., Da Costa, C., and Behrens, A. (2004) *Science* **303,** 1374–1378
32. Tetzlaff, M. T., Yu, W., Li, M., Zhang, P., Finegold, M., Mahon, K., Harper, J. W., Schwartz, R. J., and Elledge, S. J. (2004) *Proc. Natl. Acad. Sci. U. S. A.* **101,** 3338–3345
33. Clurman, B. E., Sheaff, R. J., Thress, K., Groudine, M., and Roberts, J. M. (1996) *Genes Dev.* **10,** 1979–1990
34. Won, K. A., and Reed, S. I. (1996) *EMBO J.* **15,** 4182–4193
35. Welcker, M., Singer, J., Loeb, K. R., Grim, J., Bloecher, A., Gurien-West, M., Clurman, B. E., and Roberts, J. M. (2003) *Mol. Cell* **12,** 381–392
36. Spruck, C. H., Strohmaier, H., Sangfelt, O., Muller, H. M., Hubalek, M., Muller-Holzner, E., Marth, C., Widschwendter, M., and Reed, S. I. (2002) *Cancer Res.* **62,** 4535–4539
37. Donzelli, M., Squatrito, M., Ganoth, D., Hershko, A., Pagano, M., and Draetta, G. F. (2002) *EMBO J.* **21,** 4875–4884
38. Jackman, M., Kubota, Y., den Elzen, N., Hagting, A., and Pines, J. (2002) *Mol. Biol. Cell.* **13,** 1030–1045
39. Deshaies, R. J., and Ferrell, J. E., Jr. (2001) *Cell* **107,** 819–822
40. Harper, J. W. (2002) *Trends Cell Biol.* **12,** 104–107

quencing reactions with purified PCR products were performed by using Big Dye Terminator chemistry and forward or reverse primers in separate sequencing reactions (Applied Biosystems, Foster City, CA). Reactions were analyzed by using a 3700 Sequence Analyzer (Applied Biosystems). Sequence traces were automatically analyzed by using PhredPhrap and Polyphred (*47*, *48*). For SNPs identified through this analysis, PCR Invader assays (Third Wave Technologies, Madison, WI) were designed and tested on 90 samples from the Polymorphism Discovery Resource panel (PDR90) (*49*). Successful assays were subsequently used to analyze samples from our study. Genotypes were assigned automatically by cluster analysis (M. Olivier *et al.*, in preparation). Differences among genotypes were analyzed by one-way ANOVA using STATVIEW 4.1 software (Abacus Concepts, Inc., Berkeley, CA). SNPs 1 to 4 are available in dbSNP under accession numbers ss3199913, ss3199914, ss3199915, and ss3199916, respectively.

35. Subjects were a combined subset of 501 healthy, nonsmoking Caucasian individuals aged >20 years (429 men, 72 women) who had participated in previous dietary intervention protocols (*50*, *51*) (R. M. Krauss *et al.*, unpublished data). All subjects had been free of chronic disease during the previous 5 years and were not taking medication likely to interfere with lipid metabolism. In addition, they were required to have plasma total cholesterol concentrations <6.74 mmol/liter (260 mg/dl), triacylglycerol <5.65 mmol/l (500 mg/dl), resting blood pressure <160/105 mm Hg, and body weight <130% of ideal. Each participant signed a consent form approved by the Committee for the Protection of Human Subjects at E. O. Lawrence Berkeley National Laboratory, University of California, Berkeley, and participated in a medical interview. Fasting blood samples were obtained from subjects eating their usual diets, and after 4 to 6 weeks of consuming diets containing high fat (35 to 46% energy) and low fat (20 to 24% energy) (*50*, *51*). Plasma lipid and lipoprotein measurements were performed as previously described (*50*, *51*). In addition, on the high- and low-fat diets, total lipoprotein mass was measured by analytic ultracentrifugation (*50*, *51*).
36. Of the 501 individuals in the original study, 388 were successfully genotyped by PCR amplification for the Sst I polymorphism as previously described (*16*, *28*).
37. To genotype the C/T SNP3 polymorphisms upstream of *APOAV*, oligonucleotides AV6-F-5′-GATTGATTCAAGATGCATTTAGGAC-3′ and AV6-R-5′-CCCCAGGAACTGGAGCGAAATT were used to amplify a 187-bp fragment from genomic DNA. The penultimate base in AV6-R was changed to T to create a Mse I site (TTAA) in the common allele. The PCR reactions were performed in 20 μl volumes containing 50 mmol/liter KCl, 10 mmol/liter tris (pH 8.3), 1.5 mmol/liter $MgCl_2$, 0.2 mmol/liter of each dNTP, 1 U of *Taq* DNA polymerase, and 200 pmol/liter of each primer. DNA was amplified under the following conditions: initial denaturation of 96°C for 2 min, followed by 32 cycles of 94°C for 15 s, 55°C for 30 s, and 72°C for 30 s, and a final step at 72°C for 3 min. PCR product (20 μl) was digested with 10 U of Mse I (New England Biolabs) at 37°C for 3 hours. The PCR products were size-fractionated on 3% agarose gels, stained with ethidium bromide, and visualized on an ultraviolet transilluminator.
38. S. F. Altschul, W. Gish, W. Miller, E. W. Myers, D. J. Lipman, *J. Mol. Biol.* **215**, 403 (1990).
39. K. Osoegawa *et al.*, *Genome Res.* **10**, 116 (2000).
40. I. Dubchak *et al.*, *Genome Res.* **10**, 1304 (2000).
41. G. G. Loots *et al.*, *Science* **288**, 136 (2000).
42. C. Mayor *et al.*, *Bioinformatics* **16**, 1046 (2000).
43. A. Lupas, M. Van Dyke, J. Stock, *Science* **252**, 1162 (1991).
44. H. Nielsen, J. Engelbrecht, S. Brunak, G. von Heijne, *Protein Eng.* **10**, 1 (1997).
45. C. C. Allain, L. S. Poon, C. S. Chan, W. Richmond, P. C. Fu, *Clin. Chem.* **20**, 470 (1974).
46. E. M. Beasley, R. M. Myers, D. R. Cox, L. C. Lazzeroni, *PCR Applications* (Academic Press, San Diego, CA, 1999).
47. D. A. Nickerson, V. O. Tobe, S. L. Taylor, *Nucleic Acids Res.* **25**, 2745 (1997).
48. B. Ewing, P. Green, *Genome Res.* **8**, 186 (1998).
49. C. A. Mein *et al.*, *Genome Res.* **10**, 330 (2000).
50. R. M. Krauss, D. M. Dreon, *Am. J. Clin. Nutr.* **62**, 478S (1995).
51. D. M. Dreon, H. A. Fernstrom, P. T. Williams, R. M. Krauss, *Arterioscler. Thromb. Vasc. Biol.* **17**, 707 (1997).
52. Animals were killed, and tissues were harvested for either total RNA isolation by using the RNAeasy-midi protocol (Qiagen) or for poly(A)$^+$ mRNA isolation by using the FastTrack 2.0 system (Invitrogen, Carlsbad, CA). About 10 μg of total RNA or 2 μg of poly(A)$^+$ mRNA were separated in 1.0% agarose by gel electrophoresis and the RNA was transferred to a charged nylon membrane (Ambion, Austin, TX). The RNA blots were hybridized with [α-^{32}P]dCTP random-primed *apoAV* probes in ULTRAhyb buffer (Ambion). Probe templates were generated by PCR amplification of liver cDNA with degenerate primers degApoAV-F2-5′-GCGCGTGGTGGGRGAAGACA-3′ and degApoAV-R2-TCGCGCAGCTGGTCCAGGTT-3′. Filters were washed in 2× saline sodium citrate at room temperature for 20 min and in 0.1× SSC at 42°C for 20 min, followed by autoradiography visualization.
53. M. Olivier, unpublished observations.
54. R. M. Krauss, unpublished observations.
55. R. C. Lewontin, *Genetics* **120**, 849 (1988).
56. We thank H. Hobbs, J. Fruchart, A. Plump, C. Prange-Pennacchio and members of the Rubin laboratory for thoughtful discussions; E. Gong, K. Houston, K. Lewis, W. Dean, J.-F. Cheng, I. Dubchak, J. Schwartz, V. Afzal, and X. Yang for technical support; V. Bustos, K. Sheppard, D. Zierten, A. de Witte, R. Freudenberg, J. Bushard, A. Almendras, and A. Indap for assistance with sequencing and genotyping; and P. Blanche, L. Holl, and J. Orr for performing lipoprotein measurements. This work was supported by the National Dairy Promotion and Research Board in cooperation with the National Dairy Council and NIH-NHBLI grant HL-18574 (R.M.K., E.M.R.), the NIH-NHLBI Programs for Genomic Application Grant HL66681 (E.M.R.), through the U.S. Department of Energy under contract no. De-AC03-76SF00098 (E.M.R.), HL-53917 (J.C.C.), and an appointment to the Alexander Hollaender Distinguished Postdoctoral Fellowship Program sponsored by the U.S. Department of Energy, Office of Biological and Environmental Research, and administered by the Oak Ridge Institute for Science and Education (L.A.P.).

30 July 2001; accepted 4 September 2001

Phosphorylation-Dependent Ubiquitination of Cyclin E by the SCF^{Fbw7} Ubiquitin Ligase

Deanna M. Koepp,[1,2,3] Laura K. Schaefer,[1,2,3]* Xin Ye,[1]* Khandan Keyomarsi,[4] Claire Chu,[1] J. Wade Harper,[1] Stephen J. Elledge[1,2,3]†

Cyclin E binds and activates the cyclin-dependent kinase Cdk2 and catalyzes the transition from the G_1 phase to the S phase of the cell cycle. The amount of cyclin E protein present in the cell is tightly controlled by ubiquitin-mediated proteolysis. Here we identify the ubiquitin ligase responsible for cyclin E ubiquitination as SCF^{Fbw7} and demonstrate that it is functionally conserved in yeast, flies, and mammals. Fbw7 associates specifically with phosphorylated cyclin E, and SCF^{Fbw7} catalyzes cyclin E ubiquitination in vitro. Depletion of Fbw7 leads to accumulation and stabilization of cyclin E in vivo in human and *Drosophila melanogaster* cells. Multiple F-box proteins contribute to cyclin E stability in yeast, suggesting an overlap in SCF E3 ligase specificity that allows combinatorial control of cyclin E degradation.

Passage through the cell cycle is controlled by the activity of cyclin-dependent kinases (CDKs) (*1*). Cyclin E is the regulatory subunit of Cdk2 and controls the G_1 to S phase transition, which is rate-limiting for proliferation. Cyclin E is tightly regulated by ubiquitin-mediated proteolysis, which requires phosphorylation on Thr^{380} and Cdk2 activation (*2*–*4*). Failure to properly regulate cyclin E accumulation can lead to accelerated S phase entry (*5*), genetic instability (*6*), and tumorigenesis (*7*). Elucidating the mechanism controlling cyclin E destruction has important implications for understanding control of cell proliferation during development and its subversion by tumorigenesis.

The formation of polyubiquitin-protein conjugates, which are recognized and destroyed by the 26*S* proteasome, involves three components that participate in a cascade of ubiquitin transfer reactions: a ubiquitin-activating enzyme (E1), a ubiquitin-conjugating enzyme (E2), and a specificity factor (E3) called a ubiquitin ligase (*8*). E3s control the specificity of target protein selection and therefore are key to controlling individual target protein abundance.

The SCF (Skp1/Cullin/F-box protein) comprises a large family of modular E3s that control ubiquitination of many substrates in a phosphorylation-dependent manner (*9*). SCF complexes contain four subunits: Skp1, Cul1 (Cdc53), Rbx1, and an F-box–containing pro-

[1]Department of Biochemistry and Molecular Biology, [2]Department of Molecular and Human Genetics, [3]Howard Hughes Medical Institute, Baylor College of Medicine, Houston, TX, 77030, USA. [4]Department of Experimental Radiation Oncology, M. D. Anderson Cancer Center, Houston, TX 77030, USA

*These authors contributed equally to this work.
†To whom correspondence should be addressed. E-mail: selledge@bcm.tmc.edu

tein. F-box proteins, over 50 of which have been identified in mammals (*10*, *11*), bind Skp1 through the F-box motif (*12*) and mediate substrate specificity of SCF complexes by binding substrates through protein-protein interaction domains, often WD40 repeats or leucine-rich repeats (LRRs) (*13*, *14*).

Several observations suggest that accumulation of cyclin E might be controlled through the SCF pathway. Cyclin E, like many SCF substrates, requires phosphorylation for destruction, and mice lacking Cul1 accumulate cyclin E (*15*, *16*). Because Cul3 mutant mice also show increased amounts of cyclin E (*17*), it is not clear if the effects of either cullin are direct. Stability of cyclin E expressed in *Saccharomyces cerevisiae* depends on phosphorylation of Thr^{380}, suggesting a conserved mechanism in yeast and mammals (*3*). Therefore, we exploited the genetics of *S. cerevisiae* to explore the contribution of SCF to cyclin E ubiquitination. We used a stability assay to perform a pulse-chase analysis of cyclin E protein in wild-type and *skp1-11*, *cdc34-2*, or *cdc53-1* mutants. To prevent cell cycle position effects, we arrested cells in S phase by addition of 200 mM hydroxyurea throughout the experiment. Cyclin E was unstable in wild-type cells but stabilized in SCF mutant cells (Fig. 1A). We examined cyclin E stability in yeast F-box protein mutant strains *cdc4-1*, *grr1*, *ydr219*, *yjl149*, *yml088/ufo1*, *ynl230/ela1*, *ynl311*, and *yor080/dia2*. Cyclin E was stabilized in *cdc4-1* strains to an extent similar to that seen with core SCF mutants and was also stabilized in *yor080* mutants (Fig. 1A). Cdc4 and Yor080 contain WD40 and LRR motifs, respectively. We incubated recombinant SCF^{Cdc4} and SCF^{Yor080} complexes with recombinant cyclin E–Cdk2, E1, Cdc34 (E2), Ub, and adenosine triphosphate (ATP) (Fig. 1B). Ubiquitination of cyclin E was detected with both complexes in an F-box– and ubiquitin-dependent manner (Fig. 1B). Ubiquitination was also stimulated by phosphorylated cyclin E as it was largely prevented when catalytically inactive cyclin E–$Cdk2^{KD}$ complexes were used as substrate (Fig. 1B).

To find the mammalian F-box protein that recognizes cyclin E, we surveyed previously identified F-box proteins (*11*) for those that bound cyclin E either after coexpression in insect cells or in vitro using ^{35}S-methionine–labeled translation products and immobilized glutathione *S*-transferase (GST)–cyclin E–CDK2 complexes. Seventeen F-box proteins were tested, including 16 that contained either WD40 or LRR motifs (*18*). Of these, only the WD40-containing Fbw7 (*19*) bound specifically to GST–cyclin E–Cdk2 but not to GST alone (Fig. 1C) (*20*). This interaction was specific

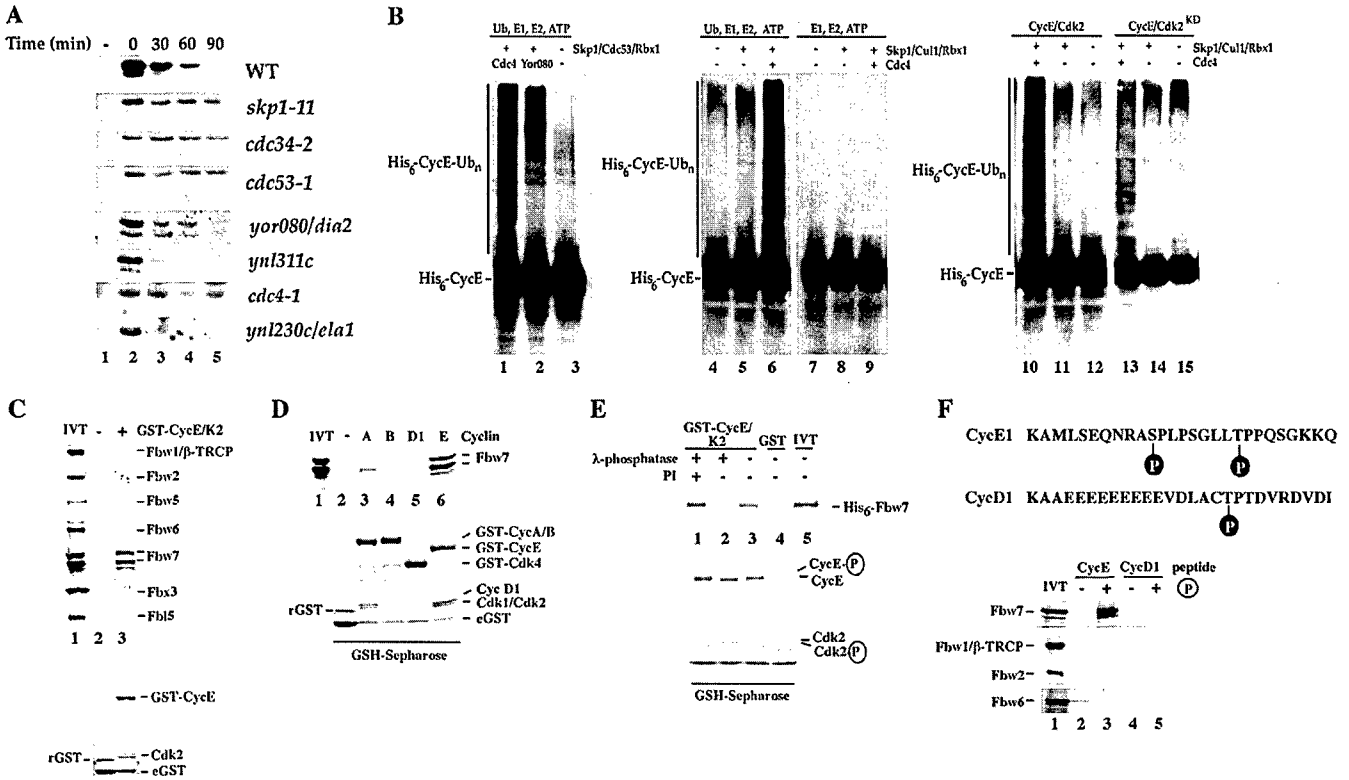

Fig. 1. Interaction between cyclin E and SCF components in yeast and mammalian cells. (**A**) Stabilization of cyclin E in *skp1-11*, *cdc34-2*, *cdc53-1*, *cdc4-1*, and *yor080* mutants (*12*, *30*). Strains of the indicated genotypes were grown in medium containing raffinose; cyclin E expression was induced for 1 hour by galactose addition and at time = 0 was repressed by addition of glucose. Cells were harvested at the indicated times, and the abundance of cyclin E was determined by immunoblotting. Extracts from uninduced cells are shown in lane 1. WT, wild type. (**B**) Cyclin E is ubiquitinated in vitro by SCF complexes. SCF^{Cdc4} or SCF^{Yor080} complexes were purified from insect cells (*13*) and supplemented with ubiquitin (Ub), E1, Cdc34 (E2), and ATP, as indicated, before addition of His_6–cyclin E–Cdk2 purified from insect cells (*13*). (**C**) GST–cyclin E–Cdk2 binds Fbw7. Immobilized GST–cyclin E–Cdk2 (lane 3) or GST (lane 2) was incubated with in vitro–translated F-box proteins (*31*, *32*). Lane 1 contains in vitro translation (IVT) product (33% of input). The bottom panel shows GST–cyclin E–Cdk2 and GST as detected by Coomassie staining. The positions of endogenous insect cell GST protein (eGST) and recombinant GST (rGST) are indicated. (**D**) Fbw7 preferentially binds cyclin E–Cdk2. The indicated Cdk complexes (lanes 2 to 6) were purified from insect cells and used for in vitro binding with Fbw7 as above. Cyclins were fused to GST for affinity purification, except for cyclin D1 where GST-Cdk4 is used. (**E**) Phosphorylation-dependent association of Fbw7 with cyclin E–Cdk2. Immobilized GST–cyclin E–Cdk2 was treated with λ-phosphatase in the presence (lane 1) or absence (lane 2) of phosphatase inhibitors (PI) before in vitro binding to His_6-Fbw7. Untreated GST–cyclin E–Cdk2 (lane 3) and GST (lane 4) were used as controls. Binding reactions were performed as in (C). (**F**) Immobilized cyclin E– or cyclin D–derived peptides with or without phosphorylation were incubated with Fbw7, Fbw1 (β-TRCP), Fbw2, and Fbw6 IVT products as in (C). The peptide sequence and sites of phosphorylation (P) are indicated (*33*).

for cyclin E as Fbw7 did not interact tightly with other cyclin-Cdk complexes (Fig. 1D). The interaction between Fbw7 and cyclin E was phosphorylation-dependent (Fig. 1E). Furthermore, Fbw7 bound specifically to a phosphopeptide containing the region of cyclin E required genetically for ubiquitination (Fig. 1F). Thus, the properties of Fbw7 are consistent with the predicted properties of a cyclin E ubiquitin ligase.

The mouse and human Fbw7 cDNA encodes a protein of 627 amino acids containing seven WD40 repeats (Fig. 2, A and B). The presence of stop codons in all three reading frames of the 5′ untranslated region (UTR) indicates that the encoded open reading frame (ORF) is full-length. Database searches revealed substantial sequence similarity with *Caenorhabditis elegans sel-10*, which is involved in the presenilin (*sel-12*) and Notch/lin-12 pathways (*21*), and the predicted protein encoded by *Drosophila melanogaster* CG15010 (*DmFbw7*). Among *S. cerevisiae* F-box proteins, Fbw7 is 28% identical to Cdc4 (Fig. 2A). The relationship between *sel-10* and a partial cDNA containing two COOH-terminal WD40 repeats from Fbw7 was noted previously (*21*). The extreme NH_2-terminus of Fbw7 contains a 23-residue stretch (residues 7 to 29) of highly hydrophobic amino acids recognized by the SMART protein analysis program as a transmembrane domain (*22*).

To examine the importance of the WD40 motifs in cyclin E recognition, we searched for basic residues located on the surface of the β-propeller structure that are conserved in Hs-Fbw7, Cdc4, Sel-10, and DmFbw7 but not in other Fbw proteins. Such residues would be candidates for phosphorylation-dependent interaction with ubiquitination targets. Arg^{417}, Arg^{457}, and Arg^{495}, located in WD40 repeats 3, 4, and 5, met these criteria (Fig. 2, A and D). These residues were independently replaced with alanine, and the resulting proteins were tested for binding to GST–cyclin E in vitro. Mutation of Arg^{417} or Arg^{457} abolished binding to cyclin E, whereas mutation of Arg^{495} reduced binding (Fig. 2C).

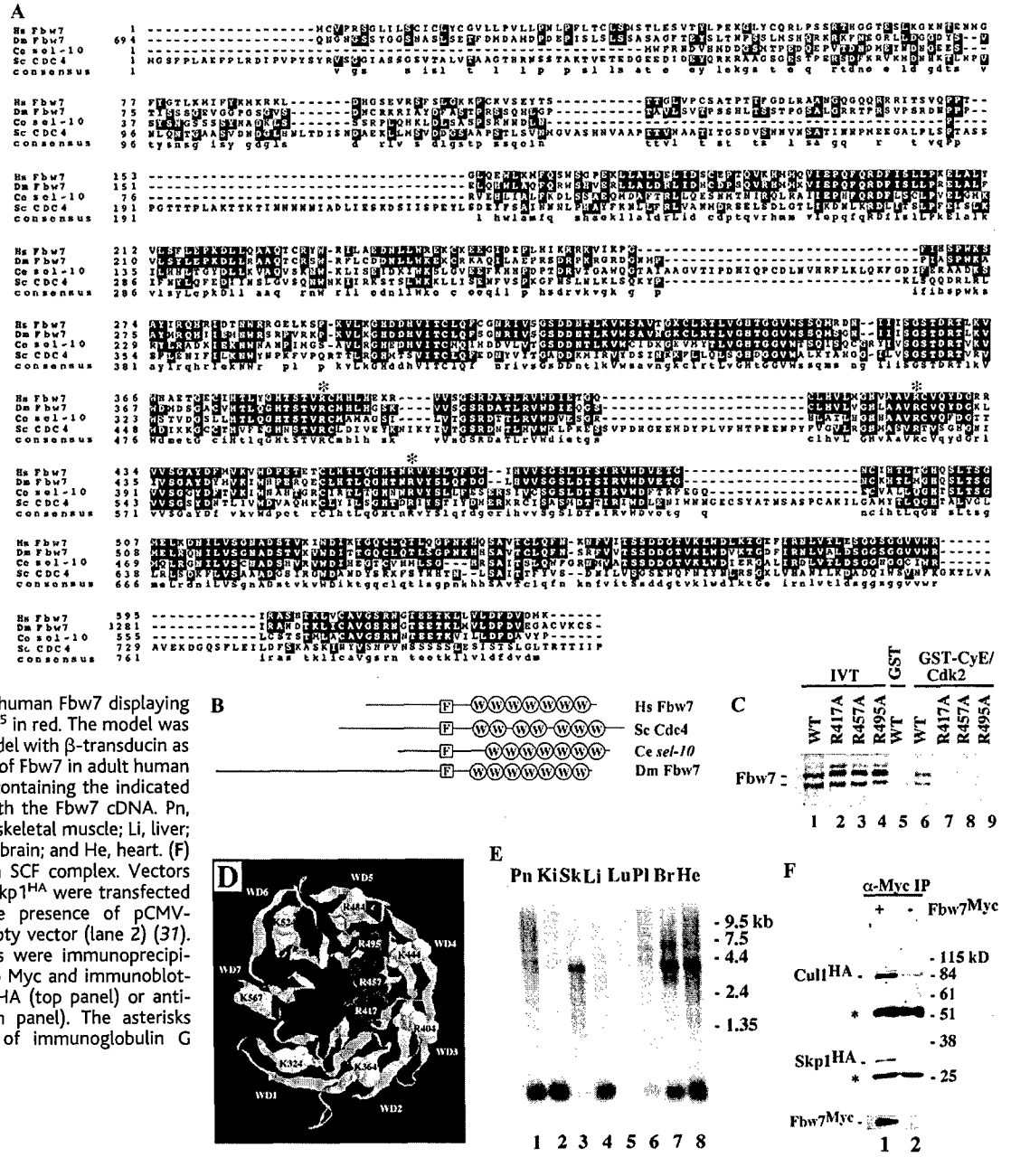

Fig. 2. Characterization of the WD40-repeat–containing F-box protein, Fbw7. **(A)** Conservation between human (Hs) Fbw7 and *C. elegans* (Ce) *sel-10*, *S. cerevisiae* (Sc) Cdc4, and *D. melanogaster* (Dm) Fbw7 (*33*). Identical residues are shaded black and similarities are shaded gray. Asterisks indicate conserved arginine residues required for cyclin E binding. **(B)** Domain structures of Fbw7 homologs. F, F-box; W, WD40 repeat. **(C)** Three surface arginines on Fbw7 are required for binding cyclin E. Wild-type (WT) and mutant Fbw7 IVT products were used for binding with GST–cyclin E–Cdk2 (lanes 6 to 9) or GST (lane 5). One-third of the input is shown (lanes 1 to 4). **(D)** Model of the β-propeller structure of human Fbw7 displaying Arg^{417}, Arg^{457}, and Arg^{495} in red. The model was generated with Swissmodel with β-transducin as template. **(E)** Expression of Fbw7 in adult human tissues. Northern blots containing the indicated mRNAs were probed with the Fbw7 cDNA. Pn, pancreas; Ki, kidney; Sk, skeletal muscle; Li, liver; Lu, lung; Pl, placenta; Br, brain; and He, heart. **(F)** Fbw7 assembles into an SCF complex. Vectors expressing $Cul1^{HA}$ and $Skp1^{HA}$ were transfected into 293T cells in the presence of pCMV-$Fbw7^{Myc}$ (lane 1) or empty vector (lane 2) (*31*). After 48 hours, extracts were immunoprecipitated with antibodies to Myc and immunoblotted with antibodies to HA (top panel) or antibodies to Myc (bottom panel). The asterisks indicate the positions of immunoglobulin G heavy and light chains.

Fbw7 mRNA is abundant in adult brain, heart, and skeletal muscle, tissues with a high percentage of terminally differentiated cells (Fig. 2E). Cotransfection of vectors encoding Myc-tagged Fbw7 with hemagglutinin (HA)-tagged Cul1 and HA-tagged Skp1 in 293T cells allowed detection of Fbw7 in SCF complexes, consistent with involvement of Fbw7 in ubiquitination (Fig. 2F).

We tested cyclin E ubiquitination in reticulocyte lysates in which either Fbw7 or Fbw2 had been translated. Ubiquitinated forms of cyclin E were observed in the presence of Fbw7 but not Fbw2 (Fig. 3A). Fbw7-dependent ubiquitination of cyclin E was also achieved in more purified systems. His_6-Fbw7 was affinity-purified on immobilized GST–cyclin E–Cdk2 (Fig. 3, B and C) or antibodies to His_6 (Fig. 3D) and used in ubiquitination reactions. Cyclin E ubiquitination was dependent on Fbw7 (Fig. 3, B and C) and was stimulated by Cul1-Rbx1 (Fig. 3, B to D). A small fraction of Fbw7 was associated with endogenous Cul1 in reticulocyte lysates (*20*). The pattern of conjugates was distinctly different when a form of ubiquitin that cannot undergo polyubiquitination (GST-Ub^{RA}) was included in the reaction mixture (Fig. 3C), indicating that the larger forms of cyclin E are ubiquitin conjugates. The ubiquitination reaction was also stimulated by phosphorylation of cyclin E (Fig. 3D) and was reduced when the cyclin E Thr^{380} → Ala (T380A) mutant was used as substrate (Fig. 3E).

If Fbw7 is rate-limiting for controlling cyclin E abundance, overexpression of Fbw7 should lead to decreased amounts of cyclin E. To test this, we transfected 293T cells with vectors encoding cytomegalovirus (CMV) promoter–driven cyclin E, Cdk2, and either Fbw7 or empty vector and assayed cyclin E amounts by immunoblotting. Cells cotransfected with Fbw7 reproducibly had smaller amounts of cyclin E but constant amounts of Cdk2 (Fig. 4A).

Conversely, inhibition of Fbw7 should lead to increased accumulation of cyclin E. To test this, we used the small interfering RNA (siRNA) technique to reduce expression of Fbw7 in HeLa cells (*23*). Cells transfected with a double-stranded RNA (dsRNA) oligo corresponding to Fbw7 showed increased accumulation of cyclin E when compared with cells transfected with a control dsRNA oligo (Fig. 4B). Amounts of Cdk2 and bulk Cdk2 activity remained unaffected (Fig. 4B) (*20*). The amount of p27 was similar in both Fbw7- and green fluorescent protein (GFP)–inhibited cells at the 48-hour time point, indicating that the accumulation of cyclin E in Fbw7-inhibited cells was not substantially influenced by p27 (*20*). To assess the effect of Fbw7 on cyclin E stability, we used the siRNA-inhibited cells for a pulse-chase analysis of cyclin E (*2*). Cells were labeled in vivo with ^{35}S-methionine, samples were taken at the indicated times after replacement with medium containing unlabeled methionine, and cyclin E was immunoprecipitated (Fig. 4C). In the GFP siRNA cells, cyclin E was unstable, whereas in Fbw7-inhibited cells, cyclin E remains stable for the course of the experiment. Immunoblotting of the immunoprecipitates indicated that cyclin E amounts remained constant throughout the experiment.

We also used the RNA interference (RNAi) technique to ablate Fbw7 in *D. melanogaster* (S2) cells (*24*). Transfection of S2 cells with dsRNAs corresponding to various portions of the *DmFbw7* gene reduced amounts of DmFbw7 mRNA (Fig. 4D) and increased accumulation of cyclin E protein but not that of a control protein, Mle1 (Fig. 4D). In contrast, amounts of cyclin E mRNA were unaltered or slightly reduced, indicating that DmFbw7 regulates cyclin E through a posttranscriptional mechanism. Control dsRNAs had no effect on DmFbw7 or cyclin E (Fig. 4E). RNAi with the COOH-terminal fragment of Fbw7 was less efficient in destabilizing Fbw7 mRNA; thus, smaller increases in cyclin E accumulation were observed.

In this report, we show that SCF^{Fbw7}-related ligases control the stability of cyclin E in a manner conserved through evolution. The finding that different E3s can control cyclin E levels in yeast may have implications for control of cell proliferation in mammals. Such a role would allow multiple signals to be independently integrated through different E3s to control cyclin E levels and cell proliferation. This could allow tissues to exert combinatorial control of proliferation and differentiation, consistent with the tissue-specific expression of

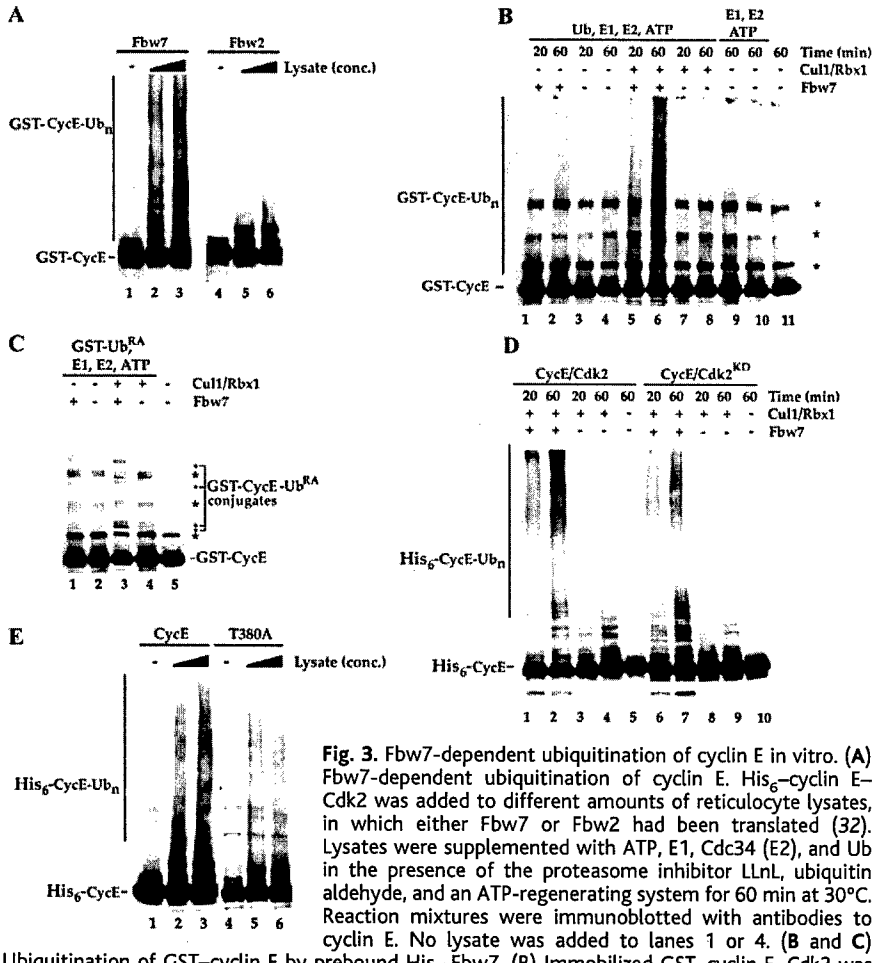

Fig. 3. Fbw7-dependent ubiquitination of cyclin E in vitro. **(A)** Fbw7-dependent ubiquitination of cyclin E. His_6–cyclin E–Cdk2 was added to different amounts of reticulocyte lysates, in which either Fbw7 or Fbw2 had been translated (*32*). Lysates were supplemented with ATP, E1, Cdc34 (E2), and Ub in the presence of the proteasome inhibitor LLnL, ubiquitin aldehyde, and an ATP-regenerating system for 60 min at 30°C. Reaction mixtures were immunoblotted with antibodies to cyclin E. No lysate was added to lanes 1 or 4. **(B and C)** Ubiquitination of GST–cyclin E by prebound His_6-Fbw7. (B) Immobilized GST–cyclin E–Cdk2 was incubated with reticulocyte extracts in the presence or absence of Fbw7. Beads were supplemented with E1, Cdc34 (E2), ATP, and either ubiquitin (Ub; 100 μg/ml) or GST-Ub^{RA} (100 μg/ml). Where indicated, 50 ng of a purified Cul1-Rbx1 complex was added. The asterisks indicate the positions of three proteins that cross react with the monoclonal antibodies to cyclin E. (C) As in (B), but GST-Ub^{RA} was used in place of ubiquitin. **(D)** Cyclin E phosphorylation enhances ubiquitination of cyclin E by SCF^{Fbw7}. Reticulocyte lysates with or without His_6-Fbw7 were immunoprecipitated with antibodies to His tag, supplemented with cyclin E–Cdk2 (or cyclin E–$Cdk2^{KD}$), E1, Cdc34 (E2), ubiquitin, and ATP and incubated at room temperature for the indicated time. Samples were treated as in (B). **(E)** Phophorylation of Thr^{380} enhances ubiquitination of cyclin E. Reactions were performed as in (A), but cyclin E T380A was also used as substrate.

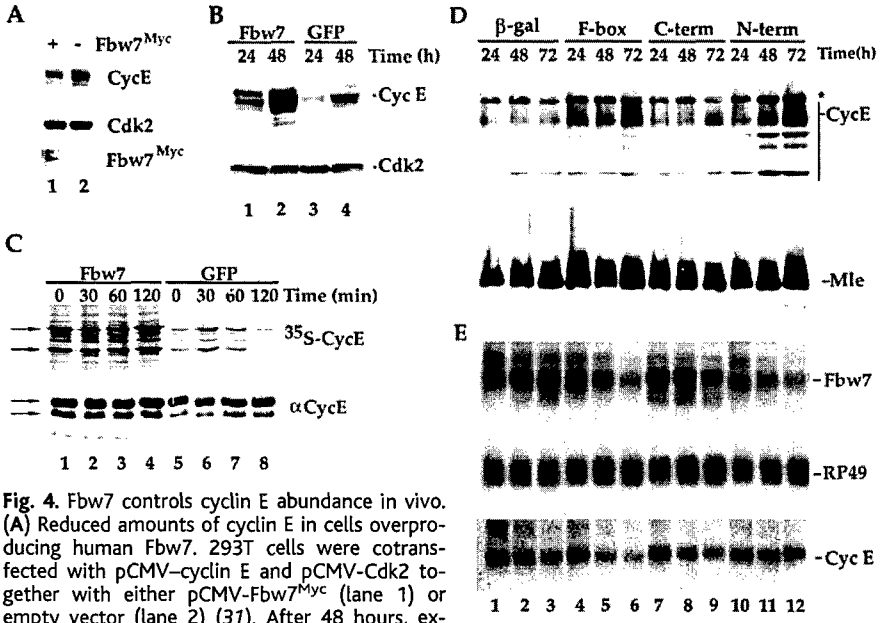

Fig. 4. Fbw7 controls cyclin E abundance in vivo. **(A)** Reduced amounts of cyclin E in cells overproducing human Fbw7. 293T cells were cotransfected with pCMV–cyclin E and pCMV-Cdk2 together with either pCMV-$Fbw7^{Myc}$ (lane 1) or empty vector (lane 2) (*31*). After 48 hours, extracts were prepared and immunoblotted with antibodies to Cdk2, cyclin E, or Myc. **(B)** Accumulation of cyclin E in HeLa cells transfected with Fbw7 siRNA but not GFP siRNA. Cells were transfected as described (*23, 34*). At the indicated times, cells were harvested and cell lysates were generated. Samples were immunoblotted with antibodies to cyclin E or Cdk2. **(C)** Cyclin E is stable in Fbw7-inhibited cells. Cells were transfected as in (B), and pulse-chase analysis was performed as described (*2*). Medium containing unlabeled methionine was added at time = 0. Samples were also immunoblotted with monoclonal antibodies to cyclin E (bottom panel). Arrows indicate the two major forms of cyclin E. **(D and E)** Accumulation of *DmCycE* in response to ablation of *DmFbw7* by RNA interference. S2 cells were transfected with dsRNA corresponding to the NH_2-terminal (N-term), COOH-terminal (C-term), or F-box region of *DmFbw7* or against β-galactosidase (β-gal) as a control (*34*). At the indicated times, cells were harvested and used to generate protein extracts and total RNA. (D) Cell extracts were immunoblotted with polyclonal antibodies against *DmCycE* or *maleless* (Mle). (E) Messenger RNA was subjected to Northern blotting with probes directed toward *DmFbw7*, *DmCycE*, or a ribosomal RNA (RP49).

Fbw7. Cells lacking the F-box protein Skp2 also accumulate cyclin E (*25*). However, this effect may be an indirect result of the accumulation of the Skp2 substrate, p27 (*26, 27*). Individual E3s often control the ubiquitination of multiple substrates (*9*); therefore, controlling accumulation of cyclin E through expression of a particular E3 may limit the function of other signaling pathways as a consequence. Thus, using different E3s to control cyclin E might lead to regulation of different constellations of signaling pathways in a tissue-specific manner. It is likely that Fbw7 controls the ubiquitination of other proteins in addition to cyclin E. Putative substrates include Notch and Presenilin proteins, as the *C. elegans* homolog *sel-10* has been implicated in the control of both Notch and Presenilin signaling (*21, 28*).

As a negative regulator of cyclin E, Fbw7 is a potential tumor suppressor. Consistent with this, we have observed that amounts of Fbw7 mRNA are decreased in breast tumor lines that have increased amounts of cyclin E (see supplemental Web figure 1 on *Science* Online at www.sciencemag.org/cgi/content/full/294/5540/173/DC1). Thus far, we have not identified mutations in the Fbw7 gene in these or other tumors. However, Fbw7 maps to 4q32, a site of loss of heterozygosity in a number of cancers (*29*). Additional studies will be required to resolve Fbw7's role in tumorigenesis.

References and Notes

1. C. J. Sherr, J. M. Roberts, *Genes Dev.* **13**, 1501 (1999).
2. B. E. Clurman, R. J. Sheaff, K. Thress, M. Groudine, J. M. Roberts, *Genes Dev.* **10**, 1979 (1996).
3. K. A. Won, S. I. Reed, *EMBO J.* **15**, 4182 (1996).
4. S. V. Ekholm, S. I. Reed, *Curr. Opin. Cell Biol.* **12**, 676 (2000).
5. M. Ohtsubo, J. M. Roberts, *Science* **259**, 1908 (1993).
6. C. H. Spruck, K. A. Won, S. I. Reed, *Nature* **401**, 297 (1999).
7. K. Keyomarsi, D. Conte Jr., W. Toyofuku, M. P. Fox, *Oncogene* **11**, 941 (1995).
8. A. Hershko, H. Heller, S. Elias, A. Ciechanover, *J. Biol. Chem.* **258**, 8206 (1983).
9. D. M. Koepp, J. W. Harper, S. J. Elledge, *Cell* **97**, 431 (1999).
10. C. Cenciarelli *et al.*, *Curr. Biol.* **9**, 1177 (1999).
11. J. T. Winston, D. M. Koepp, C. Zhu, S. J. Elledge, J. W. Harper, *Curr. Biol.* **9**, 1180 (1999).
12. C. Bai *et al.*, *Cell* **86**, 263 (1996).
13. D. Skowyra, K. L. Craig, M. Tyers, S. J. Elledge, J. W. Harper, *Cell* **91**, 209 (1997).
14. Y. G. Hsiung *et al.*, *Mol. Cell. Biol.* **21**, 2506 (2001).
15. M. J. Dealy *et al.*, *Nature Genet.* **23**, 245 (1999).
16. Y. Wang *et al.*, *Curr. Biol.* **9**, 1191 (1999).
17. J. D. Singer, M. Gurian-West, B. Clurman, J. M. Roberts, *Genes Dev.* **13**, 2375 (1999).
18. F-box proteins tested for cyclin E binding include Fbw1 (β-TRCP), Fbw2 (MD6), Fbw5, Fbw6, Fbw7, Fbl1 (Skp2), Fbl2, Fbl3a, Fbl4, Fbl5, Fbl6, Fbl7, Fbl8, Fbl11, Fbl12, and Fbx3. The Fbw6 construct for in vitro translation was generated from an expressed sequence tag (EST) previously named Fbx29 (GenBank accession number AF176707) (*11*).
19. We previously identified the F-box motif in EST clone AI836688 as Fbx30 (*11*). Further sequence analysis of a longer cDNA (GenBank accession number AY033553) revealed WD40 repeats, and it was renamed Fbw7 according to convention (*10, 11*).
20. D. M. Koepp, L. K. Schaefer, X. Ye, K. Keyomarsi, J. W. Harper, S. J. Elledge, unpublished results.
21. E. J. Hubbard, G. Wu, J. Kitajewski, I. Greenwald, *Genes Dev.* **11**, 3182 (1997).
22. See http://smart.embl-heidelberg.de.
23. S. M. Elbashir *et al.*, *Nature* **411**, 494 (2001).
24. S. M. Hammond, E. Bernstein, D. Beach, G. J. Hannon, *Nature* **404**, 293 (2000).
25. K. Nakayama *et al.*, *EMBO J.* **19**, 2069 (2000).
26. A. C. Carrano, E. Eytan, A. Hershko, M. Pagano, *Nature Cell Biol.* **1**, 193 (1999).
27. C. Spruck *et al.*, *Mol. Cell* **7**, 639 (2001).
28. G. Wu, E. J. Hubbard, J. K. Kitajewski, I. Greenwald, *Proc. Natl. Acad. Sci. U.S.A.* **95**, 15787 (1998).
29. S. Knuutila *et al.*, *Am. J. Pathol.* **155**, 683 (1999).
30. Description of the yeast F-box protein mutants will be presented elsewhere. The Fbw7 ORF lacking the stop codon was amplified by polymerase chain reaction from the EST 3347354 and inserted into pCR2.1 and pcDNA3.1 Myc-His. The His_6-Fbw7 vector was generated similarly except that the amplified ORF contained a stop codon.
31. 293T cells were transfected with Lipofectamine (Invitrogen). For association of cyclin E–Cdk2 and other cyclins with F-box proteins in vitro, immobilized GST-cyclin-Cdk or GST was incubated (1 hour, 4°C) with ^{35}S-methionine–labeled in vitro–translated F-box proteins and washed four times before electrophoresis. In some experiments, GST–cyclin E–Cdk2 was treated with 400 units of λ-phosphatase for 60 min at 30°C and then washed twice before binding.
32. SCF complexes were assembled by coexpression of Flag-Skp1, Cdc53, Rbx1, and either Cdc4 or Yor080 in insect cells and used as described (*13*). Some SCF^{Cdc4} complexes were assembled on GSH-Sepharose (Amersham Pharmacia) with human GST-Cul, Skp1, and Rbx1. His_6-tagged E1 enzyme and Cdc34-E2 were purified from yeast and bacteria, respectively. For ubiquitination in crude extracts, reticulocyte lysates programmed with either Fbw7 or Fbw2 were supplemented with an ATP regeneration system, E1 (100 ng), Cdc34 (E2) (300 ng), ubiquitin (5 μg), and His_6-cyclin E-Cdk2. For ubiquitination of GST–cyclin E prebound to SCF^{Fbw7}, GST–cyclin E–Cdk2 was incubated with reticulocyte lysate programmed with Fbw7 or lysate lacking Fbw7 at 4°C (60 min). Washed complexes were supplemented as described above. To examine ubiquitination by immune complexes containing His_6-Fbw7, we supplemented in vitro–translated His_6-Fbw7 immobilized on antibody to His tag beads as described above.
33. Single-letter abbreviations for the amino acid residues are as follows: A, Ala; C, Cys; D, Asp; E, Glu; F, Phe; G, Gly; H, His; I, Ile; K, Lys; L, Leu; M, Met; N, Asn; P, Pro; Q, Gln; R, Arg; S, Ser; T, Thr; V, Val; W, Trp; and Y, Tyr.
34. RNA interference was performed as described (*24*) except that Effectene (Qiagen) was used for transfection. dsRNAs corresponded to nucleotides 1 to 505 (NH_2-terminal), 2678 to 3159 (F-box), and 3469 to 3981 (COOH-terminal) of the Fbw7 coding region. The siRNA oligo corresponded to nucleotides 713 to 735 of the human Fbw7 coding region.

35. We thank C. Lehner, M. Kuroda, T. Orr-Weaver, R. Duronio, M. Tyers, J. Roberts, I. Greenwald, A. Newman, H. Zheng, and S. Reed for gifts of reagents, plasmids, and helpful discussions and D. Liu for technical assistance. D.M.K. is a fellow with the Helen Hay Whitney Foundation. This work was supported by grants from the NIH and the Department of Defense. S.J.E. is an Investigator with the Howard Hughes Medical Institute.

8 August 2001; accepted 13 August 2001
Published online 30 August 2001;
10.1126/science.1065203
Include this information when citing this paper.

CORRESPONDENCE

Systematic analysis and nomenclature of mammalian F-box proteins

Jianping Jin,[1] Timothy Cardozo,[2] Ruth C. Lovering,[3] Stephen J. Elledge,[4] Michele Pagano,[2,5] and J. Wade Harper[1,6]

[1]Department of Pathology, Harvard Medical School, Boston, Massachusetts 02115, USA; [2]Department of Pathology, New York University School of Medicine, New York, New York 10016, USA; [3]HUGO Gene Nomenclature Committee, Department of Biology, University College London, London, NW1 2HE, United Kingdom; [4]Partners Center for Genetics and Genomics, Department of Genetics, Howard Hughes Medical Institute, Harvard Medical School, Boston, Massachusetts 02115, USA

Much of the targeted protein ubiquitylation that occurs in eukaryotes is performed by cullin-based E3 ubiquitin ligases, which form a superfamily of modular E3s. The best understood cullin-based E3 is the SCF ubiquitin ligase (Feldman et al. 1997; Skowyra et al. 1997), which is composed of a modular E3 core containing CUL1 and RBX1 (also called ROC1), and a substrate specificity module composed of SKP1 and a member of the F-box family of proteins (Cardozo and Pagano 2004). The CUL1/RBX1 complex functions as a scaffold to assemble the E2 ubiquitin conjugating enzyme with the substrate specificity module (Zheng et al. 2002). CUL1 interacts with RBX1 through its C terminus and with SKP1 through its N terminus. The interaction of F-box proteins with SKP1 occurs through the F-box motif, an ~40-amino acid motif first identified in budding yeast Cdc4p and human cyclin F, the latter giving the name to the entire family (Bai et al. 1996). F-box proteins contain additional protein interaction domains that bind ubiquitylation targets. The overall architecture of SCF complexes is conserved in the superfamily of SCF-like ubiquitin ligases that use cullin proteins as a scaffold. All cullins characterized to date (CUL1–5) are known to interact with RBX1 or RBX2 but use distinct specificity modules, which generally display structural and functional similarities with the SKP1/F-box protein module. For example, CUL2 and CUL5 are known to interact with the SKP1-like protein elongin C, which, in turn, interacts with F-box protein-like specificity factors called BC/SOCS-box proteins (Deshaies 1999; Guardavaccaro and Pagano 2003). In addition, CUL3 interacts with the BTB/POZ family of proteins, which appear to merge the functions of SKP1 and the F-box protein into a single polypeptide (Furukawa et al. 2003; Geyer et al. 2003; Pintard et al. 2003; Xu et al. 2003), with the BTB domain displaying structural relationships with SKP1 (Schulman et al. 2000; Xu et al. 2003). Cul4 forms a complex wherein DDB1/DDB2 and CSA proteins appear to function as substrate specificity modules (Groisman et al. 2003). Thus, the current expectation is that all cullin-containing ligases will share the modular nature of the original SCF family of ligases.

A major strategy employed by the SCF is the use of extended protein families as specificity factors. In 1999, we reported the identification of 47 F-box proteins in mammals (Cenciarelli et al. 1999; Winston et al. 1999). These proteins fell into three major classes, depending on the types of substrate interaction domains identified in addition to the F-box motif. The two largest classes of interaction domains are WD40 repeats (Smith et al. 1999) and leucine-rich repeats (LRRs) (Kobe and Kajava 2001). A third generic class of F-box proteins contained various other types of protein interaction domains or no recognizable domains. These classes of F-box proteins were designated FBWs, FBLs, and FBXs, respectively, followed by a numerical identifier (Cenciarelli et al. 1999; Winston et al. 1999). Paralogous genes in the same species used the same number followed by a letter (a, b, ...) representing the individual genes in the paralogous group. The Human Genome Organization (HUGO) Gene Nomenclature Committee adopted a related four-letter gene nomenclature: FBXW, FBXL, and FBXO, respectively, where "O" in FBXO refers to "other" domains. Since this initial work, subsequent efforts, particularly cDNA and genomic sequencing projects, have facilitated the further identification of F-box protein-coding genes. However, the inconsistent use of nomenclature standards has greatly limited the utility of the sequence database. This inconsistency is due in part to the rapid pace of research in this area that has precluded coordination of gene names. A survey of F-box proteins in GenBank revealed several issues: (1) several different F-box protein

Supplemental material is available at http://www.genesdev.org.
Corresponding authors.
[5]E-MAIL michele.pagano@med.nyu.edu; FAX (212) 263-5107.
[6]E-MAIL wade_harper@hms.harvard.edu; FAX (617) 432-6591.
Article and publication date are at http://www.genesdev.org/cgi/doi/10.1101/gad.1255304.

Table 1. *Mammalian F-box proteins*

F-box protein	Revised HUGO gene symbol	Aliases	Human Entrez gene ID	Human location	Mouse accession	% identity	Mouse location	Fly ortholog	Worm ortholog	Other domains (c)
FBXW1 (β-TRCP1)	*BTRC*	Fwd1, FBXW1A	8945	10q24.32	NM 009771	99	19C3	*slmb* (CG3412)	*lin-23* (K10B2.1)	
FBXW2	*FBXW2*	Fwd2, MD6	26190	9q34	NM 013890	98	2B			
FBXW4 (Dactylin)	*SHFM3*	FBXW4	6468	10q24	NM 13907	92	19C3			
FBXW5	*FBXW5*		54461	9q34.3	NM 013908	88	2A3	CG9144		
FBXW7	*FBXW7*	FBXW6, Cdc4, Sel-10, Fbx30	55294	4q31.3	NM 080428	97	3E3.3	*ago* (CG15010)	*sel-10* (F55B12.3)	transmembrane domain in β-isoform
FBXW8	*FBXW8*	Fbx29, FBXO29, Fbw6	26259	12q24.23	NM_172721	71	5F			
FBXW9	*FBXW9*		84261	19p13.2	BC043658.1	64	9		T01E8.4	
FBXW10	*FBXW10*	C17orf1A	10517	17p12	XM 126264.2	62	11B2			
FBXW11 (β-TRCP2)	*FBXW11*	Hos, FBXW1B, BTRC2, Fbx1b	23291	5q35.1	NM 134015	99	11A4	*slmb* (CG3412)	*lin-23* (K10B2.1)	
FBXW12	*FBXW12*	FBXO35	285231	3p21.31						
Fbxw13	*Fbxw13*				NM 177598		9F2			
Fbxw14	*Fbxw14*	Fbx12, Fbxo12			NM 015793		9F2			
Fbxw15	*Fbxw15*				AK087669		9F2			
Fbxw16	*Fbxw16*				AK078661		9F2			
Fbxw17	*Fbxw17*				AAH40428		13A5			
Fbxw18	*Fbxw18*				XM 356193		9F2			
Fbwx19	*Fbxw19*				AK087808		9F2			
FBXL1 (SKP2)	*SKP2*	FBXL1	6502	5p13	NM 013787.1	86	15A2	CG9772		
FBXL2	*FBXL2*	Fbl3	25827	3p22.3	NM 178624.2	95	9F3	CG9003	C02F5.7	
FBXL3	*FBXL3*	Fbl3a, FBLX3A	26224	13q22	AF 176521.1	93	14E2.3			
FBXL4	*FBXL4*	Fbl5	26235	6q16.1	NM 172988.1	93	4A3	CG1839		
FBXL5	*FBXL5*	Fbl4, Fir4	26234	4p15.33	AK085100	88	5B3			
FBXL6	*FBXL6*		26233	8q24.3	NM 013909	75	15			
FBXL7	*FBXL7*	Fbl6	23194	5p15.1	AK129227.1	93	15B1	CG4221		
FBXL8	*FBXL8*		55336	16q22.1	NM 015821	61	8D3			
FBXL10	*FBXL10*		84678	12q24.31	AK129479.1	84	4A5	DG11033		PHD, ZF, Jmjc
FBXL11	*FBXL11*	Lilina, Fbl7	22992	11q13.1	BC057051	90	19A	CG11033		PHD, ZF, Jmjc
FBXL12	*FBXL12*		54850	19p13.2	AF176525.1	93	9A3			
FBXL13	*FBXL13*		222235	7q22.1	NM 177076.2	63	5A3			
FBXL14	*FBXL14*		144699	12p13.33	AK084506.1	100	6F1	*ppa* (CG9952)		
FBXL15	*FBXL15*	FBXO37	79176	10q24.32	NM 133694.1	87	19C3	CG8873		
FBXL16	*FBXL16*	C16orf22	146330	16p13.3	XM 128530.4	81	17A3.3	CG32085		
FBXL17	*FBXL17*	Fbx13, FBXO13	64839	5q21.3	XM 128716.2	93	17E1.1			
FBXL18	*FBXL18*		80028	7p22.2	Bl853840	89	5G2			
FBXL19	*FBXL19*		54620	16p11.2	NM 172748.2	95	7F3			PHD, ZF
FBXL20	*FBXL20*	Fbl2	84961	17q21.2	XM 126674.3	99	11D	CG9003	CO2F5.7	
FBXL21	*FBXL21*	FBXL3B, Fbl3B	26223	5q31	AK035290	81	13B1			
FBXL22	*FBXL22*		400380	15q22.1	NM 175206	80	9C			
FBXO1 (Cyclin F)	*CCNF*	FBX1, FBXO1	899	16p13.3	NM 007634.2	75	17A3.3			cyclin box
FBXO2	*FBXO2*	Nfb42, Fbs1, Fbg1, Ocp1	26232	1p35.21	BC027053.1	87	4E2.0			FBA
FBXO3	*FBXO3*	FBA	26273	11p13	AK004544.2	92	2E2.0			ApaG-like domain (SCOP)
FBXO4	*FBXO4*		26272	5p12	NM 134099.1	83	15A1			
FBXO5 (EMI1)	*FBXO5*	FBXO31	26271	6q25	BC053434.1	70	10A1	*Rca1* (CG10800)		IBR domain

continued on next page

Table 1. *(continued)*

F-box protein	Revised HUGO gene symbol	Aliases	Human Entrez gene ID	Human location	Mouse accession	% identity	Mouse location	Fly ortholog	Worm ortholog	Other domains (c)
FBXO6	*FBXO6*	Fbs2, Fbg2, Fbx6b	26270	1p36.23	NM 015797	75	4E2.0		C14B1.3	FBA domain
FBXO7	*FBXO7*	Fbx	25793	22q12-q13	NM 153195.1	70	10C1			UBL-domain (SCOP)
FBXO8	*FBXO8*	Fbs	26269	4q34.1	NM 015791.2	90	8B1.3			Sec7
FBXO9	*FBXO9*	Ny-ren-57	26268	6p12.3-p11.2	AK077607.1	89	9E1.0	CG5961		TPR, HNHc (SCOP)
FBXO10	*FBXO10*		26267	9p13.1	XM_194139.2	84	4B1	CG9461	K04A8.6	CASH
FBXO11	*FBXO11*		80204	2p21	XM_110248.4	98	17E5.0	CG9461	K04A8.6	CASH
FBXO15	*FBXO15*		201456	18q22.3	AF176530	60	18E4.0			
FBXO16	*FBXO16*		157574	8p21.1	NM 015795.1	81	14D1			
FBXO17	*FBXO17*	Fbg4, FBXO26	115290	19q13.2	AF176532/ NM 015796	80	7A3			FBA
FBXO18	*FBXO18*	Fbh1	84893	10p15.1	NM 015792	87	2A1			Helicase
FBXO20	*LMO7*	FBXO20	4008	13q21.33	AK129231	68	14E2.2			CH, PDZ, Lim
FBXO21	*FBXO21*		23014	12q24.23	AB093270	91	5F			
FBXO22	*FBXO22*		26263	15q23	NP 028049	96	9B			
FBXO24	*FBXO24*		26261	7q22	XM 132440	84	5G2			RCC1-fold (SCOP)
FBXO25	*FBXO25*		26260	8p23.3	NM 025785	84	8A1.1	CG11658	DY3.6	
FBXO27	*FBXO27*	Fbg5	126433	19q13.2	AK053292	79	7A3			FBA
FBXO28	*FBXO28*		23219	1q42.12	NM 175127	89	1H5	CG3428		
FBXO30	*FBXO30*		84085	6q24	XM 125493	87	10A1			
FBXO31	*FBXO31*	Fbx14, FBXO14	79791	16	AU066822/NM 133765.2	95	8.00E+01			
FBXO32	*FBXO32*	Mafbx, Atrogin-1	114907	8q24.13	NM_026346	96	15D1	CG11658	DY3.6	
FBXO33	*FBXO33*		254170	14q13.3	XM_127032	90	12C1	CG4911		RNI-like (SCOP)
FBXO34	*FBXO34*		55030	14q22.2	NM 030236.1	71	14B			
FBXO36	*FBXO36*		130888	2q37.1	NM 025386	78	1C5			
FBXO38	*FBXO38*	MOKA	81545	5q33.1	AK 031347	86	18E2.0			RNI-like (SCOP)
FBXO39	*FBXO39*		162517	17p13.2	XM 282966	78	11B4	CG2010		RNI-like (SCOP)
FBXO40	*FBXO40*		51725	3q21.1	XM 156082	80	16A1			TDL (SCOP)
FBXO41	*FBXO41*		150726	2p13.2	AK129466	80	6C3			
FBXO42	*FBXO42*		54455	1p36.23–p36.11	AK028867	89	4D3	CG6758		Kelch repeats
FBXO43	*FBXO43*		286151	8q22.3	NM_175281	70	15B3.1	*Rca1* (CG10800)		IBR domain
FBXO44	*FBXO44*	Fbx30, FBG3, FBXO6a	93611	1p36.21	NM 173401	90	4E2.0		C14B1.3	FBA domain
FBXO45	*FBXO45*		20093	3q29	BC026799	99	16A1			SPRY
FBXO46	*FBXO46*	FBXO34L	23403	9q13.3	NM 175530	80	7A2			

coding genes have been given the same gene name; (2) multiple individual F-box genes have been given several different names; (3) the nomenclature used for clearly orthologous mouse and human genes is inconsistent; (4) several genes present in GenBank encode F-box proteins but are not annotated as such; (5) mRNA sequence revisions and refinement of algorithms for detection of F-box motifs have led to the removal of some genes from the F-box category; and (6) improvements in structural domain identification suggest that genes previously designated in the FBXO subclass may be more appropriately placed in the FBXL or FBXW subclasses. The need for clear communication in this field necessitates a unified nomenclature for F-box proteins.

To develop a comprehensive nomenclature for mammalian F-box proteins, we have systematically analyzed F-box proteins in the human and mouse genomes and have organized these genes in a manner that largely conforms to previous nomenclature standards, as explained below. This nomenclature has now been adopted and implemented by the HUGO Gene Nomenclature Committee. Several factors were considered in devising the most appropriate nomenclature for the future. First, genes whose symbols were approved by the nomenclature committee prior to the discovery of these genes as F-box proteins will remain as the approved symbol. Second, the previous nomenclature used letters (a, b, ...) to indicate what appeared to be paralogous genes (e.g., *FBXL3a* and *FBXL3b*). However, because it is now appreciated that many F-box proteins exist as multiple splicing variants, the use of such a designation scheme has been avoided, necessitating the complete renaming of a small number of F-box proteins. Finally, mouse and human orthologs have been given the same symbols to facilitate comparative studies in the future. A detailed description of how the nomenclature changes have affected individual F-box genes is provided in the Supplemental Material.

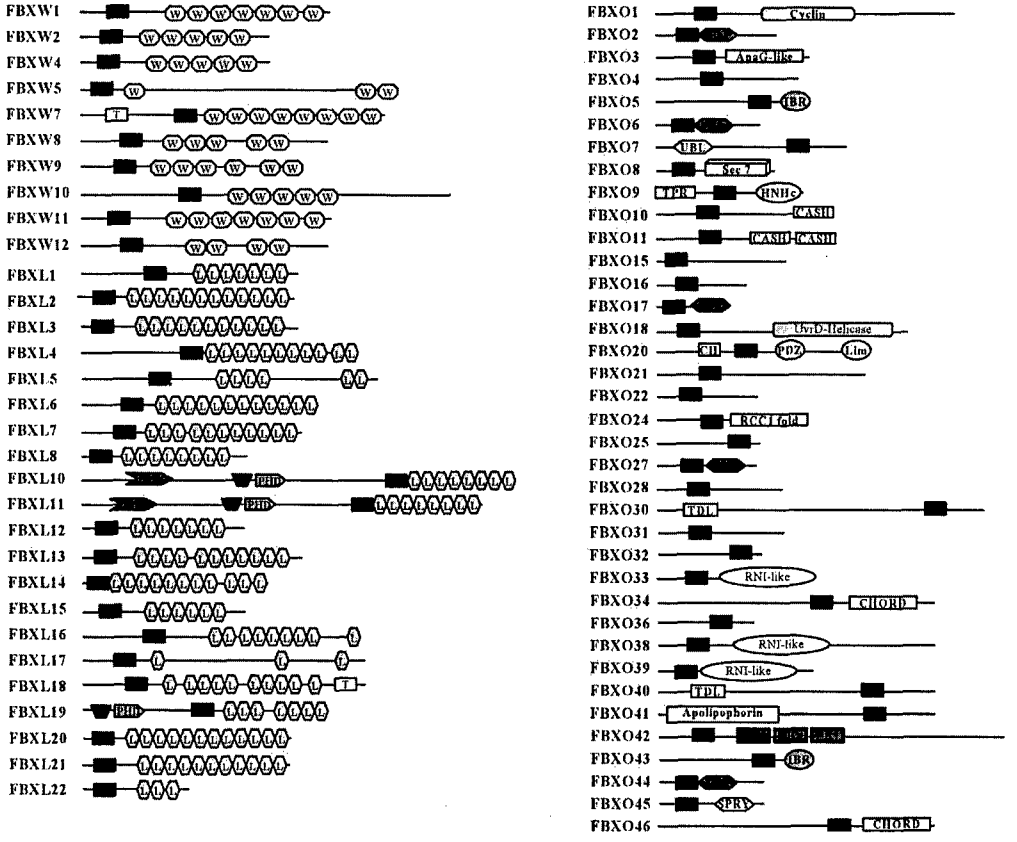

Figure 1. Domain structures of mammalian F-box proteins. Domains identified by the Hidden Markov Model algorithms of SMART or PFam include F-box motif (F), WD40 repeat (WD), leucine-rich repeat (L), transmembrane domain (T), F-box-associated domain (FBA), between-ring domain (IBR), domain in carbohydrate binding proteins and sugar hydrolases (CASH), kelch repeat (K), calponin homology domain (CH), domain found in cupin metalloenzyme family (Jmjc), domain present in PSD-95, Dlg, and ZO-1 (PDZ), zinc-binding domain found in Lin-11, Isl-1, and Mec-3 (Lim), HNH nuclease family (HNHc), novel eukaryotic zinc-binding domain (CHORD), and tetratrico peptide repeat (TPR). The following domains were found via the Structural Classification of Proteins (SCOP) database, which can be used to predict protein sequences that can adopt known protein folds: ApaG-like, which is structurally similar to bacterial ApaG; Apolipophorin, the apolipophorin-III-like fold; Ubl, the ubiquitin-like fold; TDL, which is Traf-domain like; RNI-like, which may form structure similar to that of leucine-rich repeats in placental RNase inhibitor; and RCC1, which is a possible regulator of chromatin condensation-1 fold.

Our analysis led to the identification of 68 human and 74 mouse genes encoding recognizable F-box motifs, as detected by Hidden Markov Models (Table 1; Fig. 1) (Bateman et al. 2004; Letunic et al. 2004). A phylogenetic representation of human F-box motifs is shown in Figure 2. The phylogeny of F-box domain sequences only, which gives the cleanest available view of the evolutionary signature of the family, shows two major groups of F-box proteins (an evolutionary divergence). Different protein interaction domains are scattered throughout the two groups indicating that similar domain swapping mechanisms acted on both, but ruling out that all *FBXW* subfamily members diverged from a single *FBXW* ancestor, for example.

Clear mouse orthologs were identified for all human F-box proteins except *FBXW12*, with the majority of mouse genes displaying >80% identity with their human counterparts (Table 1). In the mouse, *FBXW12*-related sequences have been dramatically expanded to seven genes (one at chromosome 13A5 [*Fbxw17*] and a cluster of six genes at chromosome 9F2 [*Fbxw13*, *Fbxw14*, *Fbxw15*, *Fbxw16*, *Fbxw18*, *Fbxw19*]). Each of these seven mouse genes is equally related to *FBXW12*, and, therefore, we are unable to unambiguously designate a mouse ortholog of human *FBXW12*. The mechanism and significance of expansion of this subclass of F-box proteins in the mouse are unknown. Three human proteins with F-box like motifs—Tome-1 (CDCA3), TBL1, and TBLR1 (TBL1XR1)—were not included because the presumptive F-box sequence did not reach the threshold sufficient for this classification.

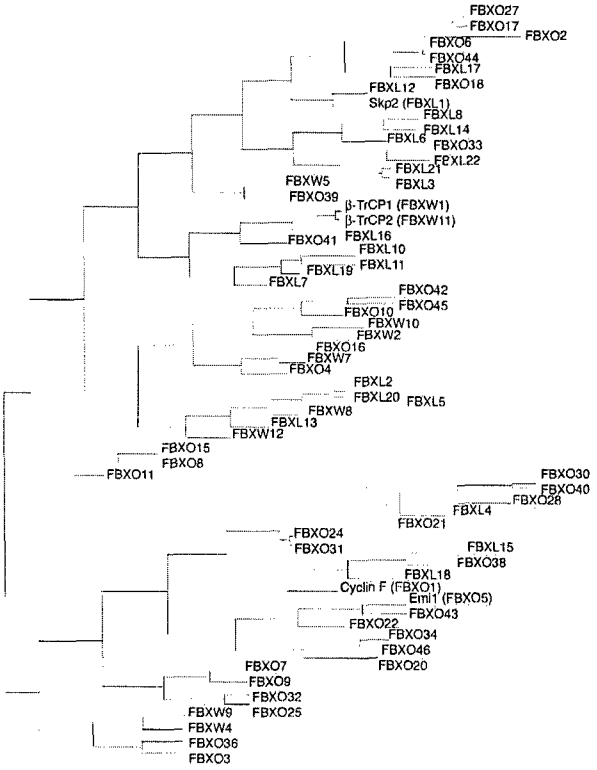

Figure 2. Phylogenetic tree depiction of interrelationships between human F-box proteins. The tree is generated from the pairwise ZEGA distances (Abagyan and Batalov 1997) within the set of amino acid sequences comprising the F-box domain only by the neighbor-joining method (Saitou and Nei 1987) as adapted in ICM software (Molsoft LLC; http://www.molsoft.com).

A combination of BLAST analyses and phylogenetic tree construction using putative substrate interaction domains together with the F-box motif revealed possible orthologs of mammalian F-box proteins in *Drosophila melanogaster* and *Caenorhabditis elegans* (Table 1; Fig. 3). The inclusion of substrate interaction domains allows confirmation of some relationships with the mammalian proteins (e.g., FBXL12 with SKP2), but also demonstrates, in comparison to the F-box domain only tree, that the phylogenetic spread of each subgroup is as wide as that of the whole family. Interestingly, the *D. melanogaster* genome contains several possible orthologs of the human FBXL series that are not found in *C. elegans* (Table 1; Fig. 3). The fact that *C. elegans* has more than 300 F-box proteins but that only a few display relationships with mammalian genes indicates significant diversification of the F-box proteins in this organism. This expansion is species-specific because the *Caenorhabditis briggsae* genome is predicted to encode a similar number of F-box proteins as found in human and mouse genomes (Stein et al. 2003). Six genes encoding F-box proteins appear to be conserved in *C. elegans*, *D. melanogaster*, and mammals: *BTRC* (*FBXW1*), *FBXW7*, *FBXL2*, *FBXO10*, *FBXO25*, and *FBXO45* (Table 1; Fig. 3). Interestingly, in mammals four of these six genes have a paralog: *FBXW1* (*BTRC*, *β-TRCP1*) for *FBXW11* (*β-TRCP2*), *FBXL20* for *FBXL2*, *FBXL11* for *FBXL10*, and *FBXO32* for *FBXO25*, respectively. The FBA-containing subclass of FBXO proteins are contained in the *C. elegans* genome but are absent in *D. melanogaster* (Table 1; Fig. 3). Thus, it is possible that much of the core SCF signaling common to metazoans is performed by a relatively small number of highly conserved F-box proteins. To date, conserved degradation pathways have been found for targets of mammalian FBXW7 and β-TRCP1/2 in both *C. elegans* and *Drosophila*. c-MYC and cyclin E are targeted by ago/FBXW7 in both *Drosophila* and mammals (Koepp et al. 2001; Moberg et al. 2001, 2004; Strohmaier et al. 2001; Tetzlaff et al. 2004; Welcker et al. 2004), and Notch is targeted by sel-10/FBXW7 in both mammals and *C. elegans* (Hubbard et al. 1997; Wu et al. 2001; Tetzlaff et al. 2004; Tsunematsu et al. 2004). Similarly, β-TRCP1/2/*slmb* has been linked to the β-catenin, IκB, and cell cycle pathways in both *Drosophila* and mammals (for review, see Maniatis 1999; Guardavaccaro and Pagano 2003).

Despite the large number of mammalian F-box proteins, in addition to β-TRCP1/2 and FBW7, only one other mammalian F-box protein has been matched to its downstream substrates, namely, SKP2 (Ang and Harper 2004; Cardozo and Pagano 2004). Interestingly, SKP2 is the product of a proto-oncogene, FBW7 is a tumor suppressor (Pagano and Benmaamar 2003; Yamasaki and Pagano 2004), and overexpression of β-TRCP1 can contribute to transformation at least in some epithelial tissues

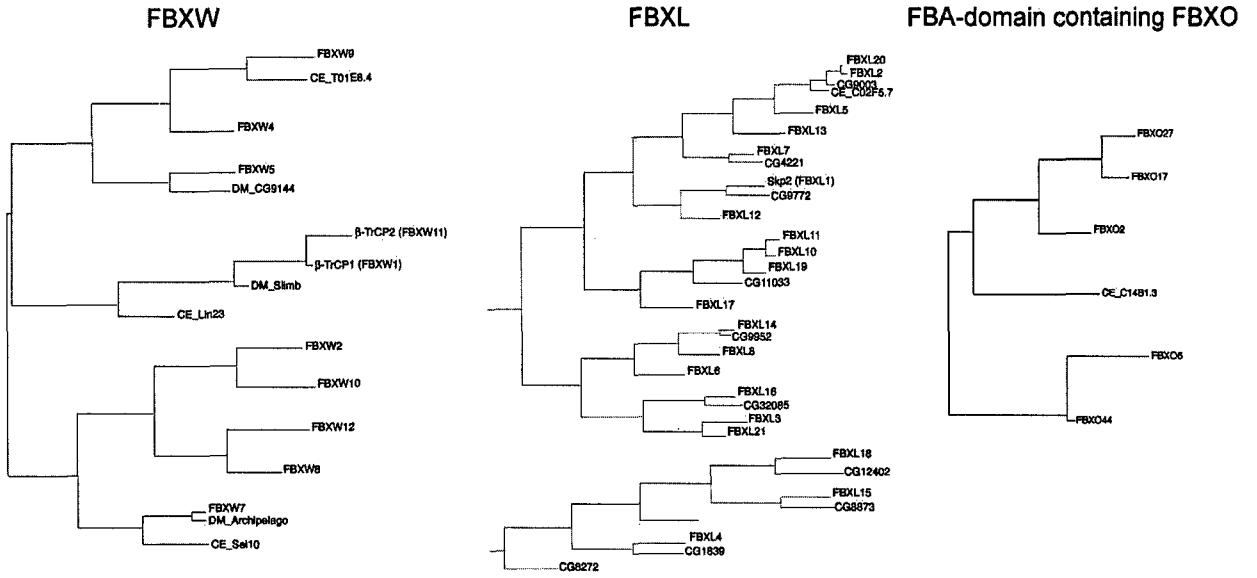

Figure 3. Phylogenetic trees for FBXW, FBXL, and FBA-domain-containing subfamilies of F-box proteins, along with orthologous sequences from *D. melanogaster* and *C. elegans*. Only the contiguous portions of the sequence corresponding to the F-box domain followed by the indicated protein interaction domain were included and aligned.

(Kudo et al. 2004). Finally, EMI1/FBXO5, an inhibitor of the mitotic ubiquitin ligase APC/C, is overexpressed in tumor cell lines and certain breast tumors (Hsu et al. 2002; van 't Veer et al. 2002). Other F-box proteins appear to play a role in different diseases. For example, Dactylin/FBW4 is encoded by *SHFM3*, the split hand–foot malformation syndrome gene 3 (Basel et al. 2003). *FBXO3* expression is increased in proliferating synovium of patients with rheumatoid arthritis (Masuda et al. 2002). FBXO32 is up-regulated during muscle atrophy (Bodine et al. 2001; Gomes et al. 2001). Thus, F-box proteins are attractive candidates for drug discovery because they play crucial roles in many important signaling pathways.

Validated protein structure prediction tools revealed inappropriately classified F-box proteins as well the association of new functional or structural domains with the F-box motif (Fig. 1). For example, certain F-box proteins previously placed in the FBXO class (e.g., FBXO13) were found to have LRRs and were reclassified accordingly (Table 1; also see Supplemental Material). FBXO14 was found to have WD40 repeats and was reclassified as FBXW12 (Table 1). Three FBXO members (FBXO33, FBXO38, and FBXO39) may display structural similarity to RNase inhibitor, the prototypical LRR, but these sequences do not reach the threshold required to be fingered as authentic LRRs based on sequence information alone (Fig. 1). Additional protein folds new to the mammalian FBX class include ubiquitin-like folds (FBXO7), TPR-like domain (FBXO9), RCC1 (FBXO24), and Kelch repeats (FBXO42). In addition to the five FBA-containing F-box proteins that bind glycosylated proteins (Cardozo and Pagano 2004), two additional proteins (FBXO10 and FBXO11) contain the CASH domain frequently found in carbohydrate-binding proteins and hydrolases (Fig. 1). Both *D. melanogaster* and *C. elegans* contain possible orthologs of *FBXO10* and/or *FBXO11* (Table 1). Finally, F-box proteins containing a SPRY domain (FBXO45 in mammals) are found in all metazoans. The SPRY domain is of unknown function but is frequently present in ryanodine receptors. Recent studies have linked the *C. elegans* SPRY domain F-box protein (C26E6.5) with presynaptic differentiation (Liao et al. 2004).

The use of this systematic nomenclature should facilitate comparative genomics and drug discovery approaches, as well as the communication of experiments designed to elaborate the functional properties of F-box proteins.

Acknowledgments

This work was supported by NIH grant AG11085 (to J.W.H. and S.J.E), and by the Department of Defense (DAMD17-01-1-0135) to J.W.H., and by NIH grants CA76584 and GM57587 to M.P. J.J. was supported by postdoctoral fellowship DAMD17-02-1-0284. S.J.E. is an investigator of the Howard Hughes Medical Institute.

References

Abagyan, R.A. and Batalov, S.V. 1997. Do aligned sequences share the same fold? *J. Mol. Biol.* **273:** 355–368.

Ang, X.L. and Harper, J.W. 2004. Interwoven ubiquitination oscillators and control of cell cycle transitions. *Sci. STKE* **2004:** pe31.

Bai, C., Sen, P., Hofmann, K., Ma, L., Goebl, M., Harper, J.W., and Elledge, S.J. 1996. SKP1 connects cell cycle regulators to the ubiquitin proteolysis machinery through a novel motif, the F-box. *Cell* **86:** 263–274.

Basel, D., DePaepe, A., Kilpatrick, M.W., and Tsipouras, P. 2003. Split hand foot malformation is associated with a reduced level of Dactylin gene expression. *Clin. Genet.* **64:** 350–354.

Bateman, A., Coin, L., Durbin, R., Finn, R.D., Hollich, V., Griffiths-Jones, S., Khanna, A., Marshall, M., Moxon, S., Sonnhammer, E.L., et al. 2004. The Pfam protein families database. *Nucleic Acids Res.* **32:** D138–D141.

Bodine, S.C., Latres, E., Baumhueter, S., Lai, V.K., Nunez, L., Clarke, B.A., Poueymirou, W.T., Panaro, F.J., Na, E., Dharmarajan, K., et al. 2001. Identification of ubiquitin ligases required for skeletal muscle atrophy. *Science* **294:** 1704–1708.

Cardozo, T. and Pagano, M. 2004. The SCF ubiquitin ligase: Insights into a molecular machine. *Nat. Rev. Mol. Cell. Biol.* **5:** 739–753.

Cenciarelli, C., Chiaur, D.S., Guardavaccaro, D., Parks, W., Vidal, M., and Pagano, M. 1999. Identification of a family of human F-box proteins. *Curr. Biol.* **9:** 1177–1179.

Deshaies, R.J. 1999. SCF and Cullin/Ring H2-based ubiquitin ligases. *Annu. Rev. Cell Dev. Biol.* **15:** 435–467.

Feldman, R.M., Correll, C.C., Kaplan, K.B., and Deshaies, R.J. 1997. A complex of Cdc4p, Skp1p, and Cdc53p/cullin catalyzes ubiquitination of the phosphorylated CDK inhibitor Sic1p. *Cell* **91:** 209–219.

Furukawa, M., He, Y.J., Borchers, C., and Xiong, Y. 2003. Targeting of protein ubiquitination by BTB–Cullin 3–Roc1 ubiquitin ligases. *Nat. Cell. Biol.* **5:** 1001–1007.

Geyer, R., Wee, S., Anderson, S., Yates, J., and Wolf, D.A. 2003. BTB/POZ domain proteins are putative substrate adaptors for Cullin 3 ubiquitin ligases. *Mol. Cell* **12:** 783–790.

Gomes, M.D., Lecker, S.H., Jagoe, R.T., Navon, A., and Goldberg, A.L. 2001. Atrogin-1, a muscle-specific F-box protein highly expressed during muscle atrophy. *Proc. Natl. Acad. Sci.* **98:** 14440–14445.

Groisman, R., Polanowska, J., Kuraoka, I., Sawada, J., Saijo, M., Drapkin, R., Kisselev, A.F., Tanaka, K., and Nakatani, Y. 2003. The ubiquitin ligase activity in the DDB2 and CSA complexes is differentially regulated by the COP9 signalosome in response to DNA damage. *Cell* **113:** 357–367.

Guardavaccaro, D. and Pagano, M. 2003. Oncogenic aberrations of Cullin-dependent ubiquitin ligases. *Oncogene* **23:** 2037–2049.

Hsu, J.Y., Reimann, J.D., Sorensen, C.S., Lukas, J., and Jackson, P.K. 2002. E2F-dependent accumulation of hEmi1 regulates S phase entry by inhibiting APC(Cdh1). *Nat. Cell Biol.* **4:** 358–366.

Hubbard, E.J., Wu, G., Kitajewski, J., and Greenwald, I. 1997. sel-10, a negative regulator of lin-12 activity in *Caenorhabditis elegans*, encodes a member of the CDC4 family of proteins. *Genes & Dev.* **11:** 3182–3193.

Kobe, B. and Kajava, A.V. 2001. The leucine-rich repeat as a protein recognition motif. *Curr. Opin. Struct. Biol.* **11:** 725–732.

Koepp, D.M., Schaefer, L.K., Ye, X., Keyomarsi, K., Chu, C., Harper, J.W., and Elledge, S.J. 2001. Phosphorylation-dependent ubiquitination of cycin E by SCF^{Fbw7} ubiquitin ligase. *Science* **294:** 173–177.

Kudo, Y., Guardavaccaro, D., Santamaria, P.G., Koyama-Nasu, R., Latres, E., Bronson, R., Yamasaki, L., and Pagano, M. 2004. Role of F-box protein βTrcp1 in mammary gland development and tumorigenesis. *Mol. Cell. Biol.* **24:** 8184–8194.

Letunic, I., Copley, R.R., Schmidt, S., Ciccarelli, F.D., Doerks, T., Schultz, J., Ponting, C.P., and Bork, P. 2004. SMART 4.0: Towards genomic data integration. *Nucleic Acids Res.* **32:** D142–D144.

Liao, E.H., Hung, W., Abrams, B., and Zhen, M. 2004. An SCF-like ubiquitin ligase complex that controls presynaptic differentiation. *Nature* **430:** 345–350.

Maniatis, T. 1999. A ubiquitin ligase complex essential for the NF-κB, Wnt/Wingless, and Hedgehog signaling pathways. *Genes & Dev.* **13:** 505–510.

Masuda, K., Masuda, R., Neidhart, M., Simmen, B.R., Michel, B.A., Muller-Ladner, U., Gay, R.E., and Gay, S. 2002. Molecular profile of synovial fibroblasts in rheumatoid arthritis depends on the stage of proliferation. *Arthritis Res.* **4:** R8.

Moberg, K.H., Bell, D.W., Wahrer, D.C.R., Haber, D.A., and Hariharan, I.K. 2001. Archipelago regulates Cyclin E levels in *Drosophila* and is mutated in human cancer cell lines. *Nature* **413:** 311–316.

Moberg, K.H., Mukherjee, A., Veraksa, A., Artavanis-Tsakonas, S., and Hariharan, I.K. 2004. The *Drosophila* F box protein archipelago regulates dMyc protein levels in vivo. *Curr. Biol.* **14:** 965–974.

Pagano, M. and Benmaamar, R. 2003. When protein destruction runs amok, malignancy is on the loose. *Cancer Cell* **4:** 251–256.

Pintard, L., Willis, J.H., Willems, A., Johnson, J.L., Srayko, M., Kurz, T., Glaser, S., Mains, P.E., Tyers, M., Bowerman, B., et al. 2003. The BTB protein MEL-26 is a substrate-specific adaptor of the CUL-3 ubiquitin-ligase. *Nature* **425:** 311–316.

Saitou, N. and Nei, M. 1987. The neighbor-joining method: A new method for reconstructing phylogenetic trees. *Mol. Biol. Evol.* **4:** 406–425.

Schulman, B.A., Carrano, A.C., Jeffrey, P.D., Bowen, Z., Kinnucan, E.R., Finnin, M.S., Elledge, S.J., Harper, J.W., Pagano, M., and Pavletich, N.P. 2000. Insights into SCF ubiquitin ligases from the structure of the Skp1–Skp2 complex. *Nature* **408:** 381–386.

Skowyra, D., Craig, K.L., Tyers, M., Elledge, S.J., and Harper, J.W. 1997. F-box proteins are receptors that recruit phosphorylated substrates to the SCF ubiquitin–ligase complex. *Cell* **91:** 209–219.

Smith, T.F., Gaitatzes, C., Saxena, K., and Neer, E.J. 1999. The WD repeat: A common architecture for diverse functions. *Trends Biochem. Sci.* **24:** 181–185.

Stein, L.D., Bao, Z., Blasiar, D., Blumenthal, T., Brent, M.R., Chen, N., Chinwalla, A., Clarke, L., Clee, C., Coghlan, A., et al. 2003. The genome sequence of *Caenorhabditis briggsae*: A platform for comparative genomics. *PLoS Biol.* **1:** E45.

Strohmaier, H., Spruck, C.H., Kaiser, P., Won, K.-A., Sangfelt, O., and Reed, S.I. 2001. Human F-box protein hCdc4 targets cyclin E for proteolysis and is mutated in a breast cancer cell line. *Nature* **413:** 316–322.

Tetzlaff, M.T., Yu, W., Li, M., Zhang, P., Finegold, M., Mahon, K., Harper, J.W., Schwartz, R.J., and Elledge, S.J. 2004. Defective cardiovascular development and elevated cyclin E and Notch proteins in mice lacking the Fbw7 F-box protein. *Proc. Natl. Acad. Sci.* **101:** 3338–3345.

Tsunematsu, R., Nakayama, K., Oike, Y., Nishiyama, M., Ishida, N., Hatakeyama, S., Bessho, Y., Kageyama, R., Suda, T., and Nakayama, K.I. 2004. Mouse Fbw7/Sel-10/Cdc4 is required for notch degradation during vascular development. *J. Biol. Chem.* **279:** 9417–9423.

van 't Veer, L.J., Dai, H., van de Vijver, M.J., He, Y.D., Hart, A.A., Mao, M., Peterse, H.L., van der Kooy, K., Marton, M.J., Witteveen, A.T., et al. 2002. Gene expression profiling predicts clinical outcome of breast cancer. *Nature* **415:** 530–536.

Welcker, M., Orian, A., Jin, J., Grim, J.A., Harper, J.W., Eisenman, R.N., and Clurman, B.E. 2004. The Fbw7 tumor suppressor regulates glycogen synthase kinase 3 phosphoryla-

tion-dependent c-Myc protein degradation. *Proc. Natl. Acad. Sci.* **101:** 9085–9090.

Winston, J.T., Koepp, D.M., Zhu, C., Elledge, S.J., and Harper, J.W. 1999. A family of mammalian F-box proteins. *Curr. Biol.* **9:** 1180–1182.

Wu, G., Lyapina, S., Das, I., Li, J., Gurney, M., Pauley, A., Chui, I., Deshaies, R.J., and Kitajewski, J. 2001. SEL-10 is an inhibitor of notch signaling that targets notch for ubiquitin-mediated protein degradation. *Mol. Cell. Biol.* **21:** 7403–7415.

Xu, L., Wei, Y., Reboul, J., Vaglio, P., Shin, T.H., Vidal, M., Elledge, S.J., and Harper, J.W. 2003. BTB proteins are substrate-specific adaptors in an SCF-like modular ubiquitin ligase containing CUL-3. *Nature* **425:** 316–321.

Yamasaki, L. and Pagano, M. 2004. Cell cycle, proteolysis and cancer. *Curr. Opin. Cell Biol.* (in press).

Zheng, N., Schulman, B.A., Song, L., Miller, J.J., Jeffrey, P.D., Wang, P., Chu, C., Koepp, D.M., Elledge, S.J., Pagano, M., et al. 2002. Structure of the Cul1–Rbx1–Skp1–F box Skp2 SCF ubiquitin ligase complex. *Nature* **416:** 703–709.